Authors' Response

Blanchard, C., et al.: Effects of emission reductions on organic aerosol in the southeastern United States. ACPD, 15, 17051-17092, 2015.

We thank the reviewers for their careful reading and helpful suggestions. Their recommendations will improve the manuscript. We summarize the reviews point-by-point, provide responses, and append a mark-up version with new text, tables, and graphs indicated in red.

Referee 1

Uncertainty analysis. Both reviewers suggest additional presentation of uncertainties. We have added uncertainties as discussed more specifically in the proposed revised text. In brief, the uncertainty of the mean OM/OC is estimated as ± 0.2 based on potential biases in the measured $PM_{2.5}$ mass concentrations and the computed sum of species. A factor of two uncertainty is estimated in the mean computed biomass burning OC (OCbb) based on potential biases in identifying non-soil potassium (nsK) as a biomass-burning tracer (Kbb) and in scaling from Kbb to OCbb (subject to the constraint that OCbb < OC). Uncertainties in the source apportionment by factor analysis are estimated using the range of results among the two primary versions of principal component analysis (PCA) along with the additional PCA sensitivity analyses and PMF analyses that we had applied to CTR and JST data. The ranges of combustion factor OC across PCAs and PMF, for example, are 0.6 $\mu g\ m^{-3}$ at YRK, 0.8 $\mu g\ m^{-3}$ at CTR, and 1.2 $\mu g\ m^{-3}$ at JST. Taking one-half the range as a measure of uncertainty yields combustion factor OC uncertainties of ± 0.3 to ± 0.6 $\mu g\ m^{-3}$. For CTR, for example, 2008 – 2013 mean OCbb is 1.6 $\mu g\ m^{-3}$ (0.8 – 2.4 $\mu g\ m^{-3}$) compared with the mean PCA1 combustion OC of 1.3 $\mu g\ m^{-3}$ (0.9 – 1.7$\mu g\ m^{-3}$).

In addition, Referee 1 recommends making more explicit comparisons of results from the different analytical approaches. Referee 1's point that when combined, the various analyses tend to present a coherent picture, is important. We have added a summary comparison (Table 5) and a discussion of the areas of agreement and disagreement among approaches. For CTR, again for example, this comparison adds additional evidence from CMB receptor modeling indicating mean combustion OC of 1.5 μg m^{-3} (± 0.9 μg m^{-3}) and area-source (fires) OC of 1.4 μg m^{-3}.

Comparisons are made with recently published studies, as indicated in the proposed revised text.

<u>Section 3.1</u> (EC-OC-SO4). Clarifying text has been added. The ratio of JST EC/CTR EC declined by 25% whereas the ratio of JST OC/CTR OC declined by 20%. While these declines are comparable, the difference suggests a greater mobile-source influence at JST than at CTR. We have noted that OC correlates with both EC and SO_4, but for different reasons (common emission sources in the case of EC and chemistry in the case of SO_4). Consequently, EC and SO_4 also correlate, but not as strongly and not as consistently across time scales.

<u>Section 3.2</u> (OM/OC). Citations have been added in the proposed revision. Laboratory RH (38%) was defined following Equation 1. It is usually less than 38% as SEARCH tries to maintain filter samples at 33 ± 2% (FRM requirement is 35 ± 5%). As noted above, the OM/OC uncertainty is estimated as ± 0.2 and explained in the proposed revised text. Comparison with published studies indicates that our mean OM/OC agrees within error with co-located AMS results when paired in time at some times and places but not others. Since our mean OC concentrations – which are well-supported by the length of the SEARCH record – are sometimes the same and sometimes differ from mean AMS OC (paired by site and time period, usually about one month duration, as calculated from AMS OA using published OM/OC), it isn’t clear that AMS is always measuring the same material as the SEARCH filter-based OC. We think that our site mean OM/OC ratios of 1.5 – 2.0 (± 0.2) support our previous statement (“POA is a major portion of OA at both urban and rural sites”), since we aren’t claiming that POA is the largest component. However, the “POA” terminology is ambiguous. We have slightly revised this statement to read “The consistency of the mean values in the range of 1.5 to 2.0 (± 0.2) indicates that relatively fresh emissions contribute a major portion of OA at both urban and rural sites.”

Section 3.3 (Biomass burning). We have added a discussion of estimated uncertainty in OCbb and concluded that it is a factor of two. We also added comparison with AMS results. Consistent with recent studies that show loss of levoglucosan and other organic markers of biomass burning on a time scale of roughly one day or even less, Xu et al. (2015a; b) were careful to note that their BBOA component likely represented only fresh biomass burning, with more aged OA from burns perhaps appearing with MO-OOA. The AMS BBOA was lower at CTR during SOAS, ~0.25 μg m^{-3} OC (using reported OM/OC for BBOA) than at JST, ~0.5 μg m^{-3} OC (during May and December 2012) and at YRK, ~0.6 μg m^{-3} OC (during December 2012 and January 2013) (Xu et al., 2015a; b). Whether or not our long-term results differ from available AMS data depends on the unknown ratio of aged biomass-burning OA to BBOA. If it is a factor of two, the sum of AMS BBOA (local--from levoglucosan tracer) and more aged material from burning would fall within our error range. Our summary comparisons across methods (see later table) suggest that our OCbb is overestimated by ~10% or more (but within our factor-of-two uncertainty estimate).

We recognize that potassium is an imperfect tracer of biomass burning. Zhang et al. (2010), for example, showed that water-soluble K and levoglucosan correlate in winter (when more biomass burning occurs in this area) but not in summer. Recent studies indicate that levoglucosan is not conservative (May et al., 2012; Bougiatioti et al., 2014), so we would expect levoglucosan to react with aging and yield a BBOA concentration biased low relative to a total. Levoglucosan will more quickly decay in the atmosphere during warmer months, possibly accounting in part for the seasonal difference. One study (presently in preliminary form) found that levoglucosan loss led to a factor-of-two underestimate of BBOA in air masses over a one-to-two day transport time (Iulia Gensch, "Chemical stability of levoglucosan in laboratory and ambient aerosol studies: an isotopic perspective", 11th International Conference on Carbonaceous Particles in the Atmosphere, Berkeley, CA, August 10 - 13, 2015).

Our computation of nsK was intended to remove the crustal component of K, and the data show that nsK correlates with K ion. Kbb has its limitations as a tracer, but does seem capable of yielding estimates within an uncertainty estimated as ~ 2x in our case. Our estimate of the scale factor between OCbb and Kbb is likely to contain a large uncertainty related to the variability of fire intensity and combustible material properties. This uncertainty is poorly characterized in the literature, although variability is documented.

The biomass burning contributions may in fact be driven by large events. If SOAS experienced few such events, some difference between AMS BBOA found in SOAS and our long-term averages would be expected. The long-term averages are a meaningful representation of the impact of biomass burning on an annual basis, and should provide a perspective that is missing from the six-week SOAS sampling campaign.

Figure S9 shows modern TC vs. Kbb. Since we calculate TCbb = 32*Kbb and OCbb = 0.9*TCbb, plotting modern TC vs. OCbb will yield the same scatter. The intent of Figure 9 is to show that the limited carbon isotope data available support our scaling factor between TCbb and Kbb (32), which is based on the southeastern regional portion of the National Emissions Inventory (e.g. Blanchard et al, 2013). In our proposed revision, we use the observed scatter in Figure S9 (slopes ranging from 22 to 82, depending on possibly unique events) to support our estimate of a factor-of-two uncertainty in scaling from Kbb to OCbb. We also added discussion of emission source profiles, which exhibit substantial variability in the ratio OCbb/Kbb across source types, and the implications of this variability for seasonal variation in OCbb and for the uncertainty in our computed OCbb concentrations.

We have added a clarifying statement in the proposed revision that the calculation of nsK assumes that the ratio of K-to-Si is the same in the coarse and fine modes. This assumption appears to us to be supported by Figures S7 and S8. Both show a strong correlation between coarse K and Si. In the fine mode, the relationship is bimodal. One limb shows that fine K vs. Si falls exactly on the line defined by coarse K vs. Si. A second limb shows higher fine K concentrations especially occurring at lower-than-average fine Si concentrations. As originally noted, we excluded high nsK values occurring July 4 – 5 and Jan 1 – 2, apparently associated with holiday fireworks.

<u>Section 3.4</u> (PCA). We have added subheadings and the suggested comparisons in the proposed revision. We also provide additional interpretations to link our factors to AMS components. We clarify that our combustion factor embodies post-emission shifts in

phase and chemistry and is not HOA identified with AMS measurements, nor should it be considered as simply POA. The combustion factor describes origins, not oxidation state or degree of aging. It tends to compare in magnitude to AMS HOA, BBOA, COA (when one or more such factors are found) and portions of MO-OOA, as would be expected to the extent that MO-OOA includes oxidized motor-vehicle exhaust, other anthropogenic combustion emissions, or biomass burning.

Our sulfate OC factor is clearly related to the isoprene OA factor found by AMS. Although our mean contributions do not always agree (possibly because SEARCH and AMS mean OC concentrations sometimes differ), the quantitative relationship of our sulfate OC factor to SO_4 is the same as the relationship between isoprene OA and SO_4, which Xu et al. (2015a; b) reported as 0.42 $\mu g\ m^{-3}$ isoprene OA per 1 $\mu g\ m^{-3}$ SO_4. Based on their reported OM/OC for isoprene OA (1.97), their result is 0.21 $\mu g\ m^{-3}$ isoprene OC per 1 $\mu g\ m^{-3}$ SO_4. For CTR (2008 – 2013, n = 383 days), we obtain 0.216 (± 0.008, 1 SE) $\mu g\ m^{-3}$ sulfate-associated OC per 1 $\mu g\ m^{-3}$ SO_4 (PCA1), 0.190 (± 0.004, 1 SE) $\mu g\ m^{-3}$ sulfate-associated OC per 1 $\mu g\ m^{-3}$ SO_4 (PCA2), 0.213 (± 0.003, 1 SE) $\mu g\ m^{-3}$ sulfate-associated OC per 1 $\mu g\ m^{-3}$ SO_4 (PMF1), and 0.211 (± 0.001, 1 SE) $\mu g\ m^{-3}$ sulfate-associated OC per 1 $\mu g\ m^{-3}$ SO_4 (PMF2) (PMF1 and PMF2 modeling approaches differ only in the weights used for the fitting species).

One of the differences between PCA1 and PCA2 is that PCA1 uses potassium ion measurements (available beginning 2008), whereas PCA2 uses the calculated Kbb (available for the whole record).

The revised text provides further explanation.

<u>Referee 2</u>

<u>Comment "A"</u> (clarify terminology and acknowledge interaction between biogenic and anthropogenic emissions). Our appendix was an attempt to conceptually acknowledge and document methodological and terminological differences. We have now expanded the introduction and clarified the interpretation of the PCA nomenclature relative to conventional use of OC and EC source terminology (please see proposed revision for

new material). Our seasonal (ozone) and sulfate PCA factors correspond within error to previous work that has linked biogenic and anthropogenic emissions. We have prepared a comparison to the manuscripts of Xu et al. (2015a, b), which appear consistent with our results. We link our sulfate factor to the isoprene SOA identified by Xu et al. (2015a, b), and we link our seasonal factor to the LO-OOA factor. The comparisons are provided in the proposed revised text.

Our combustion OC factor is identified through its correlation with CO, EC, and NO_x. This factor doesn't correlate with sulfate. (We aren't sure why the referee listed sulfate and SO_2 as part of the combustion component, as our results do not show either SO_4 or SO_2 as components of the combustion factor. We hope that our revision of the section on PCA will be clear about these distinctions). As noted, there is a separate sulfate OC factor that is consistent with the AMS isoprene OA factor. Our combustion OC factor is not linked with either isoprene or nitrate SOA, nor is it equivalent to HOA identified by AMS or to POA. It is an emission source-related factor, not a composition-based factor. We conclude that the combustion factor includes both fresh emissions and more aged and oxidized OA, all deriving from sources that co-emit CO, EC, NO_x, and, possibly, VOCs. The factor represents an observable association among combustion emissions notwithstanding the evolution of those emissions via atmospheric processes. We hope that the new comparisons and text will clarify this result.

Comment "B" (link calculated OM and biomass burning estimates to other SOAS study results). As indicated in the revised text, we provide an additional comparison of our calculated OM to the OA and OM/OC published by Xu et al (2015a, b). We also compare our biomass burning OC (OCbb) to AMS BBOA estimates and estimate uncertainties for our OCbb.

Comment "C" (context and perspective). We had previously placed most of this material in appendix. We have revised the introduction to summarize historical advances in understanding carbonaceous aerosol and have added to the supplement a table summarizing 19 studies in the SEARCH area that provide data from various types of measurements and analyses. We also note in the revised appendix the ambiguities associated with intercomparisons, both in terms of atmospheric processes and emissions, and the methods of measurement of OC components. In the latter case, comparison of observations from different sampling and analytical procedures, as well as differences in time duration from short-term campaigns to long-term averaging, would lead one to expect differences rather than exact correspondence of results.

Comment “D” (PCA exposition). Both reviewers indicated that this section was difficult to follow. We revised the text with subheadings and provided more interpretation of the PCA factors. We could not find a way to shorten this section and still provide insightful description and interpretation of the results. The PCA results are compared with the other methods and the comparison is included in the proposed revision. In the submission, the PCA results were presented in tabular form in the text, rather than as figures. Table 2 identifies the most important species associations and shows the consistency of these associations across the eight sites and two PCA applications. Table 3 lists the mean OC concentrations associated with each PCA factor. We have augmented these two tables with two new tables in the main text. New Table 4 summarizes the range of results obtained across alternative PCA (and PMF) applications. We use these comparisons to assess uncertainty. New Table 5 compares results across methods, so that the PCA apportionments can be compared with other approaches. We appreciate the diagnostic value of good figures. For example, we have examined time series of 2013 data and PCA apportionments to identify the dates when network-wide crustal OC appeared along with elevated concentrations of Al, Si, and Fe. We also examined back-trajectories for these dates.

Comment “E” (emissions summary). We are moving this section to the beginning of “Results and Discussion” to better provide the emissions context for the manuscript. We extend previous CMB receptor modeling results to 2013 (and note this in the revised text) and use the CMB results in the summary comparison of methods to show areas of agreement and disagreement. As noted by the reviewer, the CMB receptor model and the correlations of ambient trends with emission trends are inherently linear. Nonetheless, linearity explains most of the relation between emission trends and ambient trends on an annual-average basis. Even ozone appears linear in relation to ambient NO_2 concentrations when considering the annual 4th-highest ozone in relation to annual-average NO_2 (Hidy and Blanchard, 2015). We agree that nonlinearity should generally prevail between precursors and both O_3 (Blanchard et al., 2010; 2014) and SOA at finer temporal resolution.

Detailed comments. Table 1 appears to have suffered in the conversion from Word to PDF – those “x” symbols were “plus-and-minus” symbols. We will correct that problem.

OC correlates with both EC and SO_4, but for different reasons (common emission sources in the case of EC and chemistry in the case of SO_4). Consequently, EC and SO_4 also correlate, but not as strongly and not as consistently across time scales. We think our concluding statement in this section is justified (“In summary, the EC and OC measurements indicate influence of multiple emission sources or atmospheric processes affecting all SEARCH sites, though differently at urban and rural locations.”).

We have added uncertainty analyses to both sections 3.2 and 3.3, as discussed above, in the proposed revised manuscript.

The supplement figures are improved for readability.

We have revised the discussions of retene and PCA with VOC species as suggested.

Response References

Blanchard, C., Tanenbaum, S., and Hidy, G. NMOC, ozone and organic aerosol in the southeastern states. 1999-2007. 2. Ozone trends and sensitivity to NMOC emissions in Atlanta, Georgia. *Atmos. Environ*., 44, 4840-4849, 2010.

Blanchard, C. L., Tanenbaum, S., and G. Hidy. Ozone in the southeastern United States: An observation-based model using measurements from the SEARCH network. *Atmos. Environ.* 48: 192-200, 2014.

Bougiatioti, A., Stavroulas, I., Kostenidou, E., Zarmpas, P., Theodosi, C., Kouvarakis, G., Canonaco, F., Prévôt, A. S. H., Nenes, A., Pandis, S. N., Mihalopoulos, N.: Processing of biomass-burning aerosol in the eastern Mediterranean during summertime, *Atmos. Chem. Phys.*, 14, 4793–4807, www.atmos-chem-phys.net/14/4793/2014/, doi:10.5194/acp-14-4793-2014, 2014.

Hidy, G. and Blanchard, C.: Precursor reductions and ground-level ozone in the continental United States. *J. Air Waste Manage*., 65, DOI. 10.1080/10962247.2015.1079654, 2015.

May, A., Saleh, R., Hennigan, C., Donahue, N., and Robinson, A.: Volatility of organic molecular markers used for source apportionment analysis: measurements and implications for atmospheric lifetime, *Environ. Sci. Technol*., 46, 12435-12444, 2012.

Effects of Emission Reductions on Organic Aerosol in the Southeastern United States

C. L. Blanchard[1], G. M. Hidy[2], S. Shaw[3], K. Baumann[4], E. S. Edgerton[4]

[1] Envair, Albany, CA, USA

[2] Envair/Aerochem, Placitas, NM, USA

[3] Environmental Sector, Electric Power Research Institute, Palo Alto, CA, USA

[4] Atmospheric Research and Analysis, Cary, NC, USA

Correspondence to: C. L. Blanchard (cbenvair@pacbell.net)

Abstract

Long-term (1999 to 2013) data from the Southeastern Aerosol Research and Characterization (SEARCH) network are used to show that anthropogenic emission reductions led to important decreases in fine particle organic aerosol (OA) concentrations in the southeastern U.S. On average, 45% (range 25 to 63%) of the 1999 to 2013 mean organic carbon (OC) concentrations are attributed to combustion processes, including fossil fuel use and biomass burning, through associations of measured OC with combustion products such as elemental carbon (EC), carbon monoxide (CO), and nitrogen oxides (NO_x). The 2013 mean combustion-derived OC concentrations were 0.5 to 1.4 μg m^{-3} at the five sites operating in that year. Mean annual combustion-derived OC concentrations declined from 3.8 ± 0.2 μg m^{-3} (68% of total OC) to 1.4 ± 0.1 μg m^{-3} (60% of total OC) between 1999 and 2013 at the urban Atlanta, Georgia, site (JST) and from 2.9 ± 0.4 μg m^{-3} (39% of total OC) to 0.7 ± 0.1 μg m^{-3} (30% of total OC) between 2001 and 2013 at the urban Birmingham, Alabama, site (BHM). The urban OC declines coincide with reductions of motor vehicle emissions between 2006 and 2010, which may have decreased mean OC concentrations at the urban SEARCH sites by > 2 μg m^{-3}. BHM additionally exhibits a decline in OC associated with SO_2 from 0.4 ± 0.04 μg m^{-3} in 2001 to 0.2 ± 0.03 μg m^{-3} in 2013, interpreted as the result of reduced emissions from

industrial sources within the city. Analyses using non-soil potassium as a biomass burning tracer indicate that biomass burning OC occurs throughout the year at all sites. All eight SEARCH sites show an association of OC with sulfate (SO_4) ranging from 0.3 to 1.0 µg m^{-3} on average, representing ~25% of the 1999 to 2013 mean OC concentrations. Because the mass of OC identified with SO_4 averages 20 to 30% of the SO_4 concentrations, the mean SO_4-associated OC declined by ~0.5 to 1 µg m^{-3} as SO_4 concentrations decreased throughout the SEARCH region. The 2013 mean SO_4 concentrations of 1.7 to 2.0 µg m^{-3} imply that future decreases in mean SO_4-associated OC concentrations would not exceed ~0.3 to 0.5 µg m^{-3}. Seasonal OC concentrations, largely identified with ozone (O_3), vary from 0.3 to 1.4 µg m^{-3} (~20% of the total OC concentrations).

1 Introduction

In much of North America, organic aerosol (OA) represents approximately half of average $PM_{2.5}$ mass concentrations in ambient air (Kanakidou et al., 2005). OA derives from primary source emissions and secondary atmospheric processes involving reactions of volatile organic compounds (VOCs) of anthropogenic and natural origins (see appendix). The latter is widely recognized in the southeastern U.S. with its potential source of VOCs from dense vegetation (Hand et al., 2012). Initial speculation about secondary organic aerosol (SOA) in the Southeast from natural terpenoid compounds dates back to 1991 (e.g., Pandis et al., 1991). With re-evaluation of particle yields from isoprene acidic-photochemical oxidation in smog chambers, interest in natural SOA focused on this species (e.g., Kroll et al., 2006). The early 2000s investigations involving isoprene and terpenoids identified chemical mechanisms hypothetically applicable in the ambient atmosphere as well as tracers for reaction products (e.g. Hallquist et al., 2009). These hypotheses included accounting for the effect of acidity and photochemical linkages with the gas and condensed phases; a part of this chemistry involves the interactions with inorganic acids in the atmosphere—sulfur and nitrogen oxides, SO_2 and NO_x. More recently, field studies have adopted measurements from aerosol mass spectrometry combined with gas chromatograph and mass spectroscopy to track indicator species for SOA components, including species associated with isoprene- sulfur oxide or nitrogen oxide photochemistry (e.g., Gao et al., 2006; Surratt et al, 2007; Hatch et al., 2011a,b; Budisulistiorini et al., 2013; Liao et al., 2015; Lin et al., 2013; 2014; Hu et al., 2015; Kim et al., 2015; Xu et al., 2015a, b).

In parallel with advances in organic aerosol chemistry, workers explored different indirect means of estimating SOA from VOC sources. In Atlanta, Lim and Turpin (2002) used the carbon tracer method to calculate summertime SOA concentrations from collected filter samples. In the Southeast, Zheng et al. (2002; 2006) used chemical tracers extracted from filters to identify primary OA, noting that an incomplete mass balance could be SOA. Kleindienst et al. (2007; 2010) and Lewandowski et al. (2013) used chemical tracers to estimate SOA from isoprene and terpenes. The carbon tracer method was expanded for natural species using carbon isotopes (e.g., Lewis et al., 2004; Tanner et al., 2004; Zheng et al., 2006; Ding et al., 2008). The empirical approaches were explored further by Yu et al. (2007) and Blanchard et al. (2008). Identification of water-soluble carbon as an SOA indicator also has been used (e.g. Weber et al., 2007). The various evolving methods have provided operationally defined OA as indicated schematically in Figure S1.

The characterization of SOA in the Southeast is complicated by OA from open burning of vegetation (e.g., Zhang et al., 2010; Hu et al., 2015). Like other combustion sources, wildfires and prescribed burning appear to be important components of OA and SOA (e.g., Zhang et al., 2010; Hidy et al., 2014; Washenfelder et al., 2015). OA composition in the southeastern U.S. provides indications of emission source origins, but results have not been consistent across studies (Table S1). SOA particularly is known to be a complex description of emissions, followed by evaporation, condensation, and chemical interactions during species aging in the atmosphere.

The ambiguities in accounting for OA sources and the chemistry of SOA helped motivate a major suite of field experiments during the summer of 2013, the Southern Oxidant and Aerosol Study (SOAS) (SOAS, 2014) and associated campaigns that comprised the Southeast Atmosphere Study (SAS) (SAS, 2014). Ground-level measurements were located at rural sites, with many studies situated at a Southeastern Aerosol Research and

Characterization (SEARCH) network monitoring location outside Brent, near Centreville, Alabama (CTR) (e.g., Hu et al., 2015; Isaacman-VanWertz et al., 2015; Nguyen et al., 2015; Washenfelder et al., 2015; Xu et al., 2015a; b), a site estimated to be regionally representative (Hidy et al., 2014).

CTR and other SEARCH sites offer a long-term record of trace-gas and particle observations (Hidy et al., 2014) that provide insight into the effects of anthropogenic emission reductions on organic aerosol trends in the southeastern U.S. The SEARCH record complements the six-week-long SAS and SOAS investigations of key atmospheric processes and chemical reactions. Specific questions relevant to SOAS and SAS goals that can be addressed using the SEARCH data include:

1. What fraction of measured organic carbon (OC) was emitted by combustion processes, such as motor vehicle exhaust and biomass burning? How has this fraction responded to emission reductions?

2. Over a long period of record, can the fractions of OA directly emitted in the condensed phase (primary organic aerosol, POA) and of SOA formed in the atmosphere via reactions of gaseous or condensed-phase precursors be quantified or constrained based on diurnal, seasonal, and annual variations of OC, elemental (or black) carbon (EC), ozone (O_3), sulfate (SO_4), and other aerometric measurements? How have inferred SOA concentrations responded to emission reductions?

3. Do the long-term gas and particle measurements indicate how much biogenic SOA is present on daily, seasonal, or annual time scales? How has SOA of biogenic origins been affected by anthropogenic emission reductions?

This paper describes analyses of aerometric data from CTR and the other SEARCH sites that address these questions. We apply five complementary data analysis methods that provide insight into the sources of aerosol carbon in the Southeast relying on the long-term SEARCH database. Because uncertainties and differences among previous studies have been challenging to resolve due to inconsistent or ambiguous definitions and terminology used to describe carbon measurements, an appendix defines terminology and identifies unresolved questions. We adopt in part the concepts of aerosol evolution from initial emission to multiscale ambient conditions postulated by Robinson et al. (2007), noting accompanying uncertainties (e.g., Murphy and Pandis, 2010).

2 Methods

The data for this study of aerosol carbon derive primarily from long-term SEARCH measurements obtained from up to eight operating sites, comprising four urban-rural or urban-suburban pairs, between 1999 and 2013 (e.g., Hansen et al, 2003; Atmospheric Research and Analysis [ARA], 2014; Hidy et al., 2014). The dataset includes particle mass concentrations and composition, gases, and meteorological parameters (ARA, 2014) as previously described in Hansen et al. (2003) and Edgerton et al. (2005; 2006). Special data from ancillary experiments in the SEARCH network supplement the long-term data. We also use emission data derived from the EPA National Emission Inventory (NEI), augmented as described in Blanchard et al. (2013) and Hidy et al. (2014).

Multiple empirical methods are employed to understand OA sources and SOA formation in the southeastern U.S., utilizing the SEARCH data to obtain a multi-year and multi-season interpretation. The methods are: (1) comparison of observations with augmented NEI emission estimates (Hidy et al., 2014) and receptor model predictions based on the NEI, (2) comparison and correlation of measured OC with EC concentrations and use of the OC/EC ratios as indicators of combustion-related emissions and SOA formation, (3) computation of organic mass (OM)/OC ratios utilizing $PM_{2.5}$ mass and sums of species concentrations as evidence for the presence of oxidized OA, (4) estimation of biomass burning contributions to measured EC and OC using biomass burning tracers, and (5) application of receptor modeling (principal component analysis, PCA, supplemented with comparisons to positive matrix factorization, PMF) to identify and quantify atmospheric processes affecting OA concentrations. Computational details are described within the results and discussion section and in the supplemental information.

3 Results and Discussion

3.1 Emission sources and the relation of ambient to emission trends

This section incorporates previously published analyses by reference, extends them through 2013, and integrates findings. Results related to emission changes are compared with those obtained using other approaches in Section 3.6 (Synthesis).

Southeastern emissions in 2013 are shown by source category in Table S2; comparison with 2008 emissions reported in Blanchard et al. (2013) indicates reductions since 2008. Statistically significant ($p<0.001$) relationships were found between mean annual $PM_{2.5}$ EC and OC concentrations at SEARCH sites and $PM_{2.5}$ EC and OC emissions between 1999 and 2013 (Hidy et al., 2014). Ambient EC trends were significantly related to both mobile source and total EC emissions, whereas ambient OC trends were significantly related to mobile source OC emissions but not to total OC emissions (Hidy et al., 2014). $PM_{2.5}$ EC emissions in the southeastern U.S. declined by approximately half between 1996 and 2013 due to reductions of on-road and non-road motor vehicle emissions (Hidy et al., 2014). Corresponding declines occurred in on-road and non-road motor vehicle $PM_{2.5}$ OC emissions, but total $PM_{2.5}$ OC emissions showed little trend due to the dominance of relatively constant biomass burning emissions (Hidy et al., 2014). Mobile source OC emissions represent less than 10% of OC emissions in the Southeast (Blanchard et al., 2013; Hidy et al., 2014) and only 4% as of 2013 (Table S2), with biomass burning accounting for ~75% of OC emissions in emission inventories.

Using a receptor modeling approach, Blanchard et al. (2013) showed that $PM_{2.5}$ EC emissions generally account for reported mean annual EC concentrations and trends in the SEARCH network (Figure S2). Although the receptor model overpredicted EC concentrations at the Jefferson Street (JST) site in Atlanta, Georgia, and underpredicted EC concentrations at other sites, the EC trends predicted by the model from the inventory agreed with observed EC trends. Larger observed ambient EC decreases at SEARCH sites coincided with an EC emission decline occurring between 2005 and 2013 that resulted from new Environmental Protection Agency (EPA) standards for diesel engines and fuels (effective in 2007 for on-road vehicles, in mid-2010 for non-road mobile sources, and in mid-2012 for rail and marine sources) (Hidy et al., 2014). Mobile sources account for over 50% of EC emissions in the Southeast prior to 2007 (Blanchard et al., 2013) and decline to ~40% by 2013 (Table S2), so ambient EC concentrations are expected to decrease with declining mobile source EC emissions.

Contrasting with results for EC (as well as CO, NO_x, and SO_x), greater differences between receptor model-predicted OC and measured OC trends were observed (Figure S3). These differences occurred even when comparing model predictions to the fraction of measured OC that was not associated with O_3 and SO_4 (inventory OC emissions do not represent SOA deriving from biogenic emissions of isoprene and other gases). Ambient OC trends were more pronounced than trends predicted by the model from the inventory (Figure S3). However, the receptor model reproduces observed OC trends more readily for sites where the mobile source contribution is greatest (Figure S3). Receptor-modeling studies have consistently identified mobile source contributions to ambient $PM_{2.5}$ mass concentrations in Atlanta and Birmingham (e.g., Zheng et al., 2002; 2006; Baumann et al., 2008; Lee et al., 2009); a recent analysis indicated that mobile sources contributed 0.8 to 2.8 $\mu g\ m^{-3}$ to 2006 – 2010 $PM_{2.5}$ mass concentrations (between 6 – 7% and 19 – 21% of $PM_{2.5}$ mass) in Atlanta and Birmingham (Watson et al., 2015). Measured ambient concentrations of non-polar $PM_{2.5}$ OC species associated with motor vehicles, such as hopanes and steranes, declined substantially (>50 %) at BHM and JST between 2006 and 2010, linking mobile source emission reductions during those years with observed decreases in urban OC concentrations (Blanchard et al., 2014a). As noted in the appendix, emitted OC is not conservative, but is affected by evaporation and possibly recondensation as secondary species, or by augmentation by SOA derived from gas-phase emissions. A possible explanation for the observed OC trends is that diesel SOA concentrations (which were not incorporated in the receptor model predictions) were greater prior to adoption of new diesel emission regulations beginning in 2007. In addition, changes in gasoline-engine SOA concentrations may have occurred. Reductions of SO_2 emissions are also thought to have changed SO_4-associated SOA concentrations over time (Xu et al., 2015a, b), but the chemical mass balance (CMB) model is set up to predict OC that is not associated with O_3 and SO_4 (Blanchard et al., 2013).

Trends in mobile source VOC emissions paralleled trends in mobile source $PM_{2.5}$ OC and EC emissions (Hidy et al., 2014; Blanchard et al., 2013). Similar to OC emissions, mobile source VOC emissions in the southeastern U.S. declined by approximately half between 1996 and 2013 due to reductions of on-road and non-road motor vehicle emissions (Hidy et al., 2014), but total VOC emissions showed little trend due to dominance by relatively constant VOC emissions from vegetation and soils (Table S2).

In summary, emission trends partially explain observed ambient EC and OC trends. For OC, the link between inventory emissions and ambient concentrations is less definitive than is the case for links between reductions of EC, CO, NO_x, and SO_2 emissions and observed trends in ambient EC, CO, NO_y, SO_2, and $PM_{2.5}$ SO_4 concentrations (Hidy et al, 2014).

3.2 Ambient EC and OC concentrations and trends

Trends and spatial variations are evident for mean annual and seasonal EC and OC concentrations (Table 1 and Figure 1). Mean EC concentrations were 2.0 to 3.5 times greater at JST than at CTR, thereby indicating two- to three-fold greater influence of combustion sources within Atlanta compared to rural CTR because EC is a tracer of combustion (appendix). Mean OC concentrations were 1.0 to 1.8 times greater at JST than at CTR, indicating urban sources of OC possibly superimposed on a relatively high regional baseline. The ratio of JST EC to CTR EC declined from 2.8:1 to 2.1:1 between the first and third five-year periods, while the JST OC to CTR OC ratio decreased from 1.5:1 to 1.2:1 between the first and third five-year periods. Since the ratio of JST EC/CTR EC declined by 25% and the ratio of JST OC/CTR OC declined by 20%, the decreases are comparable but the difference is consistent with a greater mobile source influence at JST than at CTR. Both EC and OC concentrations exhibit decreasing trends at all SEARCH sites (Hidy et al., 2014), particularly after 2007 but with a possible rise between 2009 and 2011 (Figure 1). Higher mean monthly concentrations in 2011 were followed by further decline in 2012 and 2013 (Figure 1). Whereas long-term ambient EC and OC trends are predicted by EC and OC mobile source emission reductions (Section 3.1), changes between 2008 and 2013 are predicted from the emission inventory for EC (Figure S2) but not for OC (Figure S3).

No season consistently exhibits the highest mean EC and OC concentrations but the CTR mean OC concentrations and OC/EC ratios are highest during summer, interpreted as the influence of aging and SOA formation during warmer months. In contrast, JST mean OC and EC concentrations tend to be higher during autumn and winter (Table 1). In 2013, the ratios of OC to total carbon (TC = EC + OC) in daily-average filter samples were greatest at CTR during the SOAS campaign (Figure S4). This result suggests that rates of SOA formation at CTR during SOAS exceed SOA formation rates at other sites in the region and at other times of the year. The differences between JST and CTR mean summer OC concentrations decline from 1.1 μg m^{-3} in 1999-2003 to less than 0.1 μg m^{-3} in 2009-2013, interpreted as reductions of urban OC concentrations toward a regional baseline level (Table 1).

Mean OC/EC ratios are higher at CTR than at JST, again consistent with regional-scale aging of ambient aerosol and a relatively greater influence of SOA at CTR. The period mean OC/EC ratios at JST range from 2.3:1 to 4.0:1, suggesting variable contributions from multiple sources. For comparison, typical OC/EC ratios are ~1 in freshly emitted motor vehicle emissions (Chow et al., 2004), with important differences among vehicle types (McDonald et al., 2015), ~5:1 – 20:1 in near-source biomass burning plumes (Andreae et al., 1996; Andreae and Merlet, 2001; Hobbs et al., 1996; Lee et al., 2005), and potentially much greater than unity as oxidation and SOA formation proceed (Robinson et al., 2007).

Temporal trends in ambient EC and OC correlated within individual sites and across the SEARCH domain (e.g., CTR and JST, Figure 1), indicating regional coherence of trends and seasonal variations for both EC and OC. The strong correlation of EC and OC at all SEARCH sites, averaging times (annual, seasonal, monthly, daily), and seasons (Table S3; Figure S5) indicates that combustion processes are a major source of OC. However, significant correlations of SO_4 with both EC and OC during summer suggest the influence of SO_4 on SOA formation in summer, consistent with results from SOAS (Xu et al., 2015a, b; Budisulistiorini et al., 2015). OC correlates with both EC and SO_4, but for different reasons. Consequently, EC and SO_4 also correlate, but not as strongly and not as consistently across time scales. In summary, the EC and OC measurements indicate influence of multiple emission sources or atmospheric processes affecting all SEARCH sites, though differently at urban and rural locations.

3.3 OM/OC ratios

More oxygenated OA has higher ratios of OM/OC, so OM/OC potentially serves as an indicator of atmospheric aging (Turpin and Lim, 2001). A low value (e.g., OM/OC ~ 1.4 to 1.6) suggests little aging (i.e., POA is a large fraction of OA), whereas a high value (e.g., > 2) suggests more aging (SOA is a large fraction of OA). For comparison, OM/OC ratios are 1.2 for pentane (and higher molecular weight alkanes), 1.1 for isoprene, and 2.0 for isoprene epoxydiol (IEPOX) (a gas-phase intermediate of isoprene oxidation, yielding SOA). The average motor vehicle OM/OC ratio is ~1.2 to 1.4 (Landis et al., 2007) while biomass burning OM/OC averages ~1.4 to 1.8 (Reid et al., 2005).

We estimate the OM/OC ratio for the urban and rural SEARCH sites using a mass balance computation based on particle composition. The sum of species concentrations, including estimated particle-bound water (PBW) at laboratory temperature and relative humidity (RH), is:

$$\textit{Sum of species} = f_1 \bullet SO_4 + f_2 \bullet NO_3 + f_3 \bullet NH_4 + EC + OC + MMO + Na + Cl \qquad (1)$$

(inorganic species concentrations are from ion measurements). PBW at laboratory RH of < 38% is represented by the coefficients f_1 (1.28), f_2 (1.15), and f_3 (1.25) (Tombach, 2004, as derived from Tang et al., 1996). The coefficient f_1 is an average of the coefficients for NH_4HSO_4 (1.27) and $(NH_4)_2SO_4$ (1.29), f_2 is the coefficient for NH_4NO_3, and f_3 is a weighted average reflecting higher SO_4 than NO_3 concentrations. MMO is the sum of the concentrations of six crustal elements (Al, Ca, Fe, Mg, Si, Ti) (x-ray fluorescence [XRF] spectroscopy measurements), expressed as oxides (Hansen et al., 2003). This estimate of crustal mass is likely conservative, since it does not include Mn and the assumed Ca mass (as CaO) would be less than the mass of $CaCO_3$ (if present). The carbon components, metals, and chloride are not adjusted for retained water at laboratory temperature and humidity. This creates a potential for uncertainty in the calculation, especially in the case of OC. Atmospheric OC is known to be hygroscopic at elevated humidity, but experimental data suggest that water retention is minimal at < 38% RH for laboratory filter analysis (e.g., Malm et al., 2005; Taylor et al., 2011). Measurements made during SOAS indicate that organic-associated water was less than ~25% of total particle water in mid-day ambient samples when ambient RH was less than ~50% (Guo et al., 2015). We estimate an OC PBW uncertainty in Eq. (1) by assuming that OC PBW is 10% of OC ($f_{OC} = 1.1$), which would increase the calculated sum of species by 3% and decrease the OM/OC (calculated below) by 0.1 units on average.

The difference between $PM_{2.5}$ mass and the sum of species concentrations is denoted as "non-measured" (NM) mass:

$$NM\ mass = PM_{2.5}\ mass - Sum\ of\ species \tag{2}$$

An upper bound for OM is calculated as OM* = OC + NM mass, which assumes that all NM mass is associated with OA. Any mass that is missing from the computed sum of species would bias NM mass high, thereby also causing OM* to be higher than the true OM. Similarly, underestimation of PBW would bias NM mass and OM* high. We estimate the combined effect of missing species and PBW to result in possible overestimation of OM*/OC by up to 0.2 units on average. An opposing bias potentially arises in Equation 2, because the FRM sampler that is used by SEARCH to provide the $PM_{2.5}$ mass measurement is known to lose volatile species (e.g., inorganic particle NO_3). We recalculated Equation 1 by replacing the measured NO_3 and Cl concentrations (which are the sum of a Teflon front filter and a nylon back-up filter located in the SEARCH PCM sampler) with the Teflon filter concentrations. The effect was to reduce the calculated sum of species, which then increased the calculated OM*/OC by 0.2 units on average. Therefore, we estimate the uncertainty in the calculated OM*/OC ratios as ± 0.2 units. If no PBW is associated with inorganic species (SO_4, NO_3, NH_4), Equation 1 would underestimate OM*/OC by 0.5 units on average. However, inorganic PBW is expected even at RH < 38%, so this potential bias appears less plausible than the documented bias in FRM $PM_{2.5}$ mass concentrations.

At all SEARCH sites, NM mass concentrations averaged 1.5 to 1.9 $\mu g\ m^{-3}$ (interquartile range ~0.5 to ~2.5 $\mu g\ m^{-3}$ at all except YRK) during the most recent five-year period (2009 to 2013; Na and Cl ions were not measured prior to 2008) (Figure S6). Daily NM mass correlated with daily OC to varying degrees: r^2 was 0.2 – 0.3 at Birmingham, Alabama (BHM), Gulfport, Mississippi (GFP), (rural) Oak Grove, Mississippi (OAK), and 0.4 – 0.5 at CTR, JST, (rural) Yorkville, Georgia (YRK), (suburban) Outlying Landing Field, Pensacola, Florida (OLF), and Pensacola, Florida (PNS). The average OM*/OC varied by site from 1.5 (BHM) to 2.0 (YRK) (Figure 2) (ΔOM*/ΔOC regression slopes of 1.6 to 1.9 without intercept terms, Figure S7), which suggests a regionally characteristic but spatially and temporally variable mix of less-oxidized and more-oxidized OA. The consistency of the mean values in the range of 1.5 to 2.0 (± 0.2) indicates that relatively fresh emissions contribute a major portion of OA at both urban and rural sites with variations in the degree of oxidation or SOA mass. However, higher OM*/OC and OM*/EC occur in the warmest months (Figure 2), consistent with seasonal SOA formation and the seasonal variations discussed above. Our mean OM*/OC is lower than reported in SOAS research – for example, mean CTR OM/OC of 2.16 from aerosol mass spectroscopy [AMS] measurements (Xu et al., 2015a). For identical sampling periods, our spring 2012 mean OM*/OC was 1.34 at JST and 1.80 at YRK, which is lower than mean OM/OC of 1.93 at JST and 1.98 at YRK reported by Xu et al. (2015b). Our winter 2012-13 mean OM*/OC was 1.51 at JST and 1.56 at YRK, which is higher than mean OM/OC of 1.40 at JST and 1.31 at YRK reported by Xu et al. (2015b). Comparisons are discussed further in Section 3.5.3.

3.4 Biomass burning

Emission inventories indicate that biomass burning, including prescribed burns, wildfires, agricultural burns, and domestic heating, is the largest source of $PM_{2.5}$ OC emissions in the Southeast on an annual-average basis (Hidy et al., 2014). Prescribed burns are the largest source of biomass burning OC emissions, again on an annual basis (Hidy et al., 2014). In the Southeast, prescribed burns are employed to manage roughly 4 million hectares (ha) (~10 million acres) of land every year, primarily between January and April; wildfires may occur year-round but are more frequent in warmer months (Wade et al. 2000; Haines et al. 2001). Nearby (e.g., ~ 10 km) biomass burning plumes are sometimes evident in CTR hourly data and substantially affect observed concentrations of EC, OA, CO, NO_y, NH_3, and O_3 (Figure S8). However, the cumulative effect of widespread and potentially wide-ranging biomass burning on long-term ambient OA concentrations is more difficult to determine. The available data record does not include organic biomass burning tracers, such as levoglucosan, except during special studies such as the six-week SOAS campaign. Alternatively, non-soil potassium (K) has been used as an indicator of biomass combustion in previous studies (Calloway et al., 1989; Lewis et al., 1988; Lewis, 1996; Pachon et al., 2010; 2013) and can be determined from K measurements reported in the long-term SEARCH data. Using a single tracer species to identify and quantify biomass burning contributions to ambient OA is subject to important uncertainties, and potassium is an imperfect tracer of biomass burning. Zhang et al. (2010), for example, showed that water-soluble K and levoglucosan correlate in winter (when more biomass burning occurs in the southeastern U.S.) but not in summer. However, levoglucosan and its associated AMS markers may persist in the atmosphere for less than a day (May et al., 2012; Bougiatioti et al., 2014). Instability of organic marker species could lead to differences in AMS biomass burning OA compared with estimates made using K as a tracer.

Non-soil K (nsK) is estimated from coarse PM (PM_{coarse} or PM_{crs}, PM between 2.5 and 10 μm) and $PM_{2.5}$ XRF measurements of K and Si following the K tracer approach of Pachon et al. (2013). Briefly, the method regresses measured K against species X concentrations: $K = \alpha + \beta * X$ (where X derives primarily from crustal material). Si measurements are used to represent the crustal species, X, because Si concentrations are routinely well above the limits of detection and the correlations of Si with Al and other known crustal elements indicate few or no interfering sources of Si. The correlations of PM_{coarse} XRF K and Si are very strong, with consistent values of the slope $\beta = \Delta K/\Delta Si$ of 0.10 to 0.13 and $r^2 \sim 0.8$ at all sites (Figures S9 – S11). These slopes therefore define the expected ratio of K/Si in crustal material in the region. The ratios are lower than, but consistent with, a value of 0.15 ± 0.01 reported for data from Phoenix, AZ (Lewis et al., 2003). In contrast to PM_{crs}, $PM_{2.5}$ measurements exhibit large excesses of K over the expected K/Si ratios, indicating the presence of one or more non-crustal sources of $PM_{2.5}$ K (Figures S9 to S11). For each plot, fine-particle K vs. Si forms one “branch” that falls on the line defined by coarse-particle K vs. Si, indicating similar relationships between K and Si within fine and coarse fractions of crustal PM. High fine-particle K concentrations also occur at lower-than-average fine Si concentrations. We apply the slopes β to compute nsK = K - β*Si from $PM_{2.5}$ data (Figure S9). The agreement between computed nsK and measured water-soluble K (K ion, KI; measured beginning 2008) supports the interpretation of non-soil K as an indicator of biomass burning K (Kbb) (which is water-soluble) at rural inland sites such as CTR (Figure S9). Although computed Kbb exceeds measured K ion concentrations by ~0.02 – 0.03 μg m^{-3} on average, the difference may relate to the differing resolutions and sensitivities of the XRF and ion measurements (Figure S9). Later analyses (Section 3.5.2) link CTR Kbb with species (including CO and EC) deriving from combustion. Possibly, both K ion and computed nsK could also have a marine origin at some coastal sites (e.g., OLF) or an industrial process origin at some urban sites (e.g., BHM). Detailed review of computed nsK indicated that all nsK > 0.4 μg m^{-3} occurred on or one day after the 4th of July and January 1 US holidays, and only at urban sites (Figure S11). This result appears to indicate fireworks as a source of nsK on such occasions. Other than samples from January 1 and 2 and from July 4 and 5, we identify nsK as biomass burning K (Kbb), recognizing some uncertainty in this identification for BHM and coastal sites. Since nsK can be computed from the XRF measurements of K and Si for the full SEARCH record (1999 to 2013), whereas K ion measurements commenced in 2008, we use nsK as our biomass burning tracer. After exclusion of obvious high-K events (holiday fireworks), our identification of nsK as an indicator of biomass burning (Kbb) could introduce a bias toward overestimation in the calculation of OCbb, discussed below, if other sources of water-soluble K are important.

The ratio of TC to Kbb (TCbb/Kbb) in biomass burning is known to vary widely among fire types (e.g., wildfires differ from prescribed burns) and among fire stages (e.g., temperature, or flaming vs. smoldering). The variability of emissions among and within fires implies that biomass burning tracers are more useful for estimating average impacts than for quantifying burn contributions during individual events. We use a single average scaling factor based on consideration of emissions information (Hidy et al., 2014), which we check using the correlation of modern C with non-soil K (Figure S12). Inventory annual average TCbb/Kbb for fires is in the range 28:1 – 36:1 (Blanchard et al., 2013). For fires (prescribed burns, wildfire, agricultural field burns) plus area sources (largely open burning from agricultural, construction, and yard waste), the 2013 ratio of TCbb/Kbb is ~ 23:1 (Table S2). The ratio varies among emission source profiles from lower values of 5:1 and 7:1 (solid waste combustion and agricultural burning, respectively) to an intermediate value of 19:1 (wildfire) and higher values of 43.5:1 (slash burning) and 61:1 (residential wood combustion) (EPA, 2015; Reff et al., 2009). Our assumed fixed scaling factor of 32 for TCbb/Kbb is similar to carbon isotope data from CTR winter samples (Figure S12, CTR regression slope $\Delta TC_{modern}/\Delta Kbb = 43$), when prescribed burns are more common and SOA formation rates are lower. The higher slope of $\Delta TC_{modern}/\Delta Kbb = 71:1$ at JST could reflect a different type of biomass burning (e.g., residential wood combustion), while the lesser correlation of modern TC with non-soil K (assumed to represent Kbb) at BHM and higher slope at PNS potentially reflect source variability or the confounding influence of industrial (BHM) or marine (PNS) sources of non-soil K. The mean ratio of wood-burning OC concentrations determined by Kleindienst et al. (2010) using organic tracers (20 samples, collected in May and August 2005, paired by site and date) to Kbb concentrations is 20:1 (varying by site from 16:1 at BHM and CTR to 18:1 at PNS and 29:1 at JST). This result agrees with the inventory TCbb/Kbb of ~ 23:1 averaged across fires and area sources (Table S2) assuming that the corresponding ratio of wood-burning TC/Kbb is ~10% higher than wood-burning OC/Kbb. Since prescribed burns and residential wood combustion (higher TCbb/Kbb) generally occur during winter months, whereas wildfires, agricultural field burns, and waste burning (lower TCbb/Kbb) may occur during warmer months, our assumed fixed scaling factor of 32:1 for TCbb/Kbb likely fails to capture some of the seasonal variability in TCbb. A higher scaling ratio (e.g., $\Delta TCbb/\Delta Kbb = 32$ rather than 20) would yield higher computed TCbb and therefore higher OCbb. Based on $\Delta OC/\Delta EC$ in actual biomass burning events observed at SEARCH sites (Figure S8), we compute OCbb = 0.9*TCbb (the ratio OCbb/TCbb could be higher in some burn events). Considering the range among SEARCH sites of winter $\Delta TC_{modern}/\Delta Kbb$ (22:1 to 82:1, Figure S12), the variability of TCbb/Kbb among source types, and the possibility that Kbb could be overestimated if there are sources other than biomass burning that contribute to nsK, we estimate the uncertainty range for OCbb as -50% to +100% (factor of two) subject to the constraint that OCbb < OC.

CTR monthly-average concentrations indicate a downward trend in OC but not in computed OCbb, so that OCbb has become a larger fraction of OC at CTR since 2007 (Figure 3). The absence of trend in computed OCbb reflects the absence of trend in measured K and computed nsK. OCbb tends to be higher in winter months, when prescribed burns are more common and residential heating needs are greatest, but OCbb is present during all seasons (Figure 3) and at all SEARCH sites (Figure S13). Retene, a tracer of coniferous wood combustion, is evident at the sites where it was measured (urban BHM and JST) with a pronounced seasonal cycle (Figure S14). This seasonality could indicate that the summer OCbb has been overestimated, or it could indicate that retene loss rates are greater during warmer months. Retene emissions from prescribed burning in the Southeast are highly variable and depend largely on the amount of softwood present in the fuel. Since historical fire suppression has led to the accumulation of significant amounts of hardwood in a thick midstory of pine-dominated forests (e.g. Provencher et al., 2001, Varner et al., 2005), retene is not considered a unique indicator for prescribed burning emissions in the Southeast.

The analysis of K measurements from the SEARCH data reinforces the conclusion that biomass burning is an important component of combustion-related OA in the SEARCH domain, at all sites and in all seasons. The contribution is especially important for regional-scale OA, as suggested by the CTR data. Uncertainties in the estimation procedure and scaling factors imply that our computed CTR mean OCbb (1.6 µg m^{-3}, 1999 – 2013 average) could be up to twice as high as the true mean OCbb concentration. If so, actual mean 1999 – 2013 OCbb would be 0.8 µg m^{-3}, which is higher than AMS mean biomass burning OA (10%, or ~0.25 µg m^{-3} OC) at CTR during the six-week SOAS period (Xu et al., 2015a, b). Although the majority of brown carbon aerosol mass during SOAS is attributed to biomass burning rather than to SOA, biomass burning did not contribute the majority of OA (Washenfelder et al., 2015). As previously noted, more biomass burning occurs in the southeastern U.S. during cooler months than during mid-summer (Zhang et al., 2010), so the SOAS campaign is expected to show less biomass burning than during other months. Reported AMS mean biomass burning OA concentrations were higher at JST (~0.5 µg m^{-3} OC during May and December 2012) and at YRK (~0.6 µg m^{-3} OC during December 2012 and January 2013) (Xu et al., 2015a, b).

Due to the loss of organic tracers on a time scale of about a day or less, the biomass burning OA that is estimated using AMS is thought to yield an estimate of relatively fresh burning as compared to aged regional burning levels (Xu et al., 2015a, b). Estimates of a regional pool of more aged biomass burning OA are not available. If the reported AMS biomass burning OA concentrations are, e.g., ~50% lower than the sum of fresh and aged biomass burning OA, the resulting sum (1 μg m^{-3} OC) would fall within our OCbb uncertainty range. The lack of long-term trend in OCbb (Figure 3) occurs regardless of scaling uncertainties (assuming constant scaling of OCbb to Kbb), because no trend exists in either K or Kbb concentrations.

3.5 Principal component analysis

Important insight into the origins of ambient aerosol can be obtained with multivariate statistical methods, such as principal component analysis (PCA), which is a well-established method for PM source apportionment (Dattner and Hopke, 1982). PCA generates mathematically independent groupings of measurements based on the correlations among the measured variables (classically, the groups are geometrically orthogonal to one another). The number of groups reproduces as large a fraction of the total variance of a data set as possible subject to optimization criteria, typically explaining ~75 to 80% of the variance of, e.g., ~20 to 25 air pollutant species concentrations with ~5 to 10 groups, also known as factors or components. Although PCA factors may be identifiable with emission sources in some applications, factors fundamentally represent correlations among species and potentially reflect a variety of aerometric processes (e.g., secondary species formation, meteorological effects). In our application, we interpret PCA factors as associations among species that are indicative of variations in the chemical environment, and refer to such species associations as components for brevity. A related methodology, positive matrix factorization (PMF) (U.S. EPA, 2014), differs in part from PCA in that PMF constrains factors to positive values. This constraint is physically realistic if PCA factors are interpreted as unique emission source contributions. The negative values permitted by PCA are in fact meaningful and informative if, in addition to emissions, factors represent a larger suite of physical and chemical processes (e.g., deposition; chemical loss processes; contrasts between inland versus marine air mass transport) as well as species origins.

3.5.1 Application

We report two main versions of PCA, with additional versions used for sensitivity tests and auxiliary information. ***PCA1*** is applied to measurements made at SEARCH sites from 2008 through 2013. The 23 gas and $PM_{2.5}$ measurements comprise daily-average concentrations of $PM_{2.5}$ EC and OC (thermal-optical reflectance, TOR), daily averages of gases NH_3 (measured continuously or at 24-hour resolution) and continuous NO_x and NO_z, secondary species (daily peak 8-hour O_3, plus $PM_{2.5}$ SO_4, NH_4, and NO_3), and $PM_{2.5}$ crustal elements (XRF measurements of Al, Si, and Fe), species associated with salts ($PM_{2.5}$ Na, Cl, Mg, and Ca ions), and trace metals ($PM_{2.5}$ Zn, Cu). Both daily averages and daily 1-hour-maxima of gases (CO and SO_2) are included to match the temporal resolution of the other daily data while also potentially capturing shorter-duration plumes. Water-soluble $PM_{2.5}$ K (K ion) is included as a potential indicator of biomass combustion. Because some species used in PCA1 were not measured throughout the 15-year SEARCH program, ***PCA2*** is carried out to interpret long-term OC trends from 1999 through 2013. PCA2 excludes measurements that commenced in 2008 (water-soluble Ca, Mg, K, Na, and Cl). XRF Ca and nsK are used instead of water-soluble Ca and K, respectively. Without Na and Cl in PCA2, salt is not detectable, as will be discussed. NH_3 is excluded from PCA2, since those measurements began in 2004. Daily-average O_3 is included in PCA2 to complement daily peak 8-hour O_3.

The sensitivity of our results to the choice of statistical method is examined by comparing PCA1 and PCA2 and by using additional PCA and PMF applications. As described in Section 3.5.3, the range of results obtained from PCA1, PCA2, other PCAs, and PMF is used to estimate uncertainty. The additional PCA applications are carried out by using special data, different suites of measurements, or different measurement periods. NMOC measurements made every day at JST from 1999 through 2008 are incorporated to generate ***PCA3*** as a modification of PCA2 (no ions and only XRF elements, and shorter time period). Alternate versions of PCA2 are carried out for 2004 – 2013 CTR data to see if factor loadings are robust and relatively insensitive to the choice of seasonal indicators

(***PCA4*** and ***PCA5***). The EPA PMF model (version 5; US EPA, 2014) was applied to the same CTR and JST measurements used in PCA2. PMF requires estimates of measurement uncertainty, which may be species-specific or even sample-specific. Two sets of uncertainty estimates were employed: uniform (10% of species concentrations) (***PMF1***), and species-specific (incorporating detection limits and species uncertainties of 5 to 25% of measured concentrations) (***PMF2***).

For PCA applications, the daily OC concentrations at each site are apportioned using daily PCA factor scores. The OC apportionment is carried out by multiple regression of daily OC concentrations against daily factor scores, retaining those that are statistically significant ($p < 0.05$). Since the PCA components are orthogonal, the regression coefficients are more stable than would be the case for multiple regression against various tracer species, which are typically intercorrelated. The PMF model generates source contributions internally.

3.5.2 PCA Components

PCA1 and PCA2 reveal consistent sets of species associations, resulting in 6 – 8 principal components at each SEARCH site (Table 2). For clarity, we designate the components as: (1) combustion, (2) crustal, (3) seasonal, (4) SO_2, (5) SO_4, (6) metals, (7) salt, and (8) other. These names are used as descriptors, rather than as designated emission sources. Component characteristics are discussed below. The full orthogonal solutions are shown in the supplement (Tables S4 to S11). The values in Tables S4 to S11 are the coefficients of the linear combinations of standardized species concentrations (daily concentration less mean divided by standard deviation); each tabled value is also the correlation (r) between a given species and a particular component. High (~1) or low (~ -1) values indicate high correlation or anti-correlation, respectively; both are meaningful. A value near zero indicates little or no correlation, so values in the range of ~-0.5 to 0.5 represent associations ranging from moderate anti-correlation (-0.5) to zero correlation to moderate correlation (0.5).

The OC apportionments indicate statistically-significant relationships between OC and four to seven PCA components (Tables S12 and S13). Mean contributions of each statistically-significant component to daily OC at each site using both PCA1 and PCA2 are summarized in Table 3; these contributions are expressed as percentages of total OC in Table S14. PCA1 and PCA2 each indicate that OC is associated with multiple components at all sites. Except at YRK and OLF (PCA2 only), the overall OC associations are strongest for the combustion component (Tables S4 to S11).

The PMF source profiles varied depending on the choice of uncertainty inputs, but yielded average OC apportionments that were qualitatively comparable to PCA2 (Figure S15). The PMF crustal OC and SO_4-associated OC concentrations were comparable to PCA (Figure S16). However, PMF source profiles combined CO and O_3, whereas PCA tended to separate O_3 from CO, leading to differences in the apportionment of OC to combustion and seasonal components (Figure S16). Differences between PCA and PMF occur in part because the PCA seasonal component generally comprised contrasts (e.g., positive O_3, negative inorganic particulate NO_3) whereas PMF forced positive solutions. In these applications, PCA predicted high OC concentrations more accurately than PMF did (Figure S17).

<u>Combustion</u>. All sites exhibit a suite of species associated with combustion processes (EC, OC, CO, Kbb or K ion, NO_x or NO_z). The variations in combustion associations among sites suggest different source mixes, differences in air mass ages (e.g., fresh emissions at urban sites, more aged emissions at rural sites), or differing transport of polluted air masses. For example, NO_z is more strongly associated than NO_x with the combustion component at the two most rural sites, CTR and OAK. OC associated with the combustion factor could therefore comprise material that would be classified as either POA or SOA by other analytical approaches (e.g., HOA or MO-OOA by AMS).

Mean combustion OC ranges from 0.7 to 1.6 $\mu g\ m^{-3}$ for PCA1 (2008 – 2013) and from 1.5 to 2.6 $\mu g\ m^{-3}$ for PCA2 (1999 – 2013), except at YRK (Table 3). Daily PCA1 and PCA2 combustion OC concentrations are correlated at all sites (Figure S18). Mean absolute differences between PCA1 and PCA2 computed combustion OC range from 0.1 to 0.7 $\mu g\ m^{-3}$ (not tabled). However, the mean PCA1 and PCA2 combustion OC concentrations are averaged over different time periods, so the differences in their averages are partly due to declining EC, CO, and NO_x concentrations (Table 1). Trends in

OC components are discussed in Section 3.4.4. Mean PCA2 combustion OC ranged from 25 to 63% of mean OC concentrations (Table 3).

Various combustion processes are expected to influence individual SEARCH sites to different degrees. CTR OCbb correlates significantly ($p < 0.0001$) with PCA1 and PCA2 combustion-associated OC ($r^2 = 0.54$ and 0.58, respectively, Figure S19a), suggesting that the combustion component at CTR is primarily associated with biomass burning. Whereas OCbb is computed from Kbb (Section 3.4), PCA1 and PCA2 combustion OC concentrations are determined from the principal component association of CO, EC, and either K ion (PCA1) or Kbb (PCA2) (Table S5). The association of K ion and Kbb with CO and EC at CTR links potassium with a combustion process. At BHM and JST, multiple regression of combustion OC against NO, gas-phase organic species (Blanchard et al., 2010), and non-polar OC compounds (including PAHs and iso/anteisoalkanes, or hopanes and steranes) (Blanchard et al., 2014a) indicates an association of fresh emissions (NO) and non-oxidized organic compounds with PCA combustion OC (Figure S19b). The urban PCA combustion factor associates CO, EC, and daily-average NO_x ; 1-hour maximum NO and non-oxidized organic compound concentrations were not used in determining either PCA1 or PCA2 (Tables S4 and S7). Urban PCA combustion OC is more likely attributable primarily to motor vehicle exhaust emissions than to biomass burning.

<u>Crustal</u>. A crustal component is present at all sites, associated with Al, Si, Fe, and, to varying degrees, Ca. At BHM, Fe associates more prominently with a metals component, consistent with previous studies indicating the impact of industrial facilities (including metals fabrication) on $PM_{2.5}$ at BHM (Baumann et al., 2008; Blanchard et al., 2014b).

The mean crustal-associated OC concentrations vary from 0.1 to 0.3 μg m^{-3} at inland sites (Table 3). Coastal sites exhibit non-significant, minor, or inverse associations of OC with crustal elements (-0.1 to 0.1 μg m^{-3}, Table 3). Inverse associations indicate that OC concentrations at coastal sites are lower than average when Al, Si, and Fe concentrations are elevated. PCA1 and PCA2 crustal OC concentrations correlate (Figure S20) and crustal OC correlates with Si (Figure S21). Crustal-associated OC could derive from region-wide phenomena (e.g., transport of Saharan dust), but may also stem from ubiquitous and widely distributed activities that suspend crustal material. Potential sources include soil-derived OC (e.g., agricultural activities, construction, or road dust), or biomass burning that lofts crustal material (e.g., through plowing material into debris piles). Road dust is known to include OC among its constituents (e.g., McDonald et al., 2013). There are two episodes with high crustal OC at CTR during June 2013. Elevated concentrations of Al, Si, and Fe co-occurred at all SEARCH sites during June 9 – 13 and June 23 – 28, 2013, thus suggesting region-wide events. Back-trajectory calculations indicate southerly air flow during these times. Trajectories arrived at CTR and JST after ~24 hours overland transport from the Gulf coast, whereas trajectories arrived at OLF from overwater transport. At other times, elevated concentrations of crustal elements occur at single sites, indicating more local events.

<u>Seasonal</u>. A seasonal component is present at all sites, but in two forms: positive O_3 and NH_3 (if measured), along with negative inorganic particulate NO_3, at BHM PCA2, CTR, GFP, JST PCA1, OAK, OLF, PNS, and YRK, or with reverse signs (e.g., relatively weak negative O_3) at BHM PCA1 and JST PCA2. As noted, sign reversals represent a change in coordinate directions and need not have physical significance; however, the association of OC with the seasonal component may differ depending on sign (discussed below). We denote this component "seasonal" rather than "photochemical." While this factor has photochemical properties, it is comprised of species with seasonality variations that result from multiple processes: emissions (NH_3), photochemistry (O_3), and temperature- and RH-sensitive thermodynamic equilibrium (inorganic particulate NO_3). The seasonal component evidently represents seasonal variations not otherwise described by the seasonal variations of the crustal, SO_4, and "other" components. Because of the strong connection of the seasonal component to O_3, seasonal OC is plausibly related to the LO-OOA component reported by Xu et al., (2015a; b). LO-OOA exhibits a strong diurnal pattern, with night maxima and day minima (Xu et al., 2015a; b). However, the LO-OOA diurnal variation is opposite to O_3 diurnal variations, which exhibit daytime maxima. Since PCA was applied to daily-resolution data, it is not possible to directly compare the PCA seasonal OC to time-resolved LO-OOA. We note that meteorological conditions that result in high peak daily O_3 concentrations (with higher seasonal OC concentrations) are also conducive to nitrate radical formation, which exhibits night-time maxima and is

associated with LO-OOA (Xu et al., 2015a; b). Further comparisons are provided in Section 3.5.3.

The mean PCA1 seasonal-component OC (OC associated with higher O_3, higher NH_3, lower NO_x, or lower $PM_{2.5}$ inorganic NO_3) ranges from 0.4 to 0.6 μg m^{-3} at all sites (e.g., 23% of OC at CTR, 13% at BHM and JST, 28% at OLF), except at YRK where the average is 1.0 μg m^{-3}. The positive association with O_3 suggests that this OC component represents SOA formation from either or both anthropogenic and biogenic precursors. PCA2 seasonal OC correlates with PCA1 seasonal OC, except at JST. The JST PCA2 seasonal OC shows an inverse correlation (Figure S22), indicating that the seasonal component represents higher winter (lower O_3, higher NO_3) OC concentrations, possibly pointing to an influence from domestic wood combustion for heating. The positive association of OC with O_3 is quantified within the JST PCA2 SO_4 component. The mean absolute differences between PCA1 and PCA2 seasonal-component OC concentrations range from 0.2 to 0.5 μg m^{-3}.

Sulfate. SO_4 and NH_4 are always associated and usually represented by a single component, denoted "SO_4." However, SO_4 and NH_4 are part of the seasonal component for PNS and YRK PCA2, suggesting that differentiation of the SO_4 and seasonal components is subject to uncertainty. O_3 is associated with both seasonal and SO_4 components.

All SEARCH sites show an association of OC with SO_4 ranging from 0.3 to 0.6 μg m^{-3} on average for PCA1 and from 0.5 to 1.0 μg m^{-3} on average for PCA2 (Table 3), with PCA2 SO_4 OC representing 15 to 44% of the 1999-to-2013 mean OC concentrations (15% at BHM; 22 – 25% at CTR, GFP, JST, and OAK; 44% at OLF). Mean PCA1 associations of OC with SO_4 were 14% of OC at CTR, 15% at BHM, 18% at OLF, 10% at JST, and 11% at YRK. PCA1 and PCA2 SO_4 OC concentrations are correlated (Figure S23) with mean absolute differences in PCA1 and PCA2 SO_4-associated OC concentrations of 0.2 to 0.5 μg m^{-3}; PCA2 did not separate the seasonal and SO_4 components at PNS and YRK (Tables S10 and S11). The mass of OC associated with SO_4 averages 20 to 30% of the SO_4 concentrations (Figure S24), so that SO_4-associated OC concentrations decline over time along with decreasing SO_4 concentrations. The presence and relative importance of SO_4-associated OC is consistent with research indicating the role of SO_4 in transferring isoprene gas-phase reaction products to the condensed phase (e.g., Surratt et al., 2007; Xu et al., 2015a; b). Seasonal variations, discussed below, also support biogenic origins of SO_4-OC. The quantitative relationship of our SO_4-associated OC factor to SO_4 is the same as the relationship between isoprene OA and SO_4, which Xu et al. (2015a, b) reported as 0.42 $\mu g\ m^{-3}$ isoprene OA per 1 $\mu g\ m^{-3}$ SO_4. Based on their reported OM/OC for isoprene OA (1.97), their result is 0.21 $\mu g\ m^{-3}$ isoprene OC per 1 $\mu g\ m^{-3}$ SO_4. For CTR (2008 – 2013, n = 383 days), we obtain 0.216 (± 0.008, 1 SE) $\mu g\ m^{-3}$ SO_4-associated OC per 1 $\mu g\ m^{-3}$ SO_4 (PCA1), 0.190 (± 0.004, 1 SE) $\mu g\ m^{-3}$ SO_4-associated OC per 1 $\mu g\ m^{-3}$ SO_4 (PCA2), 0.213 (± 0.003, 1 SE) $\mu g\ m^{-3}$ SO_4-associated OC per 1 $\mu g\ m^{-3}$ SO_4 (PMF1), and 0.211 (± 0.001, 1 SE) $\mu g\ m^{-3}$ SO_4-associated OC per 1 $\mu g\ m^{-3}$ SO_4 (PMF2).

$\underline{SO_2}$. The SO_2 component, present at all sites, identifies influences of relatively fresh plumes, whether from electric generating units (EGUs), industrial, or other SO_2 sources. At CTR, NO_x is more strongly associated with the SO_2 component than with the combustion component, consistent with relatively less aged plumes and more aged general combustion influence. Differences between urban and rural sites are evident; for example, OC at CTR and YRK is not significantly related to the SO_2 factors, but OC is related to the SO_2 factors at urban sites. This difference indicates the influence of SO_2 emission sources within urban areas, consistent with visual observations and measurements made near emission sources in Birmingham (Blanchard et al., 2014b).

OC associated with SO_2, indicative of fresh emissions, accounted for 0.07 to 0.37 $\mu g\ m^{-3}$ on average (12% of OC at BHM, 2% at JST, 7% at GFP, 20% at OAK, and 10% at OLF, none at other sites using PCA1) (Tables 3 and S14). PCA1 and PCA2 SO_2 OC concentrations are correlated (Figure S25).

Salt. A salt (or saltlike) component (of marine or other origins) is evidenced by Na, Cl, and Mg in PCA1. Na appears as a separate "other" component for JST PCA1, suggesting multiple urban sources of one or more of these species, while JST PCA1 "salt" is defined by K, Cl, and Mg. These species are not necessarily unique marine tracers; various combustion processes generate Cl emissions, for example.

Coastal sites show an inverse association of OC with Na and Cl (sea salt) (Table S14) and a negative mean OC contribution from salt (Table 3). We interpret this result as evidence that OC concentrations are lower at coastal sites when marine salt species concentrations are higher (i.e., anti-correlated), indicating that marine air masses are not an important source of OC. In contrast, mean salt-associated OC ranges from 0.14 to 0.15 μg m^{-3} (BHM and YRK) to 0.64 μg m^{-3} (JST). The species associations for the BHM and JST salt components suggest urban influences precluding identification of the salt component with marine air masses. Because K is associated with the JST "salt" component (and not with the JST combustion component) and Na is associated with the JST "other" component, it is possible that JST "salt" OC represents biomass combustion while the JST combustion component primarily represents motor vehicle exhaust.

Metals. Cu and Zn appear on a metals component at six sites (BHM, CTR, GFP [PCA2], JST [PCA2], OAK, and OLF [PCA2]); otherwise, Cu and Zn are associated with combustion or are split between the metals and "other" components. The Cu and Zn correlations range from r = 0.1 to 0.3 in the full 1999 to 2013 data set, which does not suggest a simple or strong association between these two species. At JST, Cu correlates with Pb.

Other. A component designated as "other" is present for BHM PCA1, GFP PCA1, JST PCA1, PNS PCA2, and YRK PCA1 and PCA2, indicating variability at urban and near-urban (YRK) sites not otherwise represented by the major components (Table 2).

3.5.3 Intercomparisons and uncertainty

For PCA3 (Table S15), the sum of alkanes, sum of aromatics, and α-pinene are associated with the combustion component, whereas isoprene is associated predominantly with the SO_4 component. The measured alkane and aromatic species are known constituents of motor vehicle exhaust (Blanchard et al., 2010), consistent with a mobile source contribution to the JST combustion component. Correlations between α-pinene and CO, EC, and NO_x range from r = 0.5 to 0.6, mathematically associating these species, but the physical processes underlying the correlation are ambiguous (e.g., seasonal or meteorological versus common source emissions). Isoprene and pinenes can be factors in

O_3 formation, and the association of isoprene with SO_4 could arise from a common seasonality or from atmospheric chemical processes generating SOA from isoprene (Surratt et al., 2007; Xu et al., 2015a, b). Additional work is needed to more fully interpret VOC species associations.

PCA4 and PCA5 yield consistent results when NH_3 or daily-average O_3 are either included or excluded from the analysis (Table S16).

The ranges of mean OC concentrations associated with each PCA component as obtained from the various applications are listed for CTR, JST, and YRK in Table 4. Uncertainties in the mean OC concentrations associated with each PCA component are estimated as one-half the ranges for CTR and JST (comprising both PCA and PMF applications) and the full ranges for YRK (PCA applications only), which generally yield comparable uncertainties.

A summary of our PCA1 results compared to the 2012 – 2013 source apportionments reported by Xu et al. (2015a; b) is shown in Tables S17 through S19. For these comparisons, we determined the PCA1 means by matching days to each of the Xu et al. (2015a; b) multi-week study periods. The PCA1 combustion OC tends to compare in magnitude to AMS hydrocarbon-like OA (HOA), biomass burning OA (BBOA), cooking OA (COA) (when one or more such factors are found) or to more-oxidized OA (MO-OOA). The last correspondence would be expected to the extent that MO-OOA includes oxidized motor vehicle exhaust, other anthropogenic combustion emissions, or biomass burning (Xu et al., 2015a, b). As previously noted for CTR, PCA SO_4-associated OC concentrations and AMS isoprene OA concentrations exhibit nearly identical regression relationships with SO_4 concentrations. Some differences between mean PCA SO_4-associated OC and mean AMS isoprene OA (converted to OC) percentage apportionments are evident in Tables S17 through S19, however. Such differences appear to result from ambiguities in linking PCA elements with AMS designations, different numbers of factors (affecting the percentages), and differences in mean observed OA (OC) concentrations. The SEARCH and AMS mean OC concentrations are comparable for the CTR (SOAS) and YRK (winter) data. For JST (summer), JST (winter), and YRK (summer), the mean AMS OC concentrations exceed the mean SEARCH OC concentrations by 40%, 49%, and 85% respectively. The reasons for these differences are unknown, but operationally could be related to sampling and analytical methods. The SEARCH mean OC concentrations during the multi-week comparison periods are consistent with longer-term averages from 2012, 2013, and 2008 – 2013 (Tables S17 – S19). Since SEARCH reports $PM_{2.5}$ size fractions and AMS is based on PM_1 size fractions, higher AMS PM mass concentrations are not expected. No AMS component appears to correspond to the PCA crustal OC, which could relate to the difference in size fractions sampled. The PCA crustal OC concentrations are generally small except during occasional events, as previously noted.

Comparisons of our results to results reported by Kleindienst et al. (2010) are shown in Figure S26. Kleindienst et al. (2010) determined organic tracer concentrations on archived samples from the SEARCH Carbonaceous Aerosol Characterization Experiment (CACHE) archive. Twenty samples were analyzed, five each from BHM, CTR, JST, and PNS, collected during May (7, 13, 22, 28) and August (17), 2005 (Kleindienst et al., 2010). SEARCH OC measurements are made on filters from a sampler with a denuder placed upstream to remove organic gases, whereas the CACHE sampler was not denuded. The CACHE OC concentrations were ~50 – 100% higher than the SEARCH OC concentrations (Figure S26), with a CACHE average OC concentration of 7.32 $\mu g\ m^{-3}$ compared with SEARCH OC average of 4.62 $\mu g\ m^{-3}$ when restricted to the 17 samples that had both CACHE and SEARCH OC concentrations. Kleindienst et al. (2010) accounted for ~70% of the measured CACHE OC concentration using 11 source types, so their apportioned OC concentrations are roughly comparable to measured SEARCH OC concentrations. The sum of the Kleindienst et al. (2010) diesel and wood burning OC concentrations correlates highly ($r^2 = 0.83$) and agrees in magnitude (intercept = 0; slope = 1) with PCA2 combustion OC (Figure S26). Wood burning OC concentrations also correlate highly ($r^2 = 0.76$) with PCA2 combustion OC, corresponding to ~50 – 70% of the combustion OC concentrations (Figure S26). OCbb (Section 3.4) correlates less well ($r^2 = 0.38$) with wood-burning OC, and OCbb concentrations average ~30% higher than wood-burning OC concentrations (Figure S26). As previously noted, the fixed scaling factor used for estimating OCbb from Kbb does not reflect the variability among source types in OCbb/Kbb, nor does it reflect seasonal variability in their source contributions

(Section 3.4). The modest correlation of OCbb with organic tracer-based wood-burning OC concentrations is expected due to emission source variability; overprediction of wood-burning OC by OCbb is expected during summer months when the principal biomass burning sources (agricultural field burns, open burning of wastes) likely predominate and have lower OCbb/Kbb. The sum of the Kleindienst et al. (2010) diesel and wood-burning OC concentrations correlates highly ($r^2 = 0.92$) with OCbb and CO in a multiple regression model (Figure S26), supporting combustion origins of OCbb.

3.5.4 Temporal variations

Temporal variations of the 1999-to-2013 PCA2 results are described here primarily for CTR and JST, representing (as in Table 1) one rural and one urban location having extensive SEARCH data records. At JST, day-of-week variations are evident for the combustion-derived OC and for the OC associated with crustal species (Figure S27), consistent with the occurrence of weekly activity cycles for driving, construction, and other anthropogenic emission sources. Day-of-week variations are not apparent for other OC associations at JST or for any OC factors at CTR. Seasonal and SO_4–associated OC exhibit pronounced monthly variations at both CTR and JST, with higher values of SO_4–associated OC and of CTR seasonal OC occurring during warmer months (Figures S28 and S29). The patterns for CTR SO_4–associated OC (highest in July and August) and seasonal OC (higher in spring and autumn than in July) are not independent.

Mean annual combustion-derived OC concentrations decline from 3.8 ± 0.2 to 1.4 ± 0.1 μg m^{-3} between 1999 and 2013 at JST (Figures 4, S30) and from 2.9 ± 0.4 to 0.7 ± 0.1 μg m^{-3} between 2001 and 2013 at BHM (not shown). Declining combustion OC concentrations at the urban JST and BHM sites coincide with reductions of motor vehicle emissions during this time period (Section 3.1), though these urban sites may also be affected by industrial emissions. BHM additionally benefits from a decline in OC associated with SO_2 from 0.4 ± 0.04 μg m^{-3} in 2001 to 0.2 ± 0.03 μg m^{-3} in 2013, probably as a reflection of declining emissions from industrial sources within Birmingham. In contrast, combustion-derived OC at CTR does not exhibit a statistically significant decline, equaling 1.5 ± 0.1 μg m^{-3} in 1999 and 1.3 ± 0.1 μg m^{-3} in 2013

(Figures 4, S30). At CTR, downward OC trends are evident only for SO_4 and seasonal OC (mean decreases of 0.6 μg m^{-3} and 0.7 μg m^{-3}, respectively) (Figure S31). The OC associated with SO_4 at CTR exhibits declines during all seasons, with the weakest such change in winter (Figure S32).

The trend results are consistent with the combined effects of (1) regional-scale reductions of ambient SO_4 and O_3 concentrations, (2) reductions of urban OC due to declining mobile source OC and VOC emissions, and (3) likely predominance of biomass burning OC at CTR (Hidy et al., 2014). Carbon-isotope measurements from 2004 show that fossil carbon represented ~20% of CTR TC that year (Blanchard et al., 2011), indicating that mobile source or other fossil fuel emissions affect CTR to some extent. Enhanced hourly concentrations of EC, OC, and CO at CTR are associated with winds from the directions of Birmingham, Tuscaloosa, and Montgomery (Hidy et al., 2014). EC declined by ~0.3 μg m^{-3} at CTR between 1999 and 2013 (Figure 1), suggesting an influence of mobile source emission reductions that is possibly too modest to detect using our PCA methods or is masked by annual variability in biomass burning emissions. For comparison, mean EC concentrations at JST decrease by ~1.4 μg m^{-3} (Figure 1), and the overall mean EC at JST (1.35 μg m^{-3}) is ~4 times the overall mean EC at CTR (0.35 μg m^{-3}).

The trends in mean annual OC from each identified species association indicate that anthropogenic emission reductions decreased mean annual urban combustion OC concentrations by 2.4 μg m^{-3} at JST and at BHM (and, by inference, other metropolitan areas in the Southeast), and indirectly decreased SO_4 and seasonal OC by ~1.1 to 1.3 μg m^{-3} throughout the southeastern U.S. between 1999 and 2013 (Figure 4). As of 2013, the overall mean annual combustion-derived OC is 1.3 to 1.4 μg m^{-3} at CTR and JST, whereas the sum of the mean annual SO_4 and seasonal component OC is 0.4 to 0.8 μg m^{-3} at CTR and JST (Figure 4).

3.6 Synthesis

Various apportionments of $PM_{2.5}$ OC concentrations are presented in Sections 3.1, 3.4, and 3.5. These apportionments are compared and contrasted in this section. Although the apportionments utilize different methods, there is overlap of inputs. For example, Kbb is used as an input in the multivariate regressions that generate “primary” organic carbon (“POC”) and “secondary” organic carbon (“SOC”) (Blanchard et al., 2008, not discussed here), and “POC” is a fitting species used in the CMB receptor modeling. As shown in Table 5, the apportionments exhibit areas of agreement as well as certain differences. Both are summarized using ratios of the values listed in Table 5. We report averages and ranges across the sites.

Computed “POC” represents 72% (64% - 76%) of mean OC concentrations, whereas “SOC” represents 29% (25% - 38%). As noted, “SOC” is the OC that is associated with O_3 and SO_4, which constitutes a portion of SOA. “POC” is associated with EC, CO, and Kbb, but may include oxidized OC that would be identified as SOA in other analyses. For the CMB analysis, OC derived from area sources (primarily biomass burning), mobile sources, and point sources is summed to generate combustion OC. CMB combustion OC is 97% (73% - 118%) of “POC”; this level of agreement presumably is because the CMB receptor model of Blanchard et. al. (2013) used “POC” as a fitting species. The largest PCA1 and PCA2 OC components are combustion, seasonal, and SO_4-associated OC. The sum of these three components is, for PCA1, 87% (60% - 139%) of mean measured OC (the overestimate, at PNS, is balanced by negative crustal and salt components there). For PCA2, the sum of combustion, seasonal, and SO_4-associated OC is 81% (58% - 101%) of mean measured OC. Other PCA OC components contribute smaller amounts (Table 5).

PCA1 and PCA2 combustion each represent 57% (8% - 103% and 33% - 85%, respectively) of CMB combustion. Other PCA factors, including SO_2, metals, and salts (possibly denoting biomass burning when represented by K) may be related to specific types of combustion sources.

These comparisons suggest that the OCbb concentrations are likely biased high by ~10% or more, with less evident biases at inland sites. Specifically, OCbb is 99% (66% - 121%) of “POC” and 109% (79% - 142%) of CMB area-source OC concentrations. At inland sites, OCbb is 96% (79% - 111%) of CMB area-source OC concentrations, indicating approximate agreement. Although multiple analyses (OCbb, “POC”, PCA2) used Kbb as an input variable, OCbb is calculated using a fixed scaling factor between OC and Kbb.

As described, uncertainty in this scaling factor is estimated to generate a factor-of-two uncertainty in OCbb.

4. Conclusions

Fifteen years of measurements of an extensive suite of gas and particle species at eight SEARCH sites offer important insights into the sources of OA and the effects of anthropogenic emission reductions on OA concentrations in the southeastern U.S. Five analytical methods indicate that a major component (~45% on average, 1999 to 2013, all sites; intersite range 25% to 63%) of OA derives from combustion sources, including motor vehicles and biomass burning, at all urban and rural sites and throughout the year. Reductions of emissions from combustion sources decreased overall mean annual OC concentrations by 2.4 μg m^{-3} at JST and BHM (and, by inference, throughout the Atlanta and Birmingham metropolitan areas) between 1999 and 2013. OA is identified partly with an SO_4-OA relationship (~25% of OC, on average), which is consistent with hypothesized isoprene oxidation pathways. OA is also partly identified with other seasonal atmospheric processes, including atmospheric photochemical reactions (~20% of OC, on average). Reductions of anthropogenic emissions of SO_2, NO_x, and VOC suggest a decrease in SO_4-associated OC and seasonal-component OC concentrations by ~1.1 – 1.3 μg m^{-3} between 1999 and 2013 throughout the SEARCH region, implying that reductions of anthropogenic emissions affect SOA concentrations.

As of 2013, the SEARCH mean annual combustion-derived OC concentrations are 1.3 to 1.4 μg m^{-3} at CTR and JST (~60% of total OC), while the mean annual OC concentrations associated with the SO_4 and seasonal components are 0.4 to 0.8 μg m^{-3} at CTR and JST (~35% and ~22%, respectively). Additional attention to OC from combustion emissions could yield further reductions of $PM_{2.5}$ OC concentrations, now averaging ~2.5 μg m^{-3} in the southeastern U.S. Since biomass burning is a major source of OC emissions in the southeastern U.S., minimizing the stated extent and timing of these emissions could help improve regional air quality.

Additional work could improve quantitative assessments of source contributions. Carbon-isotope measurements of archived SEARCH samples are in process, and will provide further insight into the observed OA trends. Future research could also help define the sensitivity of the SO_4-associated OC and seasonal OC to ongoing reductions of anthropogenic SO_2, NO_x, and VOC emissions. Current research by many investigators is better defining the role of naturally occurring VOCs, including isoprene. The SOAS and SAS campaigns of June – July 2013 helped resolve uncertainties and ambiguities in OA chemistry specific to that time period. Extrapolation of the short-term results to seasonal and interannual time periods can be achieved through further analyses of long-term EC and OC monitoring data.

Appendix: Measurement conventions and issues

Carbonaceous aerosol is conventionally divided into EC and OC, operationally defined by measurement protocol, either by thermal differentiation or by light absorption (for clarity, protocols based on light absorption typically report data as light-absorbing carbon [LAC] or black carbon [BC], and sometimes as brown carbon [BrC], rather than as EC). EC is comprised of extended aromatic rings, and is characteristically refractory, insoluble, chemically inert, and light absorbing (Cappa, 2011). EC derives from combustion and is believed to be exclusively from primary emission sources, including motor vehicles, other transportation sources, industrial processes, and vegetation burning (Chow et al., 2010; Watson et al., 2011). OC is the carbonaceous component of OA and refers here to specific measurements, such as filter-based measurements made by thermal-optical reflectance (TOR) (Chow et al., 2005; 2007a; 2007b). Combustion sources that emit EC also emit OC.

Organic compounds that are directly emitted in the condensed phase are typically identified as POA, whereas SOA commonly refers to organic material transferring from gases to the condensed phase through chemical transformation (Kanakidou et al., 2005). Gases of varying degrees of volatility may be oxidized and incorporated into the condensed phase (Robinson et al., 2007; Huffman et al., 2009). Chemical reactions may take place in the condensed phase in the presence of water, and partitioning by phase are key elements of uncertainty in describing SOA (e.g., Carlton and Turpin, 2013; Nguyen et al., 2015; Isaacman-VanWertz et al., 2015). Atmospheric chemical reactions involving

VOCs (Hallquist et al., 2009), especially including compounds of intermediate volatility (de Gouw et al., 2011), are known to generate oxygenated reaction products on time scales of minutes to days. Secondary organic species may be associated with other secondary species, such as O_3 or SO_4, either through a common driver of photochemical oxidation processes or due to direct chemical relationships; this is an active area of research.

The initial aging of fresh, concentrated emissions begins with turbulent dilution seconds after hot exhaust effluent enters into the cooler atmosphere. Fine particle evolution then takes place more slowly over nominal ~5-7 day lifetimes as particles are mixed and transported, and lost by deposition. These processes are often referred to as “aging” of a freshly emitted aerosol. The aging processes can be chemical in nature, or may involve physical processes as well, including absorption in clouds or precipitation followed by hydrometeor evaporation.

The exceptions to the definition of SOA as material transferring from gas to condensed phases through chemical transformation include: (1) volatile or semi-volatile material that condenses into aerosol without undergoing chemical transformation (Kanakidou et al., 2005), (2) gases absorbed into hydrometeors, leaving residual aerosol on evaporation, which might be understood as either POA or SOA depending on absence or occurrence of chemical transformation (Kanakidou et al., 2005), and (3) material emitted in the condensed phase that undergoes chemical transformation, possibly shifting multiple times between gas and aerosol, and that appears as oxidized compounds on analysis of aerosol samples (Donahue et al., 2009). The last exception is especially ambiguous: such material may be classified as POA in an emission inventory, but be identified as SOA according to measurements designated as “more oxygenated aerosol (OOA)” by aerosol mass spectrometry (AMS).

Dilution sampling is routinely used to characterize exhaust emissions because it yields estimates of EC and OC at temperatures characteristic of the ambient atmosphere, but further phase exchange of POA may be expected in the real world with ongoing dilution. Photochemical chamber studies demonstrate that organic aerosol from hot exhaust emissions (e.g., diesel engine exhaust) shifts from POA to SOA dominance typically within one or more hours of photo-oxidation (Presto et al., 2014). The comparability of POA measurements from such studies to emission inventory estimates of mobile source PM is poorly characterized. For modeling, a volatility basis set (VBS) provides more realistic diluted emission estimates by recognizing that POA spans a range of volatilities, and cannot be treated as entirely nonvolatile (Robinson et al., 2007; Donahue et al., 2009; Donahue et al., 2012).

The mass concentrations of EC are approximately conserved from emission sources to receptor sites, whereas losses due to volatilization of certain $PM_{2.5}$ organic compounds readily occur. OA concentrations may increase as SOA forms not only from POA vaporization, subsequent reactions and condensation, but also, perhaps predominantly, from atmospheric reactions of gas-phase precursors. Organic mass (OM), which includes not only carbon but also other atoms (e.g., oxygen and hydrogen) that are components of OA, is not conserved. There is no accepted measure of aging in atmospheric aerosols, but some workers have adopted OM/OC as an indicator. As POA ages, the ratio of oxygen-to-carbon typically increases, increasing the mass of OM. Aerosol aging can, therefore, increase both the OM/EC ratio and the OC/EC ratio (by definition, EC concentrations are not expected to increase with the formation of species during aging). A graphical depiction of various categorizations of OA is shown in the supplement (Figure S1).

Receptor-modeling methods have identified POA source types using measurements of conservative organic tracer species (Schauer et al., 1996), indicating that motor vehicles contribute ~ 2 to 4 $\mu g\ m^{-3}$ to annual-average OC concentrations in Atlanta (e.g., Zheng et al. 2002; 2006). SEARCH thermal desportion-gas chromatograph mass spectrometer (TD-GC/MS) measurements suggest that 30 to 50% of the observed 2006 to 2010 OC trend in Atlanta, Georgia and Birmingham, Alabama could be due to changes in mobile source emissions (Blanchard et al., 2014a). These trends need not be entirely from changes in POA emissions; diesel SOA, for example, is an important component of mobile source OA (Presto et al., 2014), and is linked to EC and POA emissions. Aside from motor vehicle exhaust, biomass burning is a major source of EC and the largest source of OC emissions in the southeastern U.S. according to emission inventories, with little evidence for substantial trend between 1999 and 2013 (Hidy et al., 2014). Carbon-isotope (^{14}C) measurements at SEARCH sites indicate that on average 2 to 4 μg m^{-3} of OC is modern in origin (rural and urban sites), with ~40% fossil in Atlanta and ~60% fossil in Birmingham during 2004 and 2005 (Blanchard et al., 2011). Together, the measurements suggest the presence of a large modern-carbon contribution added to downward-trending mobile source contributions (Hidy et al., 2014).

Significant emissions of VOC from vegetation, including isoprene and terpenes, occur in the southeastern U.S. and represent a major, and possibly a dominant, source of SOA (Goldstein et al., 2009). Although incompletely quantified, SOA derived from anthropogenic and biogenic VOC products has been estimated to be ~20 to 60% of the OA observed in the southeastern U.S. (Table S1), varying among samples and especially by season (Lim and Turpin, 2002; Zheng et al., 2006; Saylor et al., 2006; Blanchard et al., 2008). Field and laboratory work over the years has refined the chemical pathways, with evidence for both aqueous and gas-phase chemistry. Ground-level filter samples from southeastern sites have yielded expected tracers of SOA-formation chemistry from biogenic precursors (Gao et al., 2006; Surratt et al., 2007; Chan et al., 2010; Hatch et al., 2011a; 2011b). The presence of naturally occurring VOCs, modulated by temperature and solar radiation, is expected to be roughly constant over a period of years, suggesting a near constant level of biogenic SOA. However, isoprene concentrations appear to have increased at Atlanta-area sites between 2002 and 2012 (Hidy et al., 2014); the reason for, and significance of, this trend for SOA trends in the Southeast is unclear. Interaction of biogenic and anthropogenic emissions potentially affect SOA formation (Weber et al., 2007; Shilling et al., 2012; Xu et al., 2015a), so biogenic SOA trends could result from anthropogenic emission reductions.

Determination of the fraction of OC not directly attributed to sources is complicated by both the influence of atmospheric processes on emissions and the methods of measurement of OC or its components. The processing of atmospheric aerosols is exceedingly complex as a result of the chemistry of volatile and non-volatile carbon emissions and interactions between chemical and meteorological processes on multiple time and space scales. Advancing knowledge about the SOC component has been inhibited by the lack of chemical detail in long-term observations and the short-term application of more recent measurement methods. Measurements of atmospheric organic carbon as POC and SOC refer to operational definitions, including those in Figure S1. Historically, measurements of OC and EC have relied on filter sampling and subsequent analysis for OC constituents in the laboratory. The filter sampling and recently introduced continuous methods provide different data for EC and OC as well as some identification of constituents resolved in space in time. However, their quantitative comparison remains problematic as indicated in this study. Continuing research, including method comparisons, and expanded detailed atmospheric observations will be required to resolve these uncertainties.

Author contributions

C. L. B., G. M. H., S. S., K. B., and E. S. E. designed the study. E. S. E. and K. B. operated the measurement program and prepared the data sets. C. L. B. carried out the statistical analyses. C. L. B. and G. M. H. wrote the manuscript with contributions from all co-authors.

Acknowledgements

The authors thank J. Jansen, E. Knipping, and the ARA staff for their contributions to this work. Funding for the SEARCH network has come from Southern Company and the Electric Power Research Institute. We are indebted to these sponsors for supporting this unique long-term measurement program.

References

Andreae, M.O. and Merlet, P.: Emission of trace gases and aerosols from biomass burning, Global Biogeochem. Cy., 15 (4), 955-966, 2001.

Andreae, M.O., Atlas, E., Cachier, H., Cofer III, W.R., Harris, G. W., Helas, G., Koppmann, R., Lacaux, J.-P., and Ward, D.E.: Trace gas and aerosol emissions from savanna fires, in: Levine, J.S., ed., Biomass Burning and Global Change, MIT Press, Cambridge MA, 278-295, 1996.

Atmospheric Research and Analysis (ARA), http://www.atmospheric-research.com/studies/SEARCH/index.html, last access 10 July 2014.

Baumann, K., Flanagan, J.B., and Jayanty, R.K.M.: Fine particulate matter source apportionment for the chemical Speciation Trends Network site at Birmingham, Alabama, using Positive Matrix Factorization, J. Air Waste Manage., 58, 27-44, 2008.

Blanchard, C. L., Hidy, G. M., Tanenbaum, S., Edgerton, E., Hartsell, B., and Jansen, J.: Carbon in southeastern aerosol particles: empirical estimates of secondary organic aerosol formation, Atmos. Environ., 42, 6710-6720, 2008.

Blanchard, C. L., Hidy, G. M., and Tanenbaum, S.: NMOC, ozone, and organic aerosol in the southeastern states, 1999-2007: 1. Spatial and temporal variations of NMOC concentrations and composition in Atlanta, Georgia, Atmos. Environ., 44, 4827-4839 doi:10.1016/j.atmosenv.2010.08.036, 2010.

Blanchard, C. L., Hidy, G. M., and Tanenbaum, S.: NMOC, ozone, and organic aerosol in the southeastern states, 1999-2007: 3. Origins of organic aerosol in Atlanta, Georgia, and surrounding areas, Atmos. Environ., 45, 1291-1302, doi:10.1016/j.atmosenv.2010.12.004, 2011.

Blanchard, C. L., Tanenbaum, S., and Hidy, G. M.: Source attribution of air pollutant concentrations and trends in the Southeastern Aerosol Research and Characterization (SEARCH) network, Environ. Sci. Technol., dx.doi.org/10.1021/es402876s, 2013.

Blanchard, C. L., Chow, J., Edgerton, E., Watson, J.G., Hidy, G. M., and Shaw, S.: Organic aerosols in the southeastern United States: speciated particulate carbon measurements from the SEARCH network, 2006-2010, Atmos. Environ., 95, 327-333, dx.doi.org/10.1016/j.atmosenv.2014.06.050, 2014a.

Blanchard, C. L., Tanenbaum, S., and Hidy, G. M.: Spatial and temporal variability of air pollution in Birmingham, Alabama, Atmos. Environ., doi:10.1016/j.atmosenv.2014.01.006, 2014b.

Bougiatioti, A., Stavroulas, I., Kostenidou, E., Zarmpas, P., Theodosi, C., Kouvarakis, G., Canonaco, F., Prévôt, A. S. H., Nenes, A., Pandis, S. N., and Mihalopoulos, N.: Processing of biomass burning aerosol in the eastern Mediterranean during summertime, Atmos. Chem. Phys., 14, 4793–4807, www.atmos-chem-phys.net/14/4793/2014/, doi:10.5194/acp-14-4793-2014, 2014.

Budisulistiorini, S., Canagaratna, R., Croteau, P., Marth, W., Baumann, K., Edgerton, E., Show, S., Knipping E., Worsnop, D., Jayne, J., Gold, A., and Surratt, J.: Real-time continuous characterization of secondary organic aerosol derived from isoprene epoxydiols in downtown Atlanta, Georgia, using the Aerodyne Chemical Speciation Monitor, Environ. Sci. Technol., 47, 5686-5694, 2013.

Budisulistiorini, S. H., Li, X., Bairai, S. T. , Renfro, J., Liu, Y., Liu, Y. J. , McKinney, K., Martin, S. T., McNeill, V. F., Pye, H. O. T., Neff, M. , Stone, E. A., Mueller, S., Knote, C., Shaw, S. L., Zhang, Z., Gold, A., and Surratt, J. D.: Examining the effects of anthropogenic emissions on isoprene-derived secondary organic aerosol formation during the 2013 Southern Oxidant and Aerosol Study (SOAS) at the Look Rock, Tennessee, ground site, Atmos. Chem. Phys. Discuss. 15, 7365-7417, doi:10.5194/acpd-15-7365-2015, 2015.

Calloway, C. P., Li, S., Buchanan, J. W., and Stevens, R. K.: A refinement of the potassium tracer method for residential wood smoke, Atmos. Environ., 23, 67-69, 1989.

Cappa, C.: Measurements of Aerosol Carbon in the Atmosphere, AAAR Tutorial, 3 October 2011, AAAR 30th Annual Conference, October 3 – 7, 2011, Orlando, FL, http://aaar.conference2011.org/content/tutorials, last access 22 May 2014, 2011.

Carlton, A. and Turpin, B.: Particle partitioning potential of organic compounds is highest in the Eastern US and driven by anthropogenic water, Atmos. Chem. Phys., 13, 10203-102114, 2013.

Chan, M. N., Surratt, J. D., Claeys, M., Edgerton, E. S., Tanner, R. L., Shaw, S. L., Zheng, M., Knipping, E. M., Eddingsaas, N. C., Wennberg, P. O., and Seinfeld, J. H.: Characterization and quantification of isoprene-derived epoxydiols in ambient aerosol in the southeastern United States, Environ. Sci. Technol., 44, 4590–4596, 2010.

Chow, J., Watson, J., Kuhns, H., Etyemezian, V., Lowenthal, D., Crow, D., Kohl, S., Engelbrecht, J., and Green, M.: Source profiles for industrial, mobile and area sources in the Big Bend Regional Aerosol Visibility and Observational Study, Chemosphere, 54, 185-208, 2004.

Chow, J. C., Watson, J. G., Chen, L.-W. A., Paredes-Miranda, G., Chang, M.-C. O., Trimble, D. L., Fung, K. K., Zhang, H., and Yu, J. Z.: Refining temperature measures in thermal/optical carbon analysis, Atmos. Chem. Phys. 5(4), 2961-2972, 1680-7324/acp/2005-5-2961, http://www.atmos-chem-phys.net/5/2961/2005/acp-5-2961-2005.pdf, last access 22 May 2015, 2005.

Chow, J. C., Watson, J. G., Chen, L.-W. A., Chang, M. C. O., Robinson, N. F., Trimble, D. L., and Kohl, S. D.: The IMPROVE_A temperature protocol for thermal/optical carbon analysis: Maintaining consistency with a long-term database, J. Air Waste Manage., 57(9), 1014-1023, 2007a.

Chow, J. C., Yu, J. Z., Watson, J. G., Ho, S. S. H., Bohannan, T. L., Hays, M. D., and Fung, K. K.: The application of thermal methods for determining chemical composition of carbonaceous aerosols: a review, J. Environ. Sci. Heal. A, 42(11), 1521-1541, 2007b.

Chow, J.C., Watson, J.G., Lowenthal, D.H., Chen, L.-W.A., and Motallebi, N.: Black and organic carbon emission inventories: review and application to California, J. Air Waste Manage., 60(4), 497-507, http://www.tandfonline.com/doi/pdf/10.3155/1047-3289.60.4.497, last access 22 May 2015, 2010.

Dattner, S. and Hopke, P., eds.: Receptor Models Applied to Contemporary Pollutions Problems: Proceedings of a Specialty Conference, Air Pollution Control Association, Publishers Choice Book Manufacturing Co., Mars, Pennsylvania, 368 pp, 1982.

de Gouw, J. A., Middlebrook, A. M., Warneke, C., Ahmadov, R., Atlas, E. L., Bahreini, R., Blake, D. R., Brock, C. A., Brioude, J., Fahey, D. W., Fehsenfeld, F. C., Holloway, J. S., Le Henaff, M., Lueb, R. A., McKeen, S. A., Meagher, J. F., Murphy, D. M., Paris, C., Parrish, D. D., Perring, A. E., Pollack, I. B., Ravishankara, A. R., Robinson, A. L., Ryerson, T. B., Schwarz, J. P., Spackman, J. R., Srinivasan, A., and Watts, L. A.: Organic aerosol formation downwind from the Deepwater Horizon oil spill, Science, 331, 1295-1299, doi:10.1126/science.1200320, 2011.

Ding, X., Zheng, M., Edgerton, E., Jansen, J., and Wang, X.: Contemporary or fossil origin: Split of estimated secondary organic carbon in the southeastern United States, Environ. Sci. Technol., 42, 9122-9128, 2008.

Donahue, N. M., Robinson, A. L., and Pandis, S. N.: Atmospheric organic particulate matter: from smoke to secondary organic aerosol, Atmos. Environ., 43, 94–106, doi:10.1016/j.atmosenv.2008.09.055, 2009.

Donahue, N. M., Kroll, J. H., Robinson, A. L., Pandis, S. N., and Robinson, A. L.: A two-dimensional volatility basis set – part 2: diagnostics of organic-aerosol evolution, Atmos. Chem. Phys., 12, 615–634, doi:10.5194/acp-12-615-2012, www.atmos-chem-phys.net/12/615/2012/, last access 22 May 2015, 2012.

Edgerton, E. S., Hartsell, B. E., Saylor, R. D., Jansen, J. J., Hansen, D. A., and Hidy, G. M.: The Southeastern Aerosol Research and Characterization Study: part 2 – filter-based measurements of $PM_{2.5}$ and PM_{coarse} mass and composition, J. Air Waste Manage., 55, 1527-1542, 2005.

Edgerton, E. S., Hartsell, B. E., Saylor, R. D., Jansen, J. J., Hansen, D. A., and Hidy, G. M.: The Southeastern Aerosol Research and Characterization Study, part 3: continuous measurements of fine particulate matter mass and composition, J. Air Waste Manage., 56, 1325-1341, 2006.

Gao, S., Surratt, J., Knipping, E., Edgerton, E., Shahgholi, M., and Seinfeld, J.: Characterization of polar organic compounds in fine aerosols in the southeastern United States: identity, origin and evolution, J. Geophys. Res., 111, doi 10.1029/2005JD006601, 2006.

Goldstein, A. H., Koven, C. D., Heald, C. L., and Fung, I. Y.: Biogenic carbon and anthropogenic pollutants combine to form a cooling haze over the southeastern United States, P. Natl. Acad. Sci. USA, 106, 8835-8840, doi: 10.1073/pnas.0904128106, 2009.

Guo, H., Xu, L., Bougiatioti, A., Cerully, K. M., Capps, S. L., Hite Jr., J. R., Carlton, A. G., Lee, S.-H., Bergin, M. H., Ng, N. L., Nenes, A., and Weber, R. J.: Fine-particle water and pH in the southeastern United States, Atmos. Chem. Phys., 15, 5211–5228, 2015.

Haines, T.K., Busby, R.L., and Cleaves, D.A.: Prescribed burning in the South: trends, purpose, and barriers, South. J. Appl. For., 25, 149-153, 2001.

Hallquist, M., Wenger, J. C., Baltensperger, U., Rudich, Y., Simpson, D., Claeys, M., Dommen, J., Donahue, N. M. , George, C., Goldstein, A. H., Hamilton, J. F., Herrmann, H., Hoffmann, T., Iinuma, Y., Jang, M., Jenkin, M. E., Jimenez, J. L., Kiendler-Scharr, A., Maenhaut, W., McFiggans, G., Mentel, Th. F., Monod, A., Prévôt, A. S. H., Seinfeld, J. H., Surratt, J. D., Szmigielski, R., and Wildt, J.: The formation, properties and impact of secondary organic aerosol: current and emerging issues, Atmos. Chem. Phys., 9, 5155–5236, 2009.

Hand, J., Schichtel, B., Pitchford, M., Malm, W., and Frank, N.: Seasonal composition of remote and urban fine particulate matter in the United States, J. Geophys. Res. Atmos. 117, DO5209, doi:10.1029/2011JD 017122, 2012.

Hansen, D.A., Edgerton, E. S., Hartsell, B. E., Jansen, J. J., Hidy, G. M., Kandasamy, K., and Blanchard, C. L.: The Southeastern Aerosol Research and Characterization Study (SEARCH): 1. overview, J. Air Waste Manage., 53, 1460-1471, 2003.

Hatch, L. E., Creamean, J. M., Ault, A. P., Surratt, J. D., Chan, M. N., Seinfeld, J. H., Edgerton, E. S., Su, Y., and Prather, K. A.: Measurements of isoprene-derived organosulfates in ambient aerosols by aerosol time-of-flight mass spectrometry, part 1:

single particle atmospheric observations in Atlanta, Environ. Sci. Technol., 45(12), 5105–5111, 2011a.

Hatch, L. E., Creamean, J. M., Ault, A. P., Surratt, J. D., Chan, M. N., Seinfeld, J. H., Edgerton, E. S., Su, Y., and Prather, K. A.: Measurements of isoprene-derived organosulfates in ambient aerosols by aerosol time-of-flight mass spectrometry, part 2: temporal variability & formation mechanisms, Environ. Sci. Technol., 45 (20), 8648–8655, 2011b.

Hidy, G. M., Blanchard, C.L, Baumann, K, Edgerton, E., Tanenbaum, S., Shaw, S., Knipping, E., Tombach, I., Jansen, J. J., and Walters, J.: Chemical climatology of the southeastern United States, 1999 – 2013, Atmos. Chem. Phys., 14, 11893–11914, doi:10.5194/acp-14-11893-2014, 2014.

Hobbs, H, Reid, J.S., Herring, J.A., Nance, J. D., Weiss, R. E, Ross, J. L., Hegg, D. A., Ottmar, R. D., and Liousse, C.: Particle and trace-gas measurements in the smoke from prescribed burns of forest products in the Pacific northwest, in: Levine, J.S., ed., Biomass Burning and Global Change, MIT Press, Cambridge MA, 607-715, 1996.

Hu, W., Campuzano-Jost, P., Palm, B., DSay, D., Ortega, A., Hayes, P., Krechner, J., Chen, Q,Kuwata, M., Liu, Y., De Sa, S., Martin, S., Hum, M., Budisulistiorini, S., Riva, M., Surratt, J., St. Clair, J., Isaacman-VanWertz, G., Yee, L., Goldstein, A., Carbone, S., Artaxo, P., DeGouw, J., Koss, A., Wisthaler, A., Mikoviny, T., Karl, T., Kaser, L., Jud, W.,Hansel, A., Docherty, K., Robinson, N., Coe, H., Allan, J., Canagaratna, M., Paulot, F., and Jimenez, J.: Characterization of a real-time tracer for isoprene epoxidiols-derived secondary organic (IEPOX-SOA) from aerosol mass spectrometer measurements, Atmos. Chem. Phys. Discuss., 15, 11223-11276, 2015.

Huffman, J. A., Docherty, K. S., Mohr, C., Cubison, M. J., Ulbrich, I. M., Ziemann, P. J., Onasch, T. B., and Jimenez, J. L.: Chemically-resolved volatility measurements of organic aerosol from different sources, Environ. Sci. Technol., 43, 5351–5357, 2009.

Isaacman-VanWertz, G., Goldstein, A., Yee, L., Kreisberg, N., Wernis, R., Moss,, J., Hering, S., de Sa, S., Martin, S., Alexander, L., Palm, B., Hu, W., Campuzano-Jost, P., Day, D., Jiminez, J., Riva, M., Surratt, J., Edgerton, E., Baumann, K., Viegas, J., Manzi, A., deSouza, R., and Artaxo, P.: Biogenic oxidation products that dominate secondary organic aerosol in forested environments actively partitioning between gas and particle phases, in preparation, 2015.

Kanakidou, M., Seinfeld, J. H., Pandis, S. N., Barnes, Dentener, F. J., Facchini, M. C., Van Dingenen, R., Ervens, B., Nenes, A., Nielsen, C. J., Swietlicki, E., Putaud, J. P., Balkanski, Y., Fuzzi, S., Horth, J., Moortgat, G. K., Winterhalter, R., Myhre, C. E. L., Tsigaridis, K., Vignati, E., Stephanou, E. G., and Wilson, J.: Organic aerosol and global climate modelling: a review, Atmos. Chem. Phys., 5, 1053–1123, www.atmos-chem-phys.org/acp/5/1053/, last access 2 September 2014, 2005.

Kim, P., Jacob, D., Fisher, J., Travis, K., Yu, K., Zhu, L., Yantosca, R., Sulprizio, Jiminez, J., Campusano-Jost, P., Froyd, K., Liao, J., Hair, J., Fenn, M., Butle, C., Wagner, N., Gordon, T., Welti, A., Wennberg, P., Crounsem J., St. Clair, j., Teng, A., Millet, D., Schwarz, J., Markovic, M., and Perring, A.: Sources, seasonality and trends of Southeast US aerosol: an integrated analysis of surface, aircraft, and satellite observations with the GEOS-CHEM chemical transport model, Atmos. Chem. Phys. Discuss., 15, 17651-17709, 2015.

Kleindienst, T., Jaoui, M., Lewandowski, M., Offenburg, J., Lewis, C., Bhave, P., and Edney, E.: Estimates of the contribution of biogenic and anthropogenic hydrocarbons to secondary organic aerosol at a southeastern US location, Atmos. Environ., 41, 8288-8300, 2007.

Kleindienst, T., Lewandowski, M., Offenburg, J., and Edney, E.: Contribution of primary and secondary sources of organic aerosol and PM2.5 at SEARCH network sites, J. Air Waste Manage. Assoc, 60, 1388-1399, 2010.

Kroll, J., Ng, N., Murphy, S., Flagan, R., and Seinfeld, J.: Secondary organic aerosol formation from isoprene photooxidation, Environ. Sci. Technol., 40, 1869-1877, 2006.

Landis, M.S., Lewis, C. W., Stevens, R. K., Keeler, G. J., Dvonch, J. T., and Tremblay, R. T.: Ft. McHenry tunnel study: source profiles and mercury emissions from diesel and gasoline powered vehicles, Atmos. Environ., 41, 8711–8724, doi:10.1016/j.atmosenv.2007.07.028, 2007.

Lee, S., Baumann, K., Schauer, J. J., Sheesley, R. J., Naeher, L. P., Meinardi, S., Blake, D. R., Edgerton, E. S., Russell, A. G., and Clements, M.: Gaseous and particulate emissions from prescribed burning in Georgia, Environ. Sci. Technol., 39, 9049-9056, 2005.

Lee, D., Balachandran, S. Pachon, J., Shankaran, R., Lee, S., Mulholland, J. A., and Russell, A. G. Ensemble-trained $PM_{2.5}$ source apportionment approach for health studies. Environ. Sci. Technol., 43, 7023–7031, 2009.

Lewandowski, M., Piletic, I., Kleindienst, T., Offenburg, J., Beaver, M., Jaoui, M., Docherty, K., and Edney, E.: Secondary organic aerosol characterization at field sites across the United States during the spring-summer period, Intern J. Environ. Anal. Chem. 93, 1084-1103, 2013.

Lewis, C. W.: Determining the sources of particulate and VOC pollutants in ambient air by radiocarbon (^{14}C) measurements, Sixth International Conference, Preservation of Our World in the Wake of Change, Jerusalem, June 30 – July 4, 1996.

Lewis, C. W., Baumgardner, R. E., and Stevens, R. K.: Contribution of woodsmoke and motor vehicle emissions to ambient aerosol mutagenicity, Environ. Sci. Technol., 22, 968-971, 1988.

Lewis, C. W., Norris, G. A., Conner, T. L., and Henry, R. C.: Source apportionment of Phoenix $PM_{2.5}$ aerosol with the UNMIX receptor model, J. Air Waste Manage., 53, 325 – 338, doi: 10.1080/10473289.2003.10466155, 2003.

Lewis, C., Klouda, G., Ellenson, W.: Radiocarbon measurement of the biogenic contribution to summertime PM-2.5 ambient aerosol in Nashville, TN, Atmos. Environ. 38, 6053-6061, 2004.

Liao, J., Froyd, K., Murphy, D., Keutsch, F., Yu, G., Wennberg, P., St. Clair, J., Crounse, J., Wisthaler, A., Mikoviny, T., Jiminez, J., Campuzano-Jost, P., Day, D., Hu, W., Ryerson, T., Pollack I., Peischl, J., Anderson, B., Ziemba, L., Blacke, D., Meinhardi, S., and Diskin, G.: Airborne measurements of organosulfates over the continental U.S., J. Geophys. Res. Atmos., 120, doi:10.1002/so14JD022378, 2015.

Lim, H. and Turpin, B.: Origins of primary and secondary organic aerosol in Atlanta: results of time-resolved measurements during the Atlanta Supersite experiment, Environ. Sci. Technol., 36, 4489-4496, 2002.

Lin, Y., Knipping, E., Edgerton, E., Shaw, S., and Surratt, J.: Investigating the influences of SO2 and NH3 levels on isoprene-derived secondary organic aerosol formation using conditional sampling approaches, Atmos. Chem. Phys., 13, 8457-8470, 2013.

Lin, Y., Budisulistiorini, S., Chu, K., Siejack, R., Zhang, H., Riva, M., Zhang, Z., Gold, A., Kautzman, K., and Surratt, J.: Light-absorbing oligomer formation in secondary organic aerosol from reactive uptake of isoprene epoxidiols, Environ. Sci. Technol., 48, 12012-12021, 2014.

Malm, W.C., Day, D., Kreidenweis, S., Collett, J., Carrico, C., McMeeking, G., and Lee, T.: Hygroscopic properties of an organic-laden aerosol, Atmos. Environ., 39, 4969-4982, 2005.

Taylor, N., Collins, D., Spencer, C., Lowenthal, D., Zielenska, B., Samburova, V., and Kumar, N.: Measurement of ambient aerosol hydration state at Great Smoky Mountains National Park in the southeastern United States, Atmos. Chem. Phys., 11, 12085-2011, doi:10.5194/acp-1112085-2011, 2011.

May, A., Saleh, R., Hennigan, C., Donahue, N., and Robinson, A.: Volatility of organic molecular markers used for source apportionment analysis: measurements and implications for atmospheric lifetime, Environ. Sci. Technol., 46, 12435-12444, 2012.

McDonald, J. D., Chow, J. C., Peccia, J., Liu, Y., Chand, R., Hidy, G. M., and Mauderly, J. L.: Influence of collection region and site type on the composition of paved road dust, Air Qual Atmos Heal, 6, 615–628, doi 10.1007/s11869-013-0200-4, 2013.

McDonald, B., Goldstein, A., and Harley, R.: Long-term trends in California mobile source emissions and ambient concentrations of black carbon and organic aerosol, Environ. Sci. Technol., 49, 5178-5188, 2015.

Murphy, B. and Pandis, S.: Exploring summertime organic aerosol formation in the eastern United States using a regional-scale budget approach and ambient measurements, J. Geophys. Res. Atmos. 115, D24216, doi:10.1029/2010JD14418, 2010.

Nguyen, E. R., Capps, S., and Carlton, A.: Decreasing aerosol water with OC trends in the southeast U.S., Environ. Sci. Technol. 49, 7843-7850, 2015.

Pachon, J. E., Balachandran, S., Hu, Y., Weber, R. J., Mulholland, J. A., and Russell, A. G.: Comparison of SOC estimates and uncertainties from aerosol chemical composition and gas phase data in Atlanta, Atmos. Environ., 44, 3907-3914, 2010.

Pachon, J. E., Weber, R. J., Zhang, X., Mulholland, J. A., and Russell, A. G. Revising the use of potassium (K) in the source apportionment of $PM_{2.5}$, Atmos. Pollut. Res., 4, 14 – 21, 2013.

Pandis, S., Paulson, S., Seinfeld, J., and Flagan, R.: Aerosol formation in the photooxidation of isoprene and b-pinene, Atmos. Environ. 25A, 1997-1991, 1991.

Presto, A. A., Gordon, T. D., and Robinson, A. L.: Primary to secondary organic aerosol: evolution of organic emissions from mobile combustion sources, Atmos. Chem. Phys., 14, 5015–5036, doi:10.5194/acp-14-5015-2014, www.atmos-chem-phys.net/14/5015/2014/, last accessed 2 September 2014, 2014.

Provencher, L., Herring, B. J., Gordon, D. R., Rodgers, H. L., Tanner, G. W., Hardesty, J. L., Brennan, L. A., and Litt, A. R.: Longleaf pine and oak responses to hardwood reduction techniques in fire-suppressed sandhills in northwest Florida, Forest Ecol. Manag., 148, 63-77, 2001.

Reff, A., Bhave, P., Simon, H., Pace, T. S., Pouliot, G. A., Mobley, D., and Houyoux, M.: Emissions inventory of PM2.5 trace elements across the United States, Environ. Sci. Technol., 43, 5790–5796, 2009.

Reid, J. S., Koppmann, R., Eck, T. F., and Eleuterio, D. P.: A review of biomass burning emissions part II: intensive physical properties of biomass burning particles, Atmos. Chem. Phys., 5, 799–825, http://www.atmos-chem-phys.net/5/799/2005/acp-5-799-2005.pdf, last accessed 10 July 2014, 2005.

Robinson, A. L., Donahue, N. M., Shrivastava, M. K., Weitkamp, E. A., Sage, A. M., Grieshop, A. P., Lane, T. E., Jeffrey R. Pierce, J. R., and Pandis, S. N.: Rethinking organic aerosols: semivolatile emissions and photochemical aging, Science, 315, 1259 – 1262, doi:10.1126/science.1133061, 2007.

Saylor, R. D., Edgerton, E. S., and Hartsell, B. E.: Linear regression techniques for use in the EC tracer method of secondary organic aerosol estimation, Atmos. Environ., 40, 7546-7556, 2006.

Schauer, J.J., Rogge, W.F., Hildemann, L.M., Mazurek, M.A., and Cass, G.R.: Source apportionment of airborne particulate matter using organic compounds as tracers, Atmos. Environ., 30, 3837-3855, 1996.

Shilling, J. E., Zaveri, R. A., Fast, J. D., Kleinman, L., Alexander, M. L., Canagaratna, M. R., Fortner, E., Hubbe, J. M., Jayne, J. T., Sedlacek, A., Setyan, A., Springston, S., Worsnop, D. R., and Zhang, Q.: Enhanced SOA formation from mixed anthropogenic and biogenic emissions during the CARES campaign, Atmos. Chem. Phys., 13, 2091-2113, doi:105194/acp-13-2091-2013, 2013.

Southeast Atmosphere Study (SAS): https://www.eol.ucar.edu/field_projects/sas, last access 2 September 2014.

Southern Oxidant and Aerosol Study (SOAS): http://soas2013.rutgers.edu/, last access 2 September 2013.

Surratt, J., Kroll, J., Kleindinst, T., Edney, E., Claeys, M., Sorooshian, A., Ng, N., Offenberg, J., Lewandowski, M., Jaoui, M., Flagan, R., and Seinfeld, J.: Evidence for organosulfates in secondary organic aerosol, Environ. Sci. Technol., 41, 517-527, 2007.

Taylor, N., Collins, D., Spencer, C., Lowenthal, D., Zielenska, B., Samburova, V., and Kumar, N.: Measurement of ambient aerosol hydration state at Great Smoky Mountains National Park in the southeastern United States, Atmos. Chem. Phys., 11, 12085-2011, doi:10.5194/acp-1112085-2011, 2011.

Tang, I. N.: Chemical and size effects of hygroscopic aerosols on light scattering coefficients, J. Geophys. Res., 101 (D14), 19245 – 19250, 1996.

Tanner, R., Parkhurst, W., and McNichol, A.: Fossil sources of ambient aerosol carbon based on ^{14}C measurements, Aerosol Sci. Technol., 38, 133-139, 2004.

Tombach, I.: Estimating Particle-Bound Water in Weighed Sulfate and Nitrate Particles Collected in the Southeast, report prepared for Southern Company, 2004.

Turpin, B. J. and H.-J. Lim: Species contributions to $PM_{2.5}$ mass concentrations: revisiting common assumptions for estimating organic mass, Aerosol Sci. Technol., 25, 602-610, 2001.

U.S. EPA: SPECIATE website, http://www.epa.gov/ttn/chief/software/speciate/ last access October 19, 2015.

U.S. EPA: Research in Action: EPA Positive Matrix Factorization (PMF) Model, http://www.epa.gov/heasd/research/pmf.html, last access 12 November 2014.

Varner, J. M., III, Gordon, D. R., Putz, F. E., and Hiers, J. K.: Restoring fire to long-unburned Pinus palustris ecosystems: novel fire effects and consequences for long-unburned ecosystems, Restor. Ecol., 13, 536-544, 2005.

Wade, D.D., Brock, B.L., Brose, P.H., Grace, J.B., Hoch, G.A., and Patterson, W.A.: Fire in eastern ecosystems, in: Brown & Smith, eds., Wildland Fire in Ecosystems: Effects of Fire on Flora, USDA Forest Service, Rocky Mountain Research Station, Gen. Tech. Rep. RMRS-42, Ogden, UT, 2000.

Washenfelder, R., Attwood, A., Brock, C., Guo, H., Xu, L., Weber, R., Ng, N., Allen, H., Ayres, B., Baumann, K., Cohen, R., Draper, C., Duffey, K., Edgerton, E., Fry, J., Jiminez, J., Palm, B., Romer, P., Stone, E., Woodridge, P., and Brown, S.: Biomass burning dominates brown carbon absorption in the rural southeastern United States. Geophys. Res. Lett., 42, doi:10.1002/2014GL062444, 2015.

Watson, J. G., Chow, J. C., Chen, L.-W. A., Lowenthal, D. H., Fujita, E. M., Kuhns, H. D., Sodeman, D. A., Campbell, D. E., Moosmüller, H., and Zhu, D.Z.: Particulate emission factors for mobile fossil fuel and biomass combustion sources, Sci. Total Environ., 409, 2384-2396, 2011.

Watson, J., Chow, J. C., Lowenthal, D. H., Chen, L.-W. A., Shaw, S., Edgerton, E. S., and Blanchard, C. L.: $PM_{2.5}$ source apportionment with organic markers in the Southeastern Aerosol Research and Characterization (SEARCH) study, J. Air Waste Manage. Assoc, 65, 1104 – 1118, doi:10.1080/10962247.2015.1063551, 2015.

Weber, R.J., Sullivan, A.P., Peltier, R.E., Russell, A., Yan, B., Zheng, M., de Gouw, J., Warneke, C., Brock, C., Holloway, J.S., Atlas, E.L., and Edgerton, E.: A study of secondary organic aerosol formation in the anthropogenic-influenced southeastern United States, J. Geophys. Res., 112, D13302, 2007.

Xu, L., Guo, H., Boyd, C. M., Klein, M., Bougiatioti, A., Cerully, K. M., Hite, J. R., Isaacman-VanWertz, G., Kreisberg, N. M., Knote, C., Olson, K., Koss, A., Goldstein, A. H., Hering, S., de Gouw, J., Baumann, K., Lee, S-H., Nenes, A., Weber, R., and Ng, N. L.: Effects of anthropogenic emissions on aerosol formation from isoprene and monoterpenes in the southeastern United States, P. Natl. Acad. Sci. USA, 112, (1) 37-42, doi:10.1073/pnas.1417609112, 2015a.

Xu, L. Suresh, S., Guo, H., Weber, R., and Ng, N.: Aerosol characterization over the southeastern United States using high-resolution aerosol mass spectrometry: spatial and seasonal variation of aerosol composition and sources with a focus on organic nitrates, Atmos. Chem. Phys., 15, 7307-7336, 2015b.

Yu, S., Bhave, P., Dennis, R., and Mathur, R.: Seasonal and regional variations of primary and secondary organic aerosols over the continental United States: semi-empirical estimates and model evaluation, Environ. Sci. Technol., 41, 4690-4697, 2007.

Zhang, X., Hecobian, A., Zheng, M., Frank, N., and Weber, R.: Biomass burning impact on PM2.5 over the southeastern US during 2007: integrating chemically speciated FRM filter measurements, MODIS fire counts and PMF analysis, Atmos. Chem. Phys., 10, 5839-6853, 2010.

Zheng, M., Cass, G. R., Schauer, J. J., and Edgerton, E. S.: Source apportionment of $PM_{2.5}$ in the southeastern United States using solvent-extractable organic compounds as tracers, Environ. Sci. Technol., 36, 2361-2371, 2002.

Zheng, M., Ke, L., Edgerton E. S., Schauer, J. J., Dong, M., and Russell, A. G.: Spatial distribution of carbonaceous aerosol in the southeastern United States using molecular markers and carbon isotope data, J. Geophys. Res., 111, D10S06, doi:10.1029/2005JD006777, 2006.

Table 1. Five-year seasonal mean EC and OC concentrations at CTR and JST with mean OC/EC.[a]

Period[b]	CTR EC	CTR OC	CTR OC/EC	JST EC	JST OC	JST OC/EC
1999-03W	0.490 ± 0.025	2.615 ± 0.154	5.34	1.725 ± 0.068	4.801 ± 0.153	2.78
1999-03Sp	0.607 ± 0.030	3.411 ± 0.154	5.62	1.410 ± 0.037	4.465 ± 0.096	3.17
1999-03Su	0.537 ± 0.020	3.541 ± 0.100	6.59	1.439 ± 0.035	4.664 ± 0.090	3.24
1999-03A	0.684 ± 0.026	3.814 ± 0.145	5.58	1.808 ± 0.060	5.264 ± 0.150	2.91
2004-08W	0.538 ± 0.036	2.348 ± 0.167	4.37	1.319 ± 0.050	4.099 ± 0.125	3.11
2004-08Sp	0.556 ± 0.029	3.269 ± 0.199	5.88	1.173 ± 0.034	4.283 ± 0.135	3.65
2004-08Su	0.528 ± 0.030	3.267 ± 0.151	6.19	1.292 ± 0.032	4.114 ± 0.077	3.19
2004-08A	0.551 ± 0.024	2.850 ± 0.120	5.17	1.375 ± 0.049	3.852 ± 0.093	2.30
2009-13W	0.402 ± 0.027	2.066 ± 0.136	5.14	0.859 ± 0.060	2.828 ± 0.155	3.29
2009-13Sp	0.354 ± 0.018	2.243 ± 0.117	6.34	0.699 ± 0.039	2.774 ± 0.128	3.97
2009-13Su	0.357 ± 0.017	2.818 ± 0.112	7.89	0.723 ± 0.024	2.870 ± 0.095	3.97
2009-13A	0.437 ± 0.024	2.579 ± 0.105	6.31	0.926 ± 0.042	2.934 ± 0.110	3.05

a. Uncertainties are one standard error of the means. OC/EC is computed as ratios of means. Propagation of errors yields one standard error of OC/EC ranging from 0.30 to 0.49 for CTR (mean 0.41) and 0.10 to 0.29 for JST (mean 0.16).

b. W = Dec, Jan, Feb; Sp = Mar, Apr, May; Su=Jun, Jul, Aug; A = Sep, Oct, Nov

Table 2. Species associated with each PCA factor (component). Component names are keyed to the species. Three species are listed in decreasing order of association for associations of 0.6 or greater (or –0.6 or smaller). Negative values indicate anti-correlation. CO^x and SO_2^x are 1-hour daily maximum CO and SO_2, respectively. O_3^x is 8-hour daily maximum O_3. PCA1, 2008 – 2013; PCA2, 1999 – 2013. N = number of days.

PCA	**Site**	**N**	**Combustion**	**Crustal**	**Seasonal**	**SO_2**	**SO_4**	**Metals**	**Salt**	**Other**
1	BHM	364	CO, NO_x, OC	Al, Si	NO_3	SO_2^x, SO_2	NH_4, SO_4	Zn, Cu, Fe	K	NO_z
1	CTR	383	EC, OC, CO	Si, Fe, Al	NH_3	SO_2, SO_2^x	SO_4, NH_4	Cu, Zn	Na, Cl, Mg	
1	GFP	100	CO, CO^x, NO_x	Si, Fe, Al	O_3^x, NH_3	SO_2, SO_2^x	NH_4, SO_4		Cl, Na, Mg	Ca
1	JST	516	CO, NO_x, EC	Si, Al, Fe	O_3^x, NH_3, -NO_3	SO_2^x, SO_2	NH_4, SO_4		K, Cl, Mg	Na
1	OAK	100	CO^x, CO	Fe, Al, Si	NH_3, O_3^x	SO_2^x, SO_2	SO_4, NH_4	NO_x, Cu, NO_z, Zn	Na, Cl, Mg	
1	OLF	327	NO_x, CO, EC	Si, Al, Fe	NH_3, O_3^x	SO_2, SO_2^x	SO_4, NH_4	Cu	Na, Mg, Cl	
1	PNS	44	CO, NO_x, EC	Si, Al, Fe	O_3^x	SO_2, SO_2^x	NH_4, SO_4		Na, Mg, Cl	
1	YRK	426	NO_x, NO_3, CO	Si, Fe, Al	O_3^x, OC, EC	SO_2^x, SO_2	SO_4, NH_4	Cu	Na, Cl, Mg	Zn
2	BHM	1513	CO, CO^x, NO_x	Al, Si	O_3, O_3^x, -NO_3	SO_2^x, SO_2	NH_4, SO_4	Zn, Cu, Fe		
2	CTR	1258	OC, EC, CO^x	Si, Fe, Al	O_3^x, O_3	SO_2, NO_x, SO_2^x	SO_4, NH_4	Cu		
2	GFP	376	CO^x, CO, NO_x	Si, Fe, Al	O_3, O_3^x	SO_2^x, SO_2	NH_4, SO_4	Cu, Zn		
2	JST	2593	CO, CO^x, NO_x	Si, Al, Fe	NO_3, -O_3^x, -O_3	SO_2^x, SO_2	NH_4, SO_4, O_3^x	Cu		
2	OAK	707	CO^x, CO, EC	Si, Fe, Al	O_3, O_3^x	SO_2^x, SO_2	SO_4, NH_4	Cu, Zn		
2	OLF	948	CO^x, CO, NO_x	Si, Fe, Al	O_3, O_3^x	SO_2^x, SO_2	NH_4, SO_4, NO_z	Zn, Cu		
2	PNS	445	EC, CO, NO_x	Si, Al, Fe	O_3^x, O_3, SO_4, NH_4	SO_2^x, SO_2		Cu		NO_z
2	YRK	1435	CO^x, NO_x, NO_3	Si, Fe, Al	O_3^x, SO_4, O_3, NH_4	SO_2^x, SO_2		Cu		Zn

Table 3. Mean OC concentrations associated with components identified by PCA1 (2008 – 2013) and PCA2 (1999 – 2013). NS = not statistically significant, NA = not applicable (component not present in PCA). Units are μg m^{-3}. Standard errors of the means ranged from 0.003 to 0.09 μg m^{-3} (up to 0.25 μg m^{-3} for PNS PCA1).

PCA	**Site**	**N**	**Combustion**	**Crustal**	**Seasonal**	**SO_2**	**SO_4**	**Metals**	**Salt**	**Other**
1	BHM	364	1.36	0.09	0.40	0.35	0.45	0.15	0.14	0.10
1	CTR	383	1.28	0.26	0.56	NS	0.33	NS	NS	NA
1	GFP	100	0.95	NS	0.45	0.15	0.25	NS	-0.41	0.62
1	JST	516	1.09	0.16	0.49	0.07	0.27	NA	0.64	0.11
1	OAK	100	0.40	NS	0.50	0.37	0.53	0.32	-0.27	NA
1	OLF	327	0.74	-0.08[a]	0.52	0.16	0.27	NS	-0.09[a]	NA
1	PNS	44	1.95	NS	0.33	NS	0.56	NA	-0.63	NA
1	YRK	426	0.14	0.14	1.09	NS	0.26	0.16	0.15	0.47
2	BHM	1513	1.60	0.19	0.47	0.38	0.57	0.48	NA	NA
2	CTR	1258	1.50	0.12	0.69	NS	0.66	NS	NA	NA
2	GFP	376	0.72	0.14	0.37	0.21	0.50	0.25	NA	NA
2	JST	2593	2.58	0.32	0.06[b]	NS	1.01[b]	0.13	NA	NA
2	OAK	707	1.50	NS	0.47	NS	0.59	NS	NA	NA
2	OLF	948	0.81	-0.06[a]	0.25	0.09	1.02	0.20	NA	NA
2	PNS	445	1.55	NS	0.45[c]	0.17	NA	NS	NA	0.36
2	YRK	1435	0.76	0.20	1.40[c]	0.05	NA	0.39	NA	0.29

a. OLF PCA1 and PCA2 crustal and PCA1 salt OC mean concentrations are negative due to inverse associations of OC with crustal and salt components at OLF (Tables S7 and S12).

b. JST PCA2 seasonal OC is associated with NO_3; JST PCA2 SO_4 component includes OC associated with O_3 (Table 2).

c. PNS and YRK PCA2 seasonal components include OC associated with SO_4 (Table 2).

Table 4. Ranges of mean OC concentrations associated with each PCA component. The time period is 2009 – 2013. For each site, multiple methods were compared using a common set of days. For CTR (6 methods), both the standard deviation and one-half the range of component mean concentrations are shown. For JST (3 methods), one-half the range of component mean concentrations is shown. For YRK (2 PCA methods), ranges are shown. YRK ranges are smaller than ranges for CTR and JST because no PMF analyses were carried out for YRK. The larger ranges for CTR and JST compared with YRK reflect the larger differences between PCA and PMF.

	CTR[a]				JST[b]		YRK[c]	
Component	Range/2 (μg m^{-3})	Range/2 (% of mean)	Std Dev (μg m^{-3})	Std Dev (% of mean)	Range/2 (μg m^{-3})	Range/2 (% of mean)	Range (μg m^{-3})	Range (% of mean)
Combustion	0.44	18	0.30	12	0.34	12	0.34	14
Crustal	0.09	4	0.07	3	0.11	4	0.09	4
Sulfate	0.15	6	0.11	4	0.19	7	0.26	11
Seasonal	0.36	15	0.25	10	0.43	15	0.12	5
SO$_2$					0.03	1	0.03	1
Metals					0.07	2	0.04	2
Salt					0.33	12	0.16	7
Other					0.05	2	0.16	7

a. Mean OC = 2.43 μg m^{-3}, n = 383 days, number of methods = 6 (4 PCA, 2 PMF)

b. Mean OC = 2.85 μg m^{-3}, n = 398 days, number of methods = 3 (2 PCA, 1 PMF)

c. Mean OC = 2.40 μg m^{-3}, n = 426 days, number of methods = 2 (2 PCA)

Table 5. Mean OC concentrations determined for the period 2008 – 2013 using four analytical approaches: (1) multivariate regression (“POC” and “SOC”, Blanchard et al., 2008), (2) calculation of OCbb from Kbb tracer, (3) PCA and PMF analysis, and (4) CMB receptor-modeling (Blanchard et al., 2013, updated). Row indentations indicate subcategories. Units are μg m^{-3} unless specified as %.

Component	**BHM**	**CTR**	**GFP**	**JST**	**OAK**	**OLF**	**PNS**	**YRK**	**Unc**[a]
OC (mean measured)	2.91	2.41	1.91	2.86	1.84	1.81	2.06	2.33	0.05
“POC”[b]	1.85	1.78	1.40	2.12	1.35	1.36	1.57	1.61	25%
OCbb	1.58	1.60	1.64	1.40	1.63	1.62	1.77	1.37	2X
PCA1 Combustion	1.36	1.28	0.95	1.07	0.40	0.85	1.95	0.13	0.3 - 0.6
PCA2 Combustion	1.09	1.47	0.45	1.83	0.87	0.60	1.26	0.49	0.3 - 0.6
PMF Combustion	NA	1.03	NA	1.22	NA	NA	NA	NA	0.3 - 0.6
CMB Combustion Total	2.54	1.52	1.33	2.16	1.42	1.47	1.89	1.49	0.87
CMB Area Sources	2.01	1.44	1.15	1.50	1.35	1.34	1.68	1.35	20 - 33%
CMB Mobile Diesel	0.20	0.02	0.05	0.27	0.01	0.05	0.04	0.04	13 - 31%
CMB Mobile Gas	0.29	0.03	0.10	0.34	0.03	0.05	0.15	0.06	17 - 41%
CMB Point Sources	0.05	0.02	0.02	0.05	0.02	0.03	0.03	0.04	5 - 6%
PCA1 Crustal	0.09	0.26	0.00	0.15	0.00	-0.14	0.00	0.14	0.09 - 0.11
PCA2 Crustal	0.20	0.12	0.17	0.35	0.00	-0.06	0.00	0.22	0.09 - 0.11
PMF Crustal	NA	0.09	NA	0.17	NA	NA	NA	NA	0.09 - 0.11
CMB Dust	0.09	0.02	0.04	0.03	0.03	0.02	0.04	0.01	9 - 22%
“SOC”[b]	1.10	0.66	0.56	0.75	0.48	0.48	0.50	0.77	25%
PCA1 Seasonal+Sulfate	0.85	0.90	0.70	0.76	1.03	1.00	0.90	1.26	0.3 - 0.5
PCA1 Seasonal	0.39	0.57	0.45	0.49	0.50	0.71	0.33	1.00	0.1 - 0.4
PCA1 Sulfate	0.45	0.33	0.25	0.27	0.53	0.29	0.56	0.26	0.2 - 0.3
PCA2 Seasonal+Sulfate	0.92	0.95	0.81	0.76	0.99	0.93	0.41	0.86	0.3 - 0.5
PCA2 Seasonal	0.51	0.53	0.40	0.05	0.40	0.28	0.41	0.86	0.1 - 0.4
PCA2 Sulfate	0.42	0.42	0.41	0.71	0.58	0.65	0.00	0.00	0.2 - 0.3
PMF Seasonal+Sulfate	NA	0.77	NA	1.32	NA	NA	NA	NA	0.3 - 0.5
PMF Seasonal	NA	0.49	NA	0.86	NA	NA	NA	NA	0.1 - 0.4
PMF Sulfate	NA	0.28	NA	0.46	NA	NA	NA	NA	0.2 - 0.3
N days (2008 - 2013, varies by analysis)	366 - 1313	383 - 606	100 -280	443 - 787	100 - 206	327 - 598	44 - 162	426 - 585	

a. Uncertainty for mean measured OC is 1 standard error of the mean. Uncertainties for PCA and PMF are taken from Section 3.5.3. Uncertainty for CMB combustion total is RMSE across sites and years, where error is defined as the difference between predicted and observed concentrations. Uncertainty for CMB components is based on uncertainties in inputs and across alternative versions of the model expressed as 1-sigma % of prediction (Blanchard et al., 2013).

b. “POC” is the sum of OC associated with EC, CO, and Kbb. “SOC” is the sum of OC associated with O_3, and SO_4. “POC” is used as a fitting species in CMB.

Figure Captions

Figure 1. Seasonal mean EC and OC concentrations at CTR and JST. All correlations among the four time series are statistically significant ($p < 0.05$): CTR EC and OC, r = 0.68 (95% CI 0.52 – 0.80); JST EC and OC, r = 0.87 (95% CI 0.79 – 0.92); CTR EC and JST EC, r = 0.76 (95% CI 0.62 – 0.85); CTR OC and JST OC, r = 0.68 (95% CI 0.51 – 0.79).

Figure 2. Statistical distributions of the ratio OM*/OC computed for daily-average measurements at SEARCH sites, 2009 – 2013. The distributions show the 10th, 25th, 50th, 75th, and 90th percentiles. OM* is the sum of measured OC and the computed difference of $PM_{2.5}$ mass minus the sum of measured species concentrations.

Figure 3. Monthly-average measured OC (solid blue line) and computed biomass burning OCbb (solid green line with surrounding shaded area indicating estimated uncertainty) at CTR. Trends in OC (dashed blue line) are statistically significant ($p < 0.05$); trends in OCbb (dashed green line) are not statistically significant.

Figure 4. Trends in source contributions to OC at CTR and JST determined from PCA2 for 1999 - 2013.

1758

1759

1760

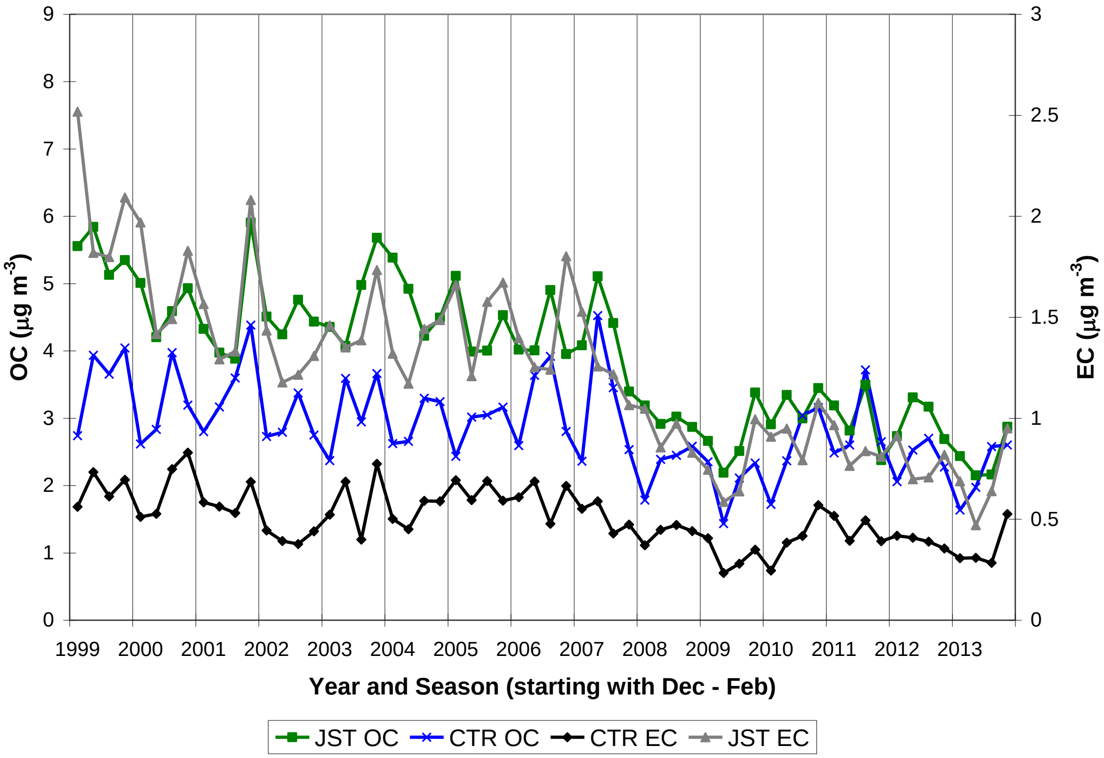

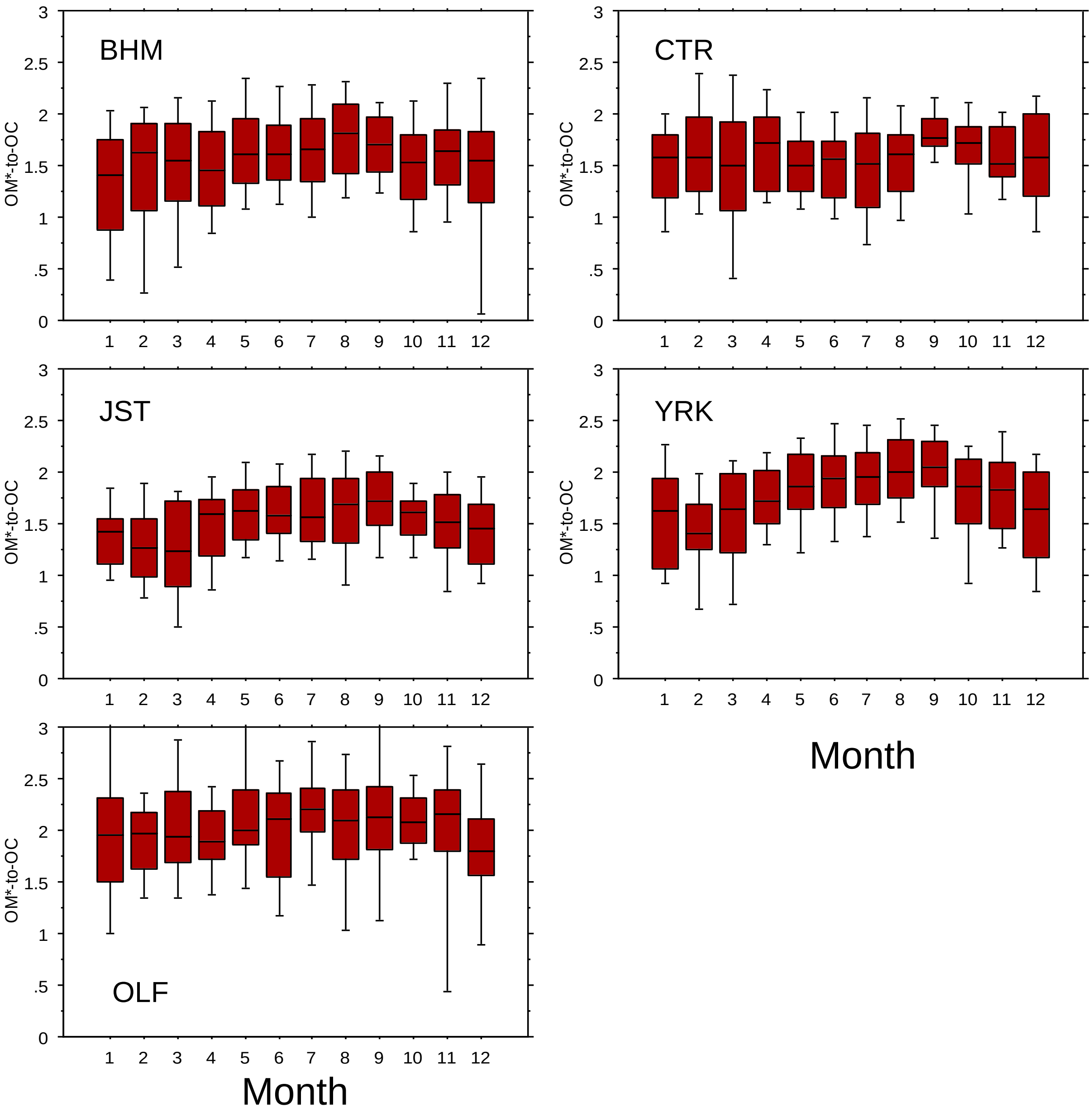
BHM
CTR
JST
YRK
OLF
OM*-to-OC
0
.5
1
1.5
2
2.5
3
1 2 3 4 5 6 7 8 9 10 11 12
Month

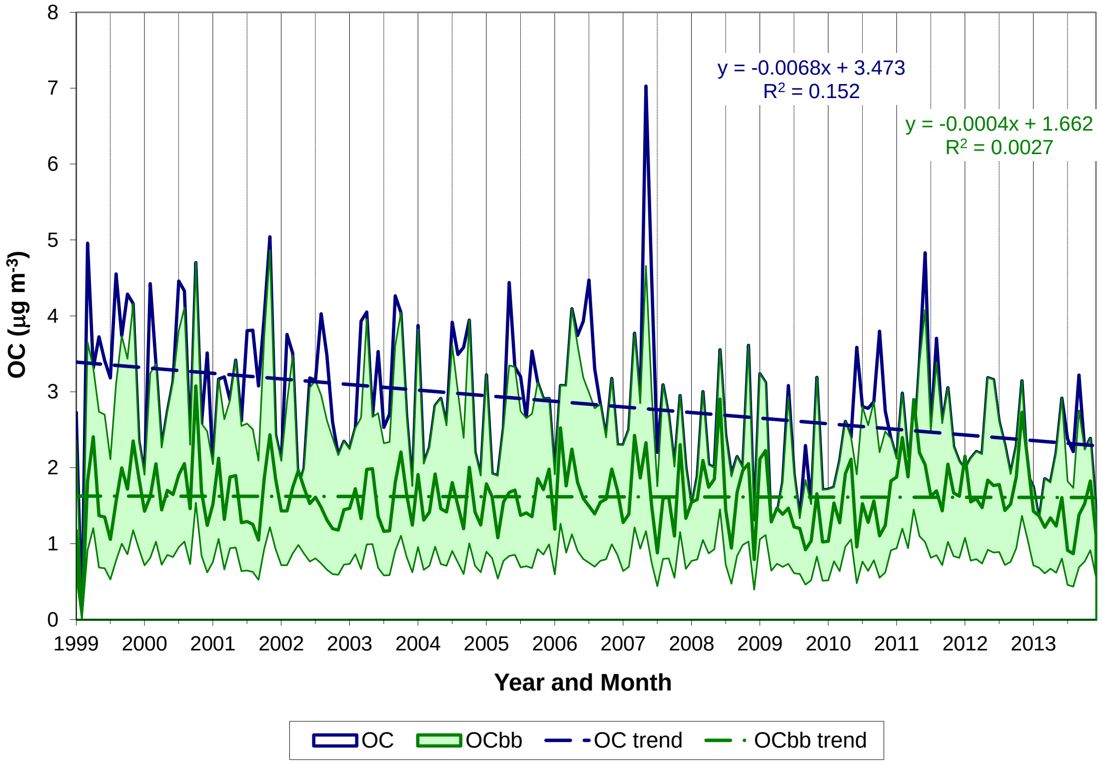
y = -0.0068x + 3.473
R² = 0.152
y = -0.0004x + 1.662
R² = 0.0027
OC (µg m⁻³)
0
1
2
3
4
5
6
7
8
1999
2000
2001
2002
2003
2004
2005
2006
2007
2008
2009
2010
2011
2012
2013
Year and Month
OC
OCbb
OC trend
OCbb trend

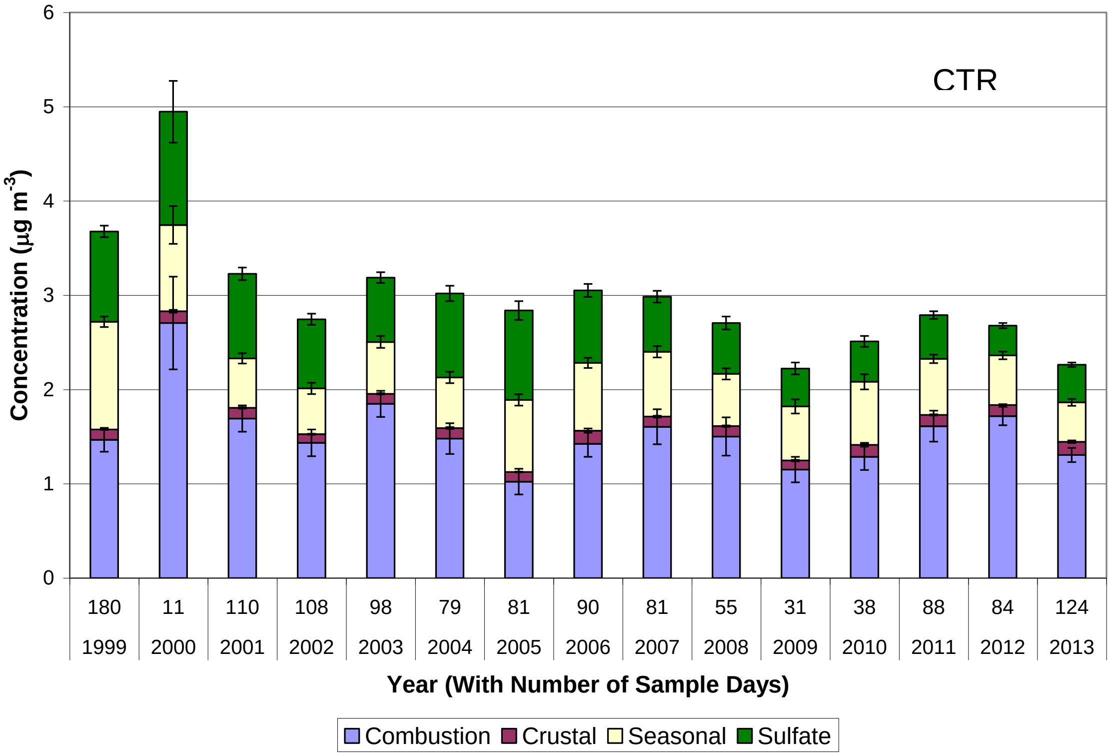
CTR
Concentration (µg m-3)
0
1
2
3
4
5
6
180
1999
11
2000
110
2001
108
2002
98
2003
79
2004
81
2005
90
2006
81
2007
55
2008
31
2009
38
2010
88
2011
84
2012
124
2013
Year (With Number of Sample Days)
Combustion
Crustal
Seasonal
Sulfate

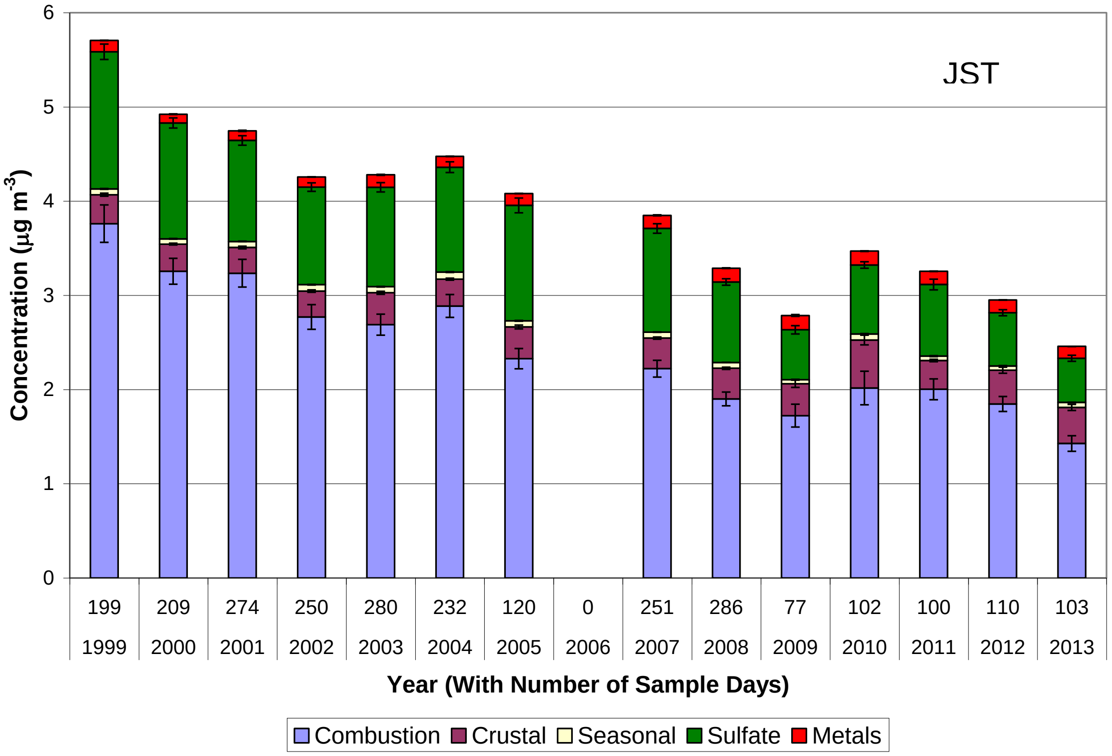
JST
Concentration (µg m-3)
0
1
2
3
4
5
6
199
1999
209
2000
274
2001
250
2002
280
2003
232
2004
120
2005
0
2006
251
2007
286
2008
77
2009
102
2010
100
2011
110
2012
103
2013
Year (With Number of Sample Days)
Combustion
Crustal
Seasonal
Sulfate
Metals

Supplemental Information

19 tables, 32 figures

Table S1. Aggregated estimates of composite OC and SOA (SOC) from various regional and local studies in the southeastern US using different methodologies. Unless otherwise stated, SOA (SOC) includes isoprene products and other products from reactions involving terpenoids and anthropogenic VOCs. Averages reported are shown for time periods listed. Investigators have used different terminologies with analytical methods (e.g., Figure S1), and analyses over different time periods, so that comparison of the OC percentages is necessarily qualitative to illustrate a range of SOC fractions, including natural components. A detailed comparison of methods, time periods, and analysis limitations is not attempted within the scope of the present study.

Investigators	**Time Period**	**Method**[a]	**Rural**		**Urban**		**Comments and Notes**
			SOC or SOA (µg m^{-3})	**%OC**	**SOC or SOA** (µg m^{-3})	**%OC**	
Lim and Turpin (2002)	Summer 99	EC Tracer	--	--	8.3	46	Regression by Deming method—ATL (JST)[e]
Saylor et al. (2006)	02	EC Tracer	1.1	30	1.8	32	Regression by York method-ATL, BHM; CTR,YRK
Zheng et al. (2006)	Sept 03-Jan 04	CMB-MM OA-POA	5.7	34	6.5	36	BHM, ATL; CTR SOC may include POA
Gao et al. (2006)	June 04	Filter MS-GC tracer; LCMS	0.3	9.1	0.2	6.3	JST, BHM; CTR total identified OA as SOA; mostly terpene derivatives
Weber et al. (2007)	June 04	Filter WSOC	--	--	2.8	58	ATL; (SOA=WSOC, estimated 70-80% biogenic)
Yu et al. (2007)	<06	Semi-empirical regional EC tracer	--	--	1.01[c]	35	semi-empirical continental-Southeast 7 sites GA, AL, SouthTN
Ding et al (2008)	04-05	CMB-MM; ^{14}C	0.6 (SOC_f) 2.5 (SOC_c)	78[g]	2.3 (SOC_f) 2.2 (SOC_c)	66[g]	SOC=fossil (SOC_f)+ contemporary (SOCc) BHM,ATL; CTR
Blanchard et al. (2008)	01-04	EC tracer; regression; mass balance; ^{14}C[b]	--	36-41	--	15-48	Annual 01-04. ATL, BHM; CTR; range depends on method used
Kleindienst et al. (2010)	05	Filter GCMS tracer; SOC mass fraction from lab. study	2.37[d]	42	2.05[d]	20	BHM, CTR (reported as SOA)
Chan et al. (2010)	Aug-Sept 08	Filter GCMS GCToFMS/tracers	0.1-1.4	(10.7 isoprene)	0.1-0.9	(7.4 isoprene)	ATL YRK; estimates from sum of isoprene products or from Kleindienst et

								al. tracer (day night separation)[g]
Zhang et al. (2010)	07	Filter WSOC	--	--	--	56		15 sites in Southeast (light absorbing WSOC=SOC)
Blanchard et al. (2013)	02-11	Integrated gas particle CMB	--	--	1.8	45		ATL composite OA = 4 ug/m3 exclude unaccounted for mass
Budisulistiorini et al (2013)	Summer 11	ACSM (AMS)	--	--	9	82 (33 isoprene)[f]		ATL. Mostly correlations between identified components of aerosol mass from PMF
Lin et al (2013)	Summer 10	Filter GC-EI-MS	--	(12-19 isoprene)[f]	--	--		YRK; OM% isoprene derivatives only; both low and High NOx contributions
Lewandowski et al. (2014)	May-Aug 05	Filter GCMS tracers; SOC mas fraction from lab study	2.37[d]	36	1.8[d]	17		ATL, BHM; CTR; differentiates biogenic SOC from anthropogenic SOC
Xu et al. (2015a, b)	June-July 13 (SOAS); ~ 1 yr (12-13-SCAPE)	HRToFMS and ACSM	4.5	89 (18 isoprene)[f]	9.1	69 (21 isoprene)[f]		ATL, CTR, (summer); PM1; OA—segregated with SOA sum of LO-OOA, MO-OOA ; seasonal isoprene OA only in summer; particle nitrate OA discussed
Liao et al. (2015)	May-June 12	(NOAA) PALMS	--	(2.2 IEPOXSO4)	--	--		Aircraft near ground values IEPOX-SO4 only
Hu et al (2015)	June-July 2013	AMS low NOx (Quant. PMF of AMS signal)	--	(17 IEPOX SO4)	--	--		Includes detils of IEPOX SO4 estimation, notes biomass burning ambiguity.
Kim et al. (2015)	Summer-fall 13	Various air-ground meas./ modeling	--	60	--	--		Integration of ground and aircraft obs.in SE. Values represent 1.5-3 km altitude; biogenic includes isoprene and terpenoid derivatives—anthropogenic SOA excluded
This study (2015)	00-13	Tracer/mass balance/PCA	2.9	39	3.9	26		CTR, ATL; SOC based on PCA1; SOC=

	using SEARCH carbon and associated data		seasonal and SO4 contributions

---

[a] Methods include analytical techniques, air quality modeling and data analysis and interpretation. Instrumentation for analysis includes thermal differentiation for OC and BC, gas chromatogrphy-mass spectroscopy (GCMS, high resolution time of flight mass spectroscopy (HRToFMS), water extraction and liquid chromatography-mass spectroscopy, aerosol mass spectroscopy (AMS), carbon isotope analysis, particle analysis laser mass spectrometer (PALMS), and aerosol chemical speciation monitor (ACSM).

[b] Data set included SEARCH public archives.

[c] Southeastern region (15 monitoring sites for OC and EC) stated in urban category, but includes rural sites.

[d] Reported as $\mu gC/m^{-3}$; estimates of SOC mainly isoprene and monoterpene derivatives

[e] The SEARCH network sites included in studies were Jefferson Street, Atlanta, GA (JST or ATL), Centreville, AL (CTR), Yorkville, GA (YRK) and Birmingham, AL (BHM). A site locator map and description is found in Hidy et al. (2014).

[f] Parentheses isoprene derivative component of OC or OA (OM) only from AMS assignment.

[g] %OC is calculated as sum of fossil and contemporary SOC; values average over four seasons

Table S2. Primary air pollutant emissions within AL, GA, MS, and NW FL in 2013. Units are 1000 metric tons per year. $PM_{2.5}$ species were determined from NEI emissions of $PM_{2.5}$ mass using SPECIATE or from the EPA MOVES model (EC and OC from on-road diesel and gasoline). Zero values indicate emissions less than one-half the smallest reported significant figure (1 or 0.1 thousand metric tons). Source categories are defined in Blanchard et al. (2013).

			Speciated $PM_{2.5}$ Emissions								
Sector	CO	NO_x	EC	OC	K	Al	Ca	Fe	Si	SO_2	VOC
Agriculture	0	0	0.0	1.1	0.8	3.3	0.9	2.1	9.1	0	0
Area	294	11	3.9	16.4	2.4	0.0	0.0	0.0	0.1	0	246
Vegetation & soil	526	43	0.0	0.0	0.0	0.0	0.0	0.0	0.0	0	5008
Commercial	5	7	0.1	0.1	0.0	0.0	0.0	0.0	0.0	4	0
Dust	0	0	0.3	6.3	1.6	4.5	6.6	4.0	14.5	0	0
EGU	25	98	0.1	0.2	0.0	0.2	0.2	0.1	0.4	247	2
Fires	1996	39	8.1	89.0	2.7	0.2	0.3	0.1	0.2	16	314
Industrial	155	162	1.3	4.8	0.7	0.8	0.4	0.4	2.3	110	132
Nonroad	686	147	5.2	2.4	0.0	0.0	0.0	0.0	0.0	3	107
Residential	35	10	0.3	2.4	0.0	0.0	0.0	0.0	0.0	0	6
On-road diesel	43	125	4.1	1.4	0.0	0.0	0.0	0.0	0.0	0	10
On-road gas	1129	133	0.3	1.3	0.0	0.0	0.0	0.0	0.0	1	60
Sum	4893	775	24	125	8	9	8	7	27	382	5886

Table S3. Correlations (r^2) among mean OC, EC, and SO_4 based on annual, seasonal, and monthly averaging periods and on daily measurements. Summer is defined as June through August, winter is December through February, autumn is September through November, and spring is March through May.

Site	Pair	Annual (n=15)	Seasonal (n=60)	Monthly (n=180)	Monthly-Winter (n=45)	Monthly-Summer (n=45)	Daily All (n = 1382-3993)	Daily 2009-13 (n = 110 - 558)	Daily-Jan (n = 106 - 338)	Daily-July (n = 150 - 345)
BHM	OC-EC	0.931	0.856	0.803	0.841	0.696	0.719	0.692	0.836	0.553
BHM	OC-SO4	0.843	0.425	0.331	0.305	0.690	0.211	0.127	0.057	0.514
BHM	EC-SO4	0.834	0.349	0.258	0.219	0.603	0.135	0.046	0.064	0.362
CTR	OC-EC	0.736	0.470	0.508	0.653	0.402	0.648	0.602	0.805	0.533
CTR	OC-SO4	0.772	0.492	0.350	0.293	0.360	0.181	0.181	0.024	0.520
CTR	EC-SO4	0.846	0.317	0.223	0.311	0.428	0.166	0.104	0.051	0.561
GFP	OC-EC	0.894	0.749	0.718	0.689	0.711	0.680	0.708	0.712	0.541
GFP	OC-SO4	0.730	0.181	0.158	0.086	0.554	0.166	0.112	0.057	0.361
GFP	EC-SO4	0.801	0.054	0.054	0.146	0.487	0.084	0.086	0.097	0.189
JST	OC-EC	0.910	0.762	0.706	0.756	0.537	0.645	0.668	0.661	0.343
JST	OC-SO4	0.854	0.276	0.191	0.350	0.552	0.099	0.084	0.144	0.365
JST	EC-SO4	0.876	0.200	0.153	0.315	0.680	0.076	0.019	0.174	0.335
OAK	OC-EC	0.731	0.666	0.647	0.904	0.397	0.842	0.594	0.964	0.605
OAK	OC-SO4	0.702	0.110	0.129	0.257	0.523	0.060	0.066	0.016	0.402
OAK	EC-SO4	0.591	0.004	0.021	0.332	0.483	0.052	0.037	0.026	0.359
OLF	OC-EC	0.840	0.701	0.574	0.673	0.517	0.590	0.684	0.748	0.520
OLF	OC-SO4	0.721	0.361	0.316	0.321	0.651	0.238	0.103	0.100	0.559
OLF	EC-SO4	0.875	0.349	0.223	0.239	0.800	0.168	0.036	0.121	0.342
PNS	OC-EC	0.930	0.858	0.767	0.770	0.539	0.724	0.902	0.779	0.490
PNS	OC-SO4	0.568	0.006	0.030	0.089	0.700	0.088	0.043	0.024	0.569
PNS	EC-SO4	0.592	0.000	0.002	0.059	0.679	0.041	0.050	0.024	0.307
YRK	OC-EC	0.839	0.636	0.546	0.774	0.489	0.554	0.651	0.705	0.413
YRK	OC-SO4	0.800	0.619	0.451	0.454	0.568	0.304	0.215	0.104	0.502
YRK	EC-SO4	0.764	0.414	0.293	0.453	0.782	0.253	0.097	0.096	0.391

Table S4. PCA1 and PCA2 orthogonal factors for SEARCH BHM daily data. PCA1: n = 364, variance explained = 78%. PCA2: n = 1513, variance explained = 77%.

PCA1	Combustion	Crustal	Seasonal	SO_2	SO_4	Metals	Salt	Other
CO	0.817	0.058	0.12	0.171	0.164	0.156	0.001	0.288
CO_max1	0.619	0.144	0.058	0.284	0.16	0.062	-0.039	0.323
NO_x	0.806	0.069	0.285	0.065	-0.034	0.295	-0.029	0.188
EC	0.744	0.068	-0.091	0.321	0.16	0.155	0.051	0.137
OC	0.784	0.063	-0.159	0.238	0.315	0.087	0.122	0.073
NO_z	0.409	0.062	0.127	-0.011	-0.007	-0.044	0.021	0.631
K	0.223	0.054	-0.035	-0.019	0.128	0.005	0.814	0.095
Al	0.106	0.949	-0.036	-0.063	0.006	0.078	0.06	0.016
Si	0.135	0.86	-0.069	0.116	0.048	0.3	0.105	0.21
Fe	0.394	0.373	0.186	0.002	0.043	0.677	-0.056	-0.135
Ca	0.237	0.199	-0.02	0.256	0.274	0.17	0.19	0.552
O_3_max8	0.282	0.062	-0.577	0.197	0.486	-0.112	-0.055	0.08
NH_3	0.552	0.129	-0.395	0.087	0.284	0.078	0.101	0.022
NO_3	0.144	-0.044	0.833	0.028	0.122	0.06	-0.048	0.108
SO_2_max1	0.296	-0.012	-0.055	0.861	0.168	0.01	0.037	0.08
SO_2	0.389	-0.002	-0.013	0.828	0.187	0.086	0.012	0.101
NH_4	0.198	-0.03	0.117	0.122	0.945	0.017	0.018	0.047
SO_4	0.111	0.056	-0.088	0.137	0.929	0.07	0.108	0.072
Na	-0.108	0.255	0.289	0.376	-0.051	-0.026	0.417	-0.266
Cl	0.649	-0.034	0.306	-0.001	-0.178	0.221	0.306	-0.106
Mg	-0.12	0.184	-0.116	0.161	0.013	0.527	0.544	0.426
Cu	0.399	0.137	0.072	-0.083	0.068	0.761	0.081	-0.124
Zn	0.083	0.052	-3.25E-04	0.106	0.001	0.858	0.015	0.188

PCA2	Combustion	Crustal	Seasonal	SO_2	SO_4	Metals
CO	0.91	0.054	-0.127	0.14	0.062	0.212
CO_max1	0.815	0.12	-0.066	0.188	0.053	0.109
NO_x	0.81	0.035	-0.264	0.116	-0.169	0.306
EC	0.758	0.082	0.094	0.228	0.136	0.28
OC	0.745	0.068	0.195	0.148	0.303	0.204
NO_z	-0.159	0.07	0.02	0.085	0.493	0.1
nsK	0.7	0.312	0.054	0.177	0.145	-0.043
Al	-0.036	0.921	0.105	-0.038	-0.036	-0.017
Si	0.309	0.894	0.075	0.109	0.028	0.126
Fe	0.289	0.566	-0.029	0.104	0.04	0.653
Ca	0.334	0.557	0.033	0.119	0.134	0.428
O_3_max8	0.267	0.086	0.78	0.101	0.422	-0.01
O_3_24hr	-0.042	0.004	0.823	0.019	0.39	-0.091
NO_3	0.197	-0.077	-0.751	0.04	0.263	0.009
SO_2_max1	0.307	0.062	0.038	0.908	0.121	0.058
SO_2	0.482	0.088	-0.001	0.793	0.196	0.129
NH_4	0.285	0.002	0.05	0.075	0.905	-0.04
SO_4	0.26	0.072	0.204	0.081	0.854	-0.002
Cu	0.145	-0.02	-0.031	-0.012	-0.018	0.72
Zn	0.224	0.14	-0.047	0.112	0.083	0.764

Table S5. PCA1 and PCA2 orthogonal factors for SEARCH CTR daily data. PCA1: n = 383, variance explained = 79%. PCA2: n = 1258, variance explained = 79%.

PCA1	Combustion	Crustal	Seasonal	SO_2	SO_4	Metals	Salt	Other
CO	0.742	-0.14	-0.118	0.194	0.205	0.238	-0.132	
CO_max1	0.669	-0.066	-0.158	0.144	0.177	0.049	-0.108	
NO_x	0.238	-0.094	-0.531	0.453	-0.152	0.361	-0.197	
EC	0.794	-0.017	0.132	0.111	0.145	0.141	-0.081	
OC	0.784	0.169	0.348	0.011	0.196	-0.002	-0.037	
NO_z	0.566	-0.016	0.055	0.487	0.19	0.342	-0.053	
K	0.769	0.085	0.095	-0.064	0.017	0.021	0.163	
Al	-0.037	0.951	0.018	-0.103	-0.054	-0.127	0.077	
Si	-0.053	0.963	0.057	-0.07	-0.036	-0.109	0.092	
Fe	0.057	0.955	0.044	0.065	0.08	0.064	0.084	
Ca	0.088	0.51	0.065	0.231	0.256	0.199	0.186	
O_3_max8	0.395	-0.068	0.593	0.299	0.231	0.255	-0.117	
NH_3	0.409	0.148	0.689	-0.025	-0.092	0.121	0.058	
NO_3	0.27	-0.046	-0.535	0.308	-0.057	0.297	0.219	
SO_2_max1	0.041	0.01	0.011	0.902	0.066	-0.06	-0.076	
SO_2	0.141	0.024	-0.102	0.917	0.142	0.051	-0.078	
NH_4	0.305	0.011	0.014	0.145	0.893	0.117	-0.051	
SO_4	0.254	0.091	0.077	0.073	0.927	0.01	-3.62E-04	
Na	-0.039	0.046	0.022	-0.025	0.018	-0.012	0.883	
Cl	-0.083	0.027	-0.085	-0.097	-0.023	0.084	0.86	
Mg	0.01	0.352	0.026	-0.065	-0.049	-0.109	0.791	
Cu	0.032	-0.004	0.068	-0.094	0.025	0.791	-0.033	
Zn	0.293	-0.042	-0.081	0.173	0.107	0.741	0.047	

PCA2	Combustion	Crustal	Seasonal	SO_2	SO_4	Metals
CO	0.682	-0.139	0.016	0.446	0.045	0.234
CO_max1	0.715	-0.082	0.017	0.397	0.002	0.169
NO_x	0.173	-0.074	-0.211	0.836	-0.025	0.039
EC	0.728	-0.044	0.217	0.189	0.357	-0.012
OC	0.765	0.057	0.311	-0.012	0.347	-0.105
NO_z	0.37	-0.017	0.522	0.41	0.222	0.035
nsK	0.741	0.26	0.19	0.023	-0.001	-0.056
Al	-0.03	0.936	-0.133	-0.169	-0.061	-0.021
Si	0.005	0.967	-0.039	-0.133	-0.024	-0.067
Fe	0.063	0.952	0.026	0.078	0.077	0.081
Ca	0.069	0.575	0.383	0.287	0.049	0.086
O_3_max8	0.244	9.53E-07	0.862	-0.014	0.333	0.016
O_3_24hr	0.204	-0.021	0.879	-0.089	0.269	0.016
NO_3	0.231	-0.021	-0.27	0.614	0.083	0.063
SO_2_max1	0.038	0.012	0.2	0.808	0.058	-0.203
SO_2	0.103	-0.001	0.208	0.878	0.09	-0.162
NH_4	0.233	-0.007	0.281	0.166	0.897	-0.038
SO_4	0.137	0.031	0.289	0.038	0.917	-0.047
Cu	0.009	0.025	-0.003	-0.163	-0.091	0.852
Zn	0.243	0.053	0.18	0.587	0.11	0.496

Table S6. PCA1 and PCA2 orthogonal factors for SEARCH GFP daily data. PCA1: n = 100, variance explained = 79%. PCA2: n = 376, variance explained = 79%.

PCA1	Combustion	Crustal	Seasonal	SO_2	SO_4	Metals	Salt	Other
CO	0.927	-0.083	0.17	0.005	0.044		-0.133	0.103
CO_max1	0.915	-0.035	0.112	-0.044	-0.045		-0.165	2.63E-04
NO_x	0.904	-0.015	-0.06	0.212	-0.162		-0.074	0.033
EC	0.753	-0.068	0.262	0.042	0.266		-0.21	0.251
OC	0.554	-0.066	0.389	0.111	0.201		-0.282	0.4
NO_z	0.45	0.087	0.421	0.031	0.306		-0.007	0.132
K	0.342	-0.083	0.35	-0.049	0.212		0.214	0.608
Al	-0.105	0.98	-0.001	-0.033	0.047		0.072	0.056
Si	-0.083	0.985	0.021	-0.029	0.041		0.05	0.06
Fe	0.124	0.98	0.02	0.032	0.039		0.033	0.043
Ca	0.059	0.195	-0.066	0.002	-0.051		-0.042	0.881
O_3_max8	0.202	0.019	0.747	-0.221	0.165		-0.291	-0.007
NH_3	0.28	0.062	0.628	-0.023	-0.186		-0.047	0.043
NO_3	0.52	-0.088	-0.152	0.049	0.433		0.245	0.286
SO_2_max1	0.044	-0.025	-0.065	0.94	-0.003		-0.12	-0.023
SO_2	0.125	-0.024	-0.041	0.956	0.019		-0.021	0.019
NH_4	0.17	-0.039	0.04	0.043	0.952		-0.078	0.023
SO_4	-0.005	0.149	0.069	-0.002	0.931		-0.042	-0.006
Na	-0.077	0.087	0.068	0.034	-0.111		0.809	-0.081
Cl	-0.114	-0.028	-0.236	-0.109	0.053		0.826	0.046
Mg	-0.374	0.352	-0.075	-0.225	-0.039		0.62	0.185
Cu	0.448	0.071	-0.437	-0.114	-0.167		-0.176	0.038
Zn	0.744	0.007	0.135	0.38	0.08		-0.016	-0.058

PCA2	Combustion	Crustal	Seasonal	SO_2	SO_4	Metals
CO	0.913	-0.109	0.053	0.022	0.158	0.083
CO_max1	0.93	-0.056	0.019	-0.013	0.014	0.057
NO_x	0.853	-0.027	-0.279	0.212	-0.095	0.188
EC	0.679	0.098	0.098	0.095	0.408	0.192
OC	0.538	0.132	0.295	0.17	0.498	0.256
NO_z	0.553	-0.017	0.098	0.196	0.16	-0.126
nsK	0.126	0.413	0.003	-0.083	0.447	0.388
Al	-0.087	0.971	-0.062	-0.034	-0.011	-0.069
Si	-0.078	0.983	-0.035	-0.035	-0.012	-0.043
Fe	0.009	0.972	-0.051	0.021	-0.005	0.048
Ca	0.024	0.887	0.117	0.004	0.073	0.159
O_3_max8	0.233	0.01	0.879	-0.088	0.287	0.056
O_3_24hr	-0.053	-0.047	0.895	-0.132	0.247	-0.019
NO_3	0.369	0.009	-0.482	-0.142	0.449	0.159
SO_2_max1	0.11	-0.019	-0.044	0.944	0.025	0.059
SO_2	0.209	-0.031	-0.109	0.92	0.093	0.049
NH_4	0.206	-0.064	0.174	0.081	0.901	-0.048
SO_4	0.05	0.025	0.284	0.078	0.849	-0.104
Cu	-0.01	0.049	0.027	-0.027	-0.148	0.793
Zn	0.198	-0.005	-0.046	0.14	0.122	0.655

Table S7. PCA1 and PCA2 orthogonal factors for SEARCH JST daily data. PCA1: n = 516, variance explained = 78%. PCA2: n = 2593, variance explained = 78%.

PCA1	Combustion	Crustal	Seasonal	SO_2	SO_4	Metals	Salt	Other
CO	0.953	0.014	-0.012	0.122	0.015		0.08	0.039
CO_max1	0.88	0.018	0.057	0.096	-0.102		0.029	0.012
NO_x	0.93	0.047	-0.097	0.211	-0.109		0.064	0.051
EC	0.883	0.059	0.175	0.108	0.133		0.08	0.103
OC	0.741	0.031	0.226	0.015	0.279		0.314	0.035
NO_z	0.447	0.02	0.373	-0.041	0.16		-0.059	0.27
K	0.346	0.064	0.071	-0.022	0.122		0.748	0.011
Al	-0.065	0.954	-0.006	-0.094	-0.004		0.097	0.025
Si	-0.045	0.97	0.014	-0.044	-0.01		0.055	0.034
Fe	0.532	0.778	0.046	0.128	0.018		0.034	0.088
Ca	0.165	0.523	0.218	0.358	0.124		0.201	-0.07
O_3_max8	0.017	0.009	0.741	-0.101	0.473		0.027	-0.108
NH_3	0.29	0.086	0.654	0.066	-0.128		0.017	0.143
NO_3	0.426	-0.119	-0.653	0.003	0.122		0.044	0.147
SO_2_max1	0.185	0.014	0.007	0.932	0.135		-0.017	-0.016
SO_2	0.343	0.004	-0.07	0.883	0.131		-0.006	-0.014
NH_4	0.155	-0.006	-0.082	0.143	0.951		0.044	0.002
SO_4	0.007	0.072	0.135	0.144	0.942		0.058	0.009
Na	0.053	0.088	-0.026	-0.008	-0.025		0.216	0.866
Cl	0.329	0.035	-0.403	0.07	-0.011		0.691	0.138
Mg	-0.109	0.457	0.15	-0.039	0.014		0.668	0.222
Cu	0.535	0.047	-0.007	0.132	-0.024		0.169	-0.327
Zn	0.749	-0.001	-0.202	0.233	0.114		0.174	-0.043

PCA2	Combustion	Crustal	Seasonal	SO_2	SO_4	Metals
CO	0.935	0.06	0.041	0.162	-0.017	
CO_max1	0.893	0.041	-0.007	0.179	-0.07	
NO_x	0.897	0.086	0.125	0.195	-0.126	
EC	0.881	0.089	0.043	0.107	0.199	
OC	0.799	0.104	0.019	-0.011	0.329	
NO_z	0.354	-0.032	0.019	0.172	0.12	
nsK	0.409	0.391	0.258	-0.195	0.168	
Al	-0.137	0.933	-0.052	-0.081	-0.043	
Si	0.033	0.961	-0.076	0.019	0.039	
Fe	0.554	0.716	-0.053	0.069	0.045	
Ca	0.386	0.585	-0.094	0.276	0.171	
O_3_max8	0.071	0.118	-0.672	-0.04	0.646	
O_3_24hr	-0.169	0.048	-0.671	-0.131	0.584	
NO_3	0.218	-0.104	0.831	0.125	0.096	
SO_2_max1	0.145	0.031	0.071	0.924	0.034	
SO_2	0.379	0.021	0.151	0.86	0.033	
NH_4	0.17	-0.031	0.107	0.132	0.935	
SO_4	0.093	0.023	-0.089	0.111	0.921	
Cu	0.115	0.034	-0.014	0.017	-0.006	
Zn	0.587	0.091	0.193	0.05	0.038	

Table S8. PCA1 and PCA2 orthogonal factors for SEARCH OAK daily data. PCA1: n = 100, variance explained = 78%. PCA2: n = 707, variance explained = 78%.

PCA1	Combustion	Crustal	Seasonal	SO_2	SO_4	Metals	Salt	Other
CO	0.623	-0.087	0.114	0.127	-0.043	0.551	-0.13	
CO_max1	0.788	-0.004	0.005	-0.091	-0.25	0.061	-0.068	
NO_x	0.085	0.078	-0.056	0.243	-0.09	0.778	0.054	
EC	0.55	-0.165	0.114	0.256	0.353	0.127	-0.058	
OC	0.58	-0.001	0.289	0.321	0.383	0.142	-0.183	
NO_z	0.223	-0.048	0.438	0.344	0.157	0.651	-0.128	
K	0.353	0.028	0.501	0.106	0.291	0.276	0.114	
Al	-0.031	0.981	-0.018	-0.062	-0.032	-0.027	0.045	
Si	-0.017	0.98	0.022	-0.064	-0.042	-0.036	0.04	
Fe	-0.035	0.982	0.009	-0.048	0.005	-0.003	0.04	
Ca	-0.07	0.775	0.151	0.041	4.30E-04	0.137	0.194	
O_3_max8	0.17	-0.182	0.71	0.135	0.315	0.147	-0.148	
NH_3	-0.029	0.363	0.814	-0.064	-0.077	-0.038	-0.043	
NO_3	0.129	-0.011	-0.011	-0.018	-0.044	0.743	0.309	
SO_2_max1	0.052	-0.059	0.045	0.921	-0.026	0.126	0.037	
SO_2	0.129	-0.052	0.052	0.824	0.077	0.423	-0.031	
NH_4	0.037	-0.084	0.128	-0.013	0.934	0.095	-0.089	
SO_4	-0.056	0.05	0.06	0.008	0.942	-0.082	0.02	
Na	-0.093	0.088	-0.036	0.008	-0.013	-0.025	0.958	
Cl	-0.054	-0.046	-0.031	0.016	-0.089	-0.055	0.929	
Mg	-0.09	0.311	-0.065	-0.041	0.006	0.041	0.88	
Cu	-0.02	0.029	0.075	0.044	0.031	0.696	0.004	
Zn	0.114	-0.075	0.092	0.155	0.121	0.6	-0.254	

PCA2	Combustion	Crustal	Seasonal	SO_2	SO_4	Metals
CO	0.797	-0.151	0.076	0.191	0.062	-0.064
CO_max1	0.813	-0.058	0.034	0.013	-0.082	-0.129
NO_x	0.505	-0.126	-0.502	0.422	-0.204	0.033
EC	0.774	-0.018	0.142	0.068	0.279	0.074
OC	0.75	0.037	0.275	0.033	0.294	-0.012
NO_z	0.691	-0.031	0.253	0.236	0.173	0.115
nsK	0.465	0.485	0.172	0.061	0.096	0.317
Al	-0.085	0.97	-0.08	-0.046	-0.033	-0.033
Si	-0.076	0.981	-0.026	-0.041	-0.03	-0.016
Fe	-0.069	0.977	-0.029	-0.023	0.018	0.02
Ca	-0.016	0.892	0.114	0.002	0.023	0.095
O_3_max8	0.198	0.014	0.901	0.096	0.223	0.043
O_3_24hr	0.229	-0.026	0.908	0.112	0.143	0.085
NO_3	0.598	6.90E-05	-0.307	-0.004	-0.006	0.288
SO_2_max1	0.02	-0.01	0.061	0.924	0.06	-0.011
SO_2	0.291	-0.039	0.1	0.887	0.095	0.026
NH_4	0.29	-0.025	0.165	0.065	0.898	0.072
SO_4	0.061	0.026	0.22	0.072	0.941	-0.041
Cu	-0.183	0.102	0.132	-0.06	-0.188	0.766
Zn	0.194	-0.014	-0.029	0.061	0.177	0.628

Table S9. PCA1 and PCA2 orthogonal factors for SEARCH OLF daily data. PCA1: n = 327, variance explained = 78%. PCA2: n = 948, variance explained = 76%.

PCA1	Combustion	Crustal	Seasonal	SO_2	SO_4	Metals	Salt	Other
CO	0.755	-0.175	0.333	0.014	0.297	-0.056	-0.093	
CO_max1	0.464	-0.043	0.438	-0.276	0.271	0.141	-0.079	
NO_x	0.761	-0.033	-0.155	-0.04	-0.138	0.208	-0.174	
EC	0.739	-0.114	0.318	0.173	0.138	-0.008	-0.117	
OC	0.674	-0.086	0.5	0.123	0.27	0.022	-0.094	
NO_z	0.395	-0.002	0.374	0.495	0.086	-0.476	-0.099	
K	0.292	0.272	0.31	0.135	0.118	-0.078	0.303	
Al	-0.106	0.958	-0.014	-0.076	0.013	0.051	0.104	
Si	-0.102	0.964	-0.026	-0.048	1.60E-04	0.089	0.115	
Fe	-0.06	0.958	-0.031	-0.022	0.03	0.117	0.143	
Ca	0.002	0.788	0.052	0.062	-0.058	-0.115	0.095	
O_3_max8	0.134	-0.195	0.635	0.303	0.347	-0.084	-0.046	
NH_3	0.039	0.105	0.801	-0.001	-0.117	0.096	-0.011	
NO_3	0.694	0.129	-0.151	0.277	-0.104	-0.353	0.179	
SO_2_max1	0.064	-0.01	0.06	0.822	0.248	0.095	-0.077	
SO_2	0.191	-0.039	0.06	0.862	0.227	0.056	-0.1	
NH_4	0.219	-0.07	0.056	0.262	0.877	-0.057	-0.072	
SO_4	0.011	0.094	0.054	0.206	0.926	0.042	0.016	
Na	-0.206	0.325	-0.085	-0.217	0.089	-0.113	0.781	
Cl	0.008	-0.007	-0.025	0.044	-0.129	0.181	0.732	
Mg	-0.218	0.483	0.001	-0.199	0.007	-0.095	0.738	
Cu	0.287	0.157	0.165	0.298	-0.027	0.668	0.099	
Zn	0.645	-0.143	-0.004	0.423	0.021	0.149	-0.008	

PCA2	Combustion	Crustal	Seasonal	SO_2	SO_4	Metals
CO	0.785	-0.152	0.006	0.195	0.309	0.129
CO_max1	0.854	-0.027	0.122	0.076	0.066	0.022
NO_x	0.676	-0.04	-0.222	0.481	-0.058	-0.023
EC	0.606	-0.055	-0.051	0.072	0.564	0.099
OC	0.509	-0.038	0.16	0.055	0.637	0.157
NO_z	0.096	-0.028	-0.08	0.011	0.663	0.013
nsK	0.141	0.328	-0.14	-0.079	0.272	0.588
Al	-0.062	0.97	-0.042	-0.056	-0.082	-0.004
Si	-0.062	0.984	-0.036	-0.035	-0.063	-0.001
Fe	-0.041	0.974	-0.032	-0.009	-0.018	0.047
Ca	-0.043	0.928	0.069	0.02	0.056	0.1
O_3_max8	0.178	-0.024	0.737	-0.074	0.537	0.11
O_3_24hr	0.038	-0.072	0.757	-0.144	0.467	0.188
NO_3	0.397	-0.008	-0.503	0.024	0.292	0.326
SO_2_max1	0.15	0.008	0.003	0.945	0.103	-0.002
SO_2	0.205	-0.032	-0.07	0.9	0.242	0.044
NH_4	0.114	-0.012	0.139	0.122	0.876	-2.62E-04
SO_4	-0.023	0.07	0.215	0.103	0.826	-0.091
Cu	-0.069	0.1	0.206	-0.118	-0.276	0.71
Zn	0.133	-0.091	0.006	0.102	0.231	0.732

Table S10. PCA1 and PCA2 orthogonal factors for SEARCH PNS daily data. PCA1: n = 44, variance explained = 84%. PCA2: n = 445, variance explained = 79%.

PCA1	Combustion	Crustal	Seasonal	SO_2	SO_4	Metals	Salt	Other
CO	0.959	0.044	0.036	0.054	0.029		-0.186	
CO_max1	0.929	0.071	0.021	-0.012	-0.121		-0.178	
NO_x	0.919	0.084	-0.069	0.08	-0.142		-0.233	
EC	0.908	-0.008	-0.087	0.067	0.279		-0.222	
OC	0.859	-0.029	0.104	0.067	0.266		-0.27	
NO_z	0.608	-0.142	0.072	0.002	0.61		-0.205	
K	0.726	-0.042	0.083	0.112	0.315		0.223	
Al	-0.109	0.971	0.009	-0.035	-0.044		-0.009	
Si	-0.09	0.971	-0.036	-0.04	-0.051		-0.011	
Fe	0.212	0.88	0.061	0.053	0.017		0.153	
Ca	-0.06	0.276	0.371	0.056	-0.203		-0.04	
O_3_max8	0.154	-0.049	0.845	0.023	0.351		-0.072	
NH_3	0.341	0.539	0.343	-0.063	-0.063		-0.433	
NO_3	0.654	0.004	-0.52	-0.019	0.405		0.06	
SO_2_max1	-0.035	0.021	-0.079	0.918	-0.02		-0.222	
SO_2	0.072	-0.041	0.061	0.933	0.097		-0.257	
NH_4	0.113	-0.057	-0.028	0.064	0.961		-0.143	
SO_4	-0.037	-0.012	0.092	0.028	0.958		-0.026	
Na	-0.244	0.022	0.049	-0.137	-0.105		0.932	
Cl	-0.03	-0.044	-0.252	-0.172	-0.047		0.876	
Mg	-0.28	0.089	0.08	-0.145	-0.111		0.906	
Cu	0.354	-0.011	0.224	0.425	0.028		0.151	
Zn	0.851	-0.001	0.071	0.011	-0.091		-0.009	

PCA2	Combustion	Crustal	Seasonal	SO_2	SO_4	Metals	Other
CO	0.893	-0.051	-0.001	0.135		0.027	-0.051
CO_max1	0.826	-0.043	0.014	0.164		0.086	-0.156
NO_x	0.862	0.01	-0.173	0.215		0.044	-0.255
EC	0.91	0.001	0.089	0.077		-0.01	0.079
OC	0.842	-0.014	0.251	0.07		-0.08	0.163
NO_z	0.079	-0.03	0.033	0.119		0.107	0.827
nsK	0.659	0.314	0.058	-0.067		0.046	0.233
Al	-0.091	0.959	0.005	-0.026		-0.081	-0.027
Si	-0.099	0.962	0.011	-0.039		-0.08	-0.016
Fe	0.195	0.914	0.008	0.02		0.017	0.002
Ca	0.142	0.672	0.077	0.123		0.266	0.016
O_3_max8	0.095	0.067	0.934	0.01		0.12	-0.068
O_3_24hr	-0.205	0.008	0.889	-0.113		0.115	-0.07
NO_3	0.681	0.017	-0.141	-0.038		-0.094	0.293
SO_2_max1	0.135	0.007	-0.03	0.954		-0.022	0.058
SO_2	0.207	0.05	-0.032	0.937		0.009	0.078
NH_4	0.282	-0.003	0.64	0.056		-0.488	0.374
SO_4	0.117	0.045	0.677	0.017		-0.497	0.338
Cu	0.153	0.049	0.068	-0.006		0.755	0.153
Zn	0.695	0.105	0.005	0.081		0.153	0.11

Table S11. PCA1 and PCA2 orthogonal factors for SEARCH YRK daily data. PCA1: n = 426, variance explained = 79%. PCA2: n = 1435, variance explained = 79%.

PCA1	Combustion	Crustal	Seasonal	SO_2	SO_4	Metals	Salt	Other
CO	0.743	-0.098	0.468	-0.073	0.198	0.058	0.024	0.105
CO_max1	0.728	-0.061	0.38	-0.079	0.118	0.166	0.064	0.104
NO_x	0.809	-0.093	-0.023	0.239	-0.131	0.046	0.07	-0.007
EC	0.308	-0.043	0.715	-0.012	0.208	0.076	0.14	0.294
OC	0.12	0.075	0.773	-0.01	0.306	0.115	0.158	0.269
NO_z	0.392	0.039	0.699	0.211	0.136	-0.126	-0.101	0.038
K	0.132	0.353	0.488	0.059	0.043	0.05	0.317	0.299
Al	-0.088	0.955	-0.014	-0.064	-0.028	0.004	0.076	0.007
Si	-0.123	0.971	-0.003	-0.015	-0.011	0.024	0.069	0.012
Fe	-0.045	0.957	0.055	0.022	0.074	0.031	0.088	0.041
Ca	0.084	0.53	0.025	0.126	0.118	0.112	0.205	-0.377
O_3_max8	-0.234	0.026	0.79	0.024	0.259	-0.043	-0.219	-0.089
NH_3	-0.012	0.02	0.623	0.093	-0.125	0.163	0.135	-0.443
NO_3	0.782	-0.05	-0.081	0.148	-0.01	-0.123	0.047	0.111
SO_2_max1	0.061	0.008	0.044	0.952	0.099	0.029	0.016	-0.005
SO_2	0.192	-0.007	0.084	0.942	0.114	0.007	-0.009	0.087
NH_4	0.124	0.012	0.25	0.142	0.922	-0.04	-0.011	0.037
SO_4	-0.07	0.07	0.253	0.097	0.932	-0.021	0.01	0.032
Na	0.024	0.15	0.116	0.011	-0.134	-0.116	0.802	0.071
Cl	0.183	0.092	-0.105	0.007	0.154	0.157	0.78	-0.102
Mg	-0.14	0.564	0.163	-0.038	-0.017	0.016	0.583	-0.092
Cu	0.028	0.091	0.071	0.03	-0.049	0.93	0.021	0.074
Zn	0.234	-0.037	0.218	0.137	0.052	0.144	-0.005	0.668
PCA2	**Combustion**	**Crustal**	**Seasonal**	**SO_2**	**SO_4**	**Metals**		**Other**
CO	0.836	-0.058	0.294	0.032		0.042		0.092
CO_max1	0.837	-0.021	0.242	0.024		0.054		0.047
NO_x	0.823	-0.061	-0.222	0.212		-0.089		0.012
EC	0.588	-0.009	0.581	0.029		0.147		0.101
OC	0.384	0.108	0.724	0.024		0.233		0.149
NO_z	0.294	-0.034	0.617	0.248		0.039		0.221
nsK	0.255	0.36	0.194	-0.049		0.516		0.221
Al	-0.12	0.936	-0.108	-0.07		0.069		-0.105
Si	-0.089	0.975	0.012	-0.02		0.05		-0.032
Fe	-0.023	0.965	0.084	-0.011		0.043		0.023
Ca	-0.032	0.65	0.301	0.086		0.004		0.412
O_3_max8	-0.217	0.039	0.883	0.043		0.058		0.125
O_3_24hr	-0.307	0.027	0.835	0.045		0.113		0.192
NO_3	0.703	-0.089	-0.064	0.179		-0.048		0.093
SO_2_max1	0.092	-0.006	0.103	0.936		-0.021		-0.028
SO_2	0.271	-0.03	0.186	0.892		-0.037		0.115
NH_4	0.302	0.028	0.825	0.094		-0.152		-0.088
SO_4	0.121	0.07	0.858	0.071		-0.151		-0.106
Cu	-0.094	0.019	-0.062	-0.027		0.876		-0.047
Zn	0.181	0.012	0.112	0.05		0.029		0.889

Table S12. Statistically significant regression results for multiple regression of OC on PCA1 factor scores. Factor composition is defined in Tables S2 through S9. Units for mean OC are $\mu g\ m^{-3}$. Factors are normalized (mean 0, variance 1), so units are $\mu g\ m^{-3}$ factor-unit^{-1} for ΔOC/Δ factor. NS = not significant; NA = not applicable (component not present).

Parameter	BHM	CTR	GFP	JST	OAK	OLF	PNS	YRK
N	364	383	100	516	100	327	44	426
r^2	0.836	0.799	0.732	0.772	0.605	0.797	0.892	0.802
Mean OC	2.904 ± 0.040	2.422 ± 0.029	2.129 ± 0.078	3.783 ± 0.052	2.545 ± 0.102	2.274 ± 0.039	2.734 ± 0.107	2.840 ± 0.040
ΔOC/ΔCombustion	1.429 ± 0.040	1.028 ± 0.031	0.918 ± 0.077	1.703 ± 0.048	0.784 ± 0.101	0.971 ± 0.038	2.011 ± 0.128	0.213 ± 0.035
ΔOC/ΔCrustal	0.100 ± 0.043	0.201 ± 0.028	NS	0.140 ± 0.023	NS	-0.116 ± 0.024	NS	0.121 ± 0.021
ΔOC/ΔSeasonal	0.371 ± 0.048	0.455 ± 0.031	0.607 ± 0.069	0.406 ± 0.038	0.424 ± 0.076	0.641 ± 0.033	0.342 ± 0.109	1.270 ± 0.037
ΔOC/ΔSO_2	0.413 ± 0.046	NS	0.161 ± 0.076	0.087 ± 0.038	0.461 ± 0.087	0.284 ± 0.053	NS	NS
ΔOC/ΔSO_4	0.570 ± 0.042	0.263 ± 0.028	0.349 ± 0.093	0.735 ± 0.056	0.594 ± 0.102	0.409 ± 0.047	0.672 ± 0.137	0.634 ± 0.049
ΔOC/ΔMetals	0.182 ± 0.039	NS	NS	NA	0.250 ± 0.095	NS	NA	0.432 ± 0.033
ΔOC/ΔSalt	0.159 ± 0.039	NS	-0.549 ± 0.095	0.669 ± 0.044	-0.268 ± 0.073	-0.122 ± 0.027	-0.532 ± 0.092	0.212 ± 0.032
ΔOC/ΔOther[a]	0.132 ± 0.051	NA	0.569 ± 0.074	0.134 ± 0.031	NA	NA	NA	0.131 ± 0.022

[a] "Other" is predominantly NO_z, Ca, Mg at BHM, Na at JST, Zn at YRK.

Table S13. Statistically significant regression results for multiple regression of OC on PCA2 factor scores. Factor composition is defined in Tables S2 through S9. Units for mean OC are $\mu g\ m^{-3}$. Factor scores are normalized (mean 0, variance 1), so the units are $\mu g\ m^{-3}$ factor-unit^{-1} for ΔOC/Δ factor. NS = not significant; NA = not applicable (PCA component not present).

Parameter	BHM	CTR	GFP	JST	OAK	OLF	PNS	YRK
N	1513	1258	376	2593	707	948	445	1435
r^2	0.750	0.800	0.728	0.751	0.682	0.711	0.800	0.750
Mean OC	3.938 ± 0.034	2.990 ± 0.023	2.296 ± 0.038	4.035 ± 0.024	2.625 ± 0.041	2.302 ± 0.025	2.668 ± 0.040	3.000 ± 0.023
ΔOC/ΔCombustion	2.097 ± 0.036	1.442 ± 0.024	0.920 ± 0.049	1.882 ± 0.023	1.641 ± 0.047	0.687 ± 0.023	1.685 ± 0.042	0.626 ± 0.021
ΔOC/ΔCrustal	0.205 ± 0.035	0.105 ± 0.024	0.176 ± 0.036	0.253 ± 0.024	NS	-0.054 ± 0.027	NS	0.180 ± 0.023
ΔOC/ΔSeasonal	0.492 ± 0.034	0.555 ± 0.022	0.436 ± 0.038	0.051 ± 0.023	0.596 ± 0.043	0.241 ± 0.025	0.519 ± 0.042	1.193 ± 0.022
ΔOC/ΔSO_2	0.420 ± 0.033	NS	0.274 ± 0.045	NS	NS	0.084 ± 0.023	0.146 ± 0.037	0.045 ± 0.021
ΔOC/ΔSO_4	0.841 ± 0.039	0.635 ± 0.023	0.776 ± 0.042	0.790 ± 0.023	0.656 ± 0.044	0.937 ± 0.026	NS	NS
ΔOC/ΔMetals	0.635 ± 0.042	NS	0.315 ± 0.032	0.103 ± 0.040	NS	0.218 ± 0.026	NS	0.389 ± 0.022
ΔOC/ΔSalt	NA	NA	NA	NA	NA	NA	NA	NA
ΔOC/ΔOther[a]	NA	NA	NA	NA	NA	NA	0.375 ± 0.039	0.237 ± 0.020

Table S14. Mean OC associated with components identified by PCA1 (2008 – 2013) and PCA2 (1999 – 2013). NS = not statistically significant, NA = not applicable (component not present in PCA). Units are percent. Mean concentrations are listed in Table 3.

PCA	Site	N	Combustion	Crustal	Seasonal	SO_2	SO_4	Metals	Salt	Other
1	BHM	364	44.7%	3.0%	13.2%	11.5%	14.8%	4.9%	4.6%	3.3%
1	CTR	383	52.7%	10.7%	23.0%		13.6%			
1	GFP	100	47.3%		22.4%	7.5%	12.4%		-20.4%[a]	30.8%
1	JST	516	38.5%	5.7%	17.3%	2.5%	9.5%		22.6%	3.9%
1	OAK	100	21.6%		27.0%	20.0%	28.6%	17.3%	-14.6%[a]	
1	OLF	327	43.8%		30.8%	9.5%	16.0%			
1	PNS	44	88.2%		14.9%		25.3%		-28.5%[a]	
1	YRK	426	5.8%	5.8%	45.2%		10.8%	6.6%	6.2%	19.5%
2	BHM	1513	43.4%	5.1%	12.7%	10.3%	15.4%	13.0%		
2	CTR	1258	50.5%	4.0%	23.2%		22.2%			
2	GFP	376	32.9%	6.4%	16.9%	9.6%	22.8%	11.4%		
2	JST	2593	62.9%	7.8%	1.5%[b]		24.6%[b]	3.2%		
2	OAK	707	58.6%		18.4%		23.0%			
2	OLF	948	35.1%	-2.6%[a]	10.8%	3.9%	44.2%	8.7%		
2	PNS	445	61.3%		17.8%[c]	6.7%				14.2%
2	YRK	1435	24.6%	6.5%	45.3%[c]	1.6%		12.6%		9.4%

a. Negative due to inverse associations of OC with crustal and salt components at (Tables S7 and S13).
b. JST PCA2 seasonal OC is associated with NO_3; JST PCA2 SO_4 component includes OC associated with O_3 (Table 2).
c. PNS and YRK PCA2 seasonal components include OC associated with SO_4 (Table 2).

Table S15. PCA3 orthogonal factors for SEARCH JST daily data. PCA3, 1999 – 2008: n = 426, variance explained = 79%. PCA2: n = 1435, variance explained = 79%.

PCA3	Combustion	Crustal	Seasonal	SO_2	SO_4	Metals	Salt	Other
CO	0.916	0.032	0.165	0.107	-0.073	0.039		0.087
CO_max1	0.86	0.023	0.113	0.13	-0.108	0.036		0.1
NO_x	0.875	0.043	0.199	0.16	-0.182	0.079		0.008
EC	0.841	0.056	0.256	0.074	0.157	0.029		0.038
OC	0.731	0.077	0.319	-0.026	0.265	0.004		0.084
NO_z	0.188	-0.04	0.05	0.059	0.075	-0.01		0.922
nsK	0.32	0.33	0.5	-0.108	0.057	-0.009		0.059
Al	-0.012	0.929	-0.025	-0.036	0.015	-0.013		-0.068
Si	0.153	0.94	0.005	0.029	0.112	0.003		0.018
Fe	0.652	0.622	0.116	0.073	0.125	0.087		-0.006
Ca	0.363	0.53	0.123	0.239	0.223	0.082		0.123
O_3_max8	0.088	0.142	-0.225	-0.049	0.859	0.071		0.153
O_3_24hr	-0.163	0.087	-0.238	-0.13	0.802	0.068		0.162
NO_3	0.077	-0.187	0.774	0.146	-0.257	-0.07		0.028
SO_2_max1	0.131	0.033	-0.01	0.941	-0.004	-0.007		-0.024
SO_2	0.332	0.006	0.117	0.881	-0.057	-0.035		0.071
NH_4	0.13	-0.095	0.345	0.063	0.848	-0.081		-0.056
SO_4	0.098	-0.016	0.149	0.05	0.905	-0.057		-0.104
Cu	0.126	0.006	0.012	0.001	0.005	0.961		-0.008
Zn	0.425	0.059	0.42	0.067	-0.011	0.146		-0.029
Alkanes	0.907	0.015	0.043	0.019	-0.087	-0.028		0.035
Aromatics	0.917	0.03	-0.008	0.011	-0.021	-0.033		0.069
Alpha pinene	0.803	0.04	-0.158	-0.047	-0.009	-0.088		-0.091
Isoprene	0.013	0.373	-0.282	0.054	0.583	-0.041		-0.136

Table S16. PCA4 (including NH_3) and PCA5 (excluding NH_3; including daily average O_3) orthogonal factors for SEARCH CTR daily data, 2004 - 2013. PCA4: n = 724, variance explained = 76%. PCA5: n = 751, variance explained = 79%.

PCA4	Combustion	Crustal	Seasonal	SO_2	SO_4	Metals	Salt	Other
CO	0.733	-0.135	0.019	0.223	-0.044	0.313		
CO_max1	0.731	-0.076	0.026	0.196	0.01	0.177		
NO_x	0.219	-0.093	-0.258	0.82	-0.097	0.102		
EC	0.672	-0.039	0.07	0.187	0.45	-0.067		
OC	0.71	0.094	0.24	-0.043	0.458	-0.137		
NO_z	0.52	-0.003	0.089	0.359	0.425	0.188		
nsK	0.71	0.298	0.057	-0.054	0.162	-0.067		
Al	-0.052	0.946	-0.017	-0.131	-0.095	-0.058		
Si	-0.041	0.964	0.014	-0.111	-0.056	-0.087		
Fe	0.026	0.963	-0.006	0.012	0.05	0.076		
Ca	0.131	0.698	0.132	0.176	0.178	0.079		
O_3_max8	0.252	0.009	0.548	-0.005	0.604	0.164		
NH_3	0.251	0.082	0.754	0.111	-0.122	-0.027		
NO_3	0.329	-0.004	-0.488	0.442	-0.07	0.054		
SO_2_max1	0.045	0.016	0.164	0.874	0.13	-0.073		
SO_2	0.103	0.001	0.089	0.923	0.177	-0.059		
NH_4	0.196	0.009	-0.097	0.138	0.909	-0.027		
SO_4	0.081	0.048	-0.047	0.03	0.934	-0.045		
Cu	0.03	0.018	0.05	-0.175	-0.096	0.839		
Zn	0.31	0.011	-0.132	0.4	0.181	0.607		

PCA5	Combustion	Crustal	Seasonal	SO_2	SO_4	Metals	Other
CO	0.689	-0.141	0.071	0.239	-0.104	0.381	
CO_max1	0.725	-0.078	0.041	0.217	-0.055	0.221	
NO_x	0.178	-0.101	-0.25	0.823	-0.035	0.189	
EC	0.705	-0.044	0.154	0.217	0.392	-0.042	
OC	0.756	0.089	0.267	-0.013	0.368	-0.128	
NO_z	0.461	-0.005	0.415	0.401	0.265	0.248	
nsK	0.739	0.29	0.114	-0.014	0.091	-0.038	
Al	-0.038	0.944	-0.107	-0.138	-0.046	-0.05	
Si	-0.021	0.964	-0.057	-0.112	-0.026	-0.086	
Fe	0.024	0.962	0.004	0.014	0.059	0.084	
Ca	0.132	0.702	0.226	0.193	0.072	0.054	
O_3_max8	0.251	0.023	0.894	0.03	0.266	0.065	
O_3_24hr	0.21	-0.01	0.905	-0.02	0.213	0.054	
NO_3	0.191	-0.025	-0.362	0.456	0.149	0.309	
SO_2_max1	0.077	0.024	0.149	0.876	0.012	-0.131	
SO_2	0.114	0.005	0.112	0.926	0.094	-0.078	
NH_4	0.206	-0.001	0.197	0.167	0.917	0.014	
SO_4	0.122	0.042	0.227	0.059	0.913	-0.051	
Cu	0.008	0.022	0.058	-0.205	-0.134	0.77	
Zn	0.242	0.005	0.055	0.404	0.166	0.655	

Table S17. Comparison of PCA1 CTR source apportionment to Xu et al. (2015a, b).

	OC from each PCA factor (% of mean OC)			Unc (%)		AMS OC (%)	AMS OA (%)
PCA Factor	2008-13	2013	SOAS		AMS Factor[a]	SOAS	SOAS
Combustion	52	53	38	18	MO-	34	39
					BBOA	11	10
Sulfate	11	13	13	6	Isop	20	18
Seasonal	14	22	23	15	LO-	35	32
Crustal	23	13	20	4			
Fitted sum	100	100	94				
Mean OA[a]	NA	NA	NA				5.0
Mean OC[a]	2.41	2.26	2.63			2.31	
Mean OC in PCA subset[a]	2.43	2.32	2.61			NA	
OM/OC	1.58	1.66	1.36			2.16	
N days for mean OC	606	156	40				
N days in PCA subset	383	105	29				

a. MO-OOA (MO-), biomass burning OA (BBOA), isoprene OA (Isop), and LO-OOA (LO-)

b. $\mu g\ m^{-3}$

Table S18. Comparison of PCA1 JST source apportionment to Xu et al. (2015a, b).[a]

	OC from each PCA factor (% of mean OC)				Unc (%)		AMS OC (%)		AMS OA (%)	
PCA Factor	2008-13	2012	MJ 2012	ND 2012		AMS Factor[b]	MJ 2012	ND 2012	MJ 2012	ND 2012
Combustion	38	41	29	57	12	HOA	14	25	10	19
						MO-	22	26	27	31
Salt[c]	23	21	20	7	11	BBOA	10	10	10	9
Other[d]	4	4	2	12	2	COA	14	23	11	20
Sulfate	10	6	9	1	7	Isop	19		21	
SO_2	3	1	1	1	1					
Seasonal	17	18	25	11	15	LO-	21	17	21	19
Crustal	6	5	3	2	4					
Fitted sum	100	95	89	91						
Mean OA[e]	NA	NA	NA	NA					9.1	7.9
Mean OC[e]	2.88	2.98	3.36	3.65			4.70	5.45		
Mean OC in PCA subset[e]	3.78	2.90	3.36	3.65			NA	NA		
OM/OC	1.51	1.37	1.34	1.51			1.93	1.40		
N days for mean OC	904	114	8	8						
N days in PCA subset	516	109	8	8						

a. Sample periods are May 10 - Jun 2, 2012 (MJ2012) and Nov 6 - Dec 4, 2012 (ND 2012)

b. MO-OOA (MO-), biomass burning OA (BBOA), isoprene OA (Isop), and LO-OOA (LO-)

c. Associated with K, Mg, Cl

d. Associated with Na

e. µg m^{-3}

Table S19. Comparison of YRK PCA1 source apportionment to Xu et al. (2015a, b).[a]

	OC from each PCA factor (% of mean OC)						AMS OC (%)		AMS OA (%)	
PCA Factor	2008-13	2012	JJ 2012	DJ 2012	Unc (%)	AMS Factor[b]	JJ 2012	DJ 2012	JJ 2012	DJ 2012
Combustion	5	4	2	14	14	MO-	25	42	30	49
Metals[c]	21	20	11	27	2					
Salt[d]	7	5	2	11	7	BBOA		35		30
Other[e]	6	7	7	8	5					
Sulfate	11	6	5	8	11	Isop	38		36	
Seasonal	42	46	47	27	5	LO-	37	23	34	22
Crustal	6	6	11	6	4					
Fitted sum	97	95	84	102						
Mean OA[f]	NA	NA	NA	NA					11.2	3.23
Mean OC[f]	2.33	2.36	3.06	1.78			5.66	1.73		
Mean OC in PCA subset[f]	2.40	2.35	2.97	1.78			NA	NA		
OM/OC	1.78	1.77	1.8	1.56			1.98	1.31		
N days for mean OC	585	119	9	11						
N days in subset	426	97	7	10						

a. Sample periods are June 26 - July 20, 2012 (JJ2012) and December 5, 2012 - January 10, 2013 (DJ2012)

b. MO-OOA (MO-), biomass burning OA (BBOA), isoprene OA (Isop), and LO-OOA (LO-)

c. Associated with Cu

d. Associated with Na, Cl, Mg, K

e. Associated with Zn

f. $\mu g\ m^{-3}$

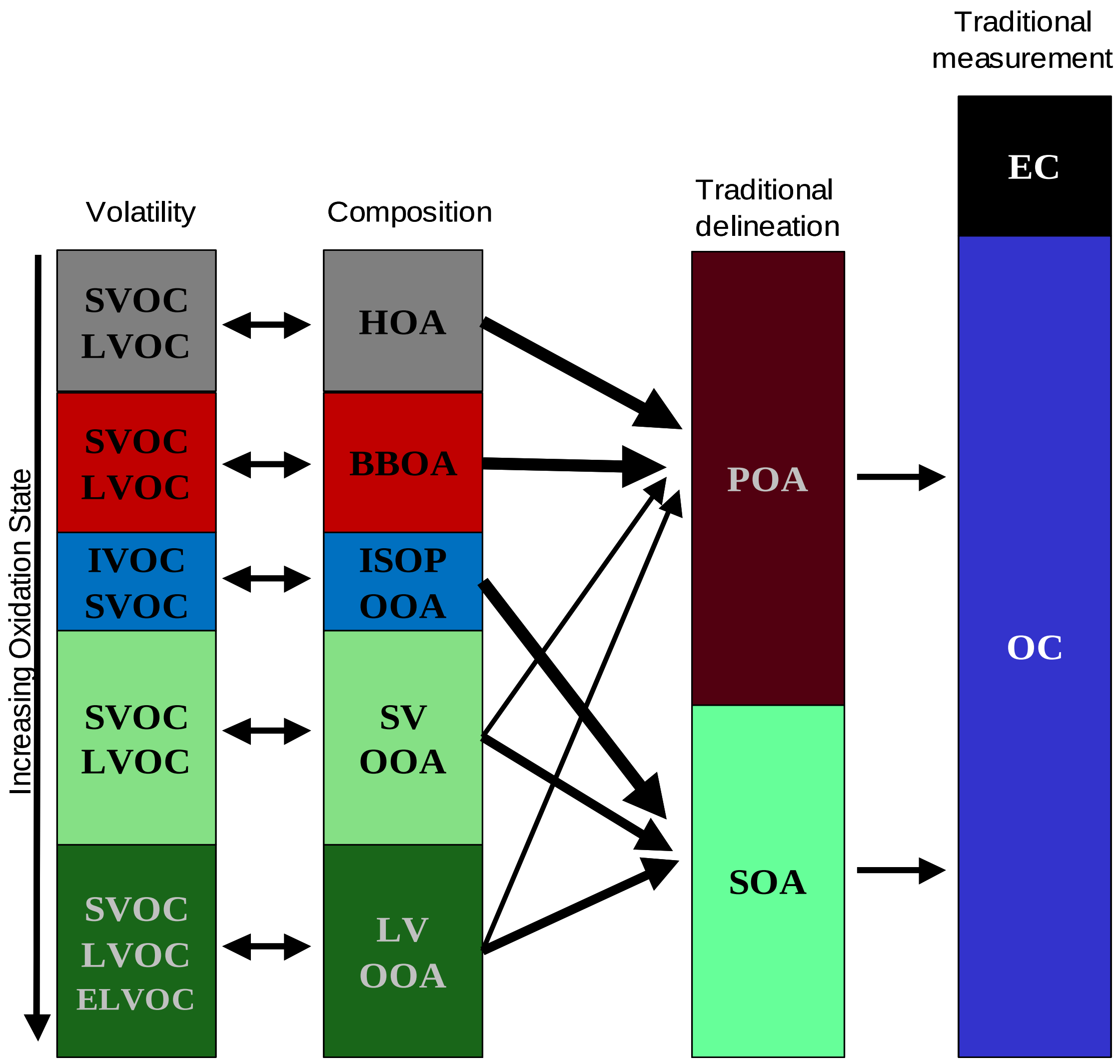

Figure S1. Graphical depiction of various categorizations of OA. Traditional measurements and delineation: EC, OC, POA, SOA as defined in the text. Composition-based categories: HOA, hydrocarbon-like OA; BBOA, biomass burning OA; ISOP OOA, isoprene-derived oxidized OA; SVOOA, semi-volatile oxidized OA (also, less-oxidized OA); LVOOA, low-volatility oxidized OA (also, more-oxidized OA). Volatility-based categories (Donahue et al., 2009; 2012): SVOC, semi-volatile OC; LVOC, low-volatility OC; IVOC, intermediate volatility OC; ELVOC, extremely low-volatility OA. Arrows denote correspondences. Composition categories (HOA, BBOA, SVOA) map to similar volatility ranges (SVOC, LVOC), but differ based on oxidation state (Donahue et al., 2012). The traditional categorization (POA, SOA), e.g., as used in emission inventories, tends to map some SVOA and LVOOA, principally organic material emitted in the condensed phase but subject to volatilization and oxidation, within POA. Traditional OC measurements do not distinguish among composition-based or volatility-based categories. Statistical analysis of multi-species data sets may identify correlations of OC with combustion products (e.g., CO, EC, NO_x) suggestive of less-oxidized OA, or with O_3 and SO_4, suggestive of more-oxidized OA.

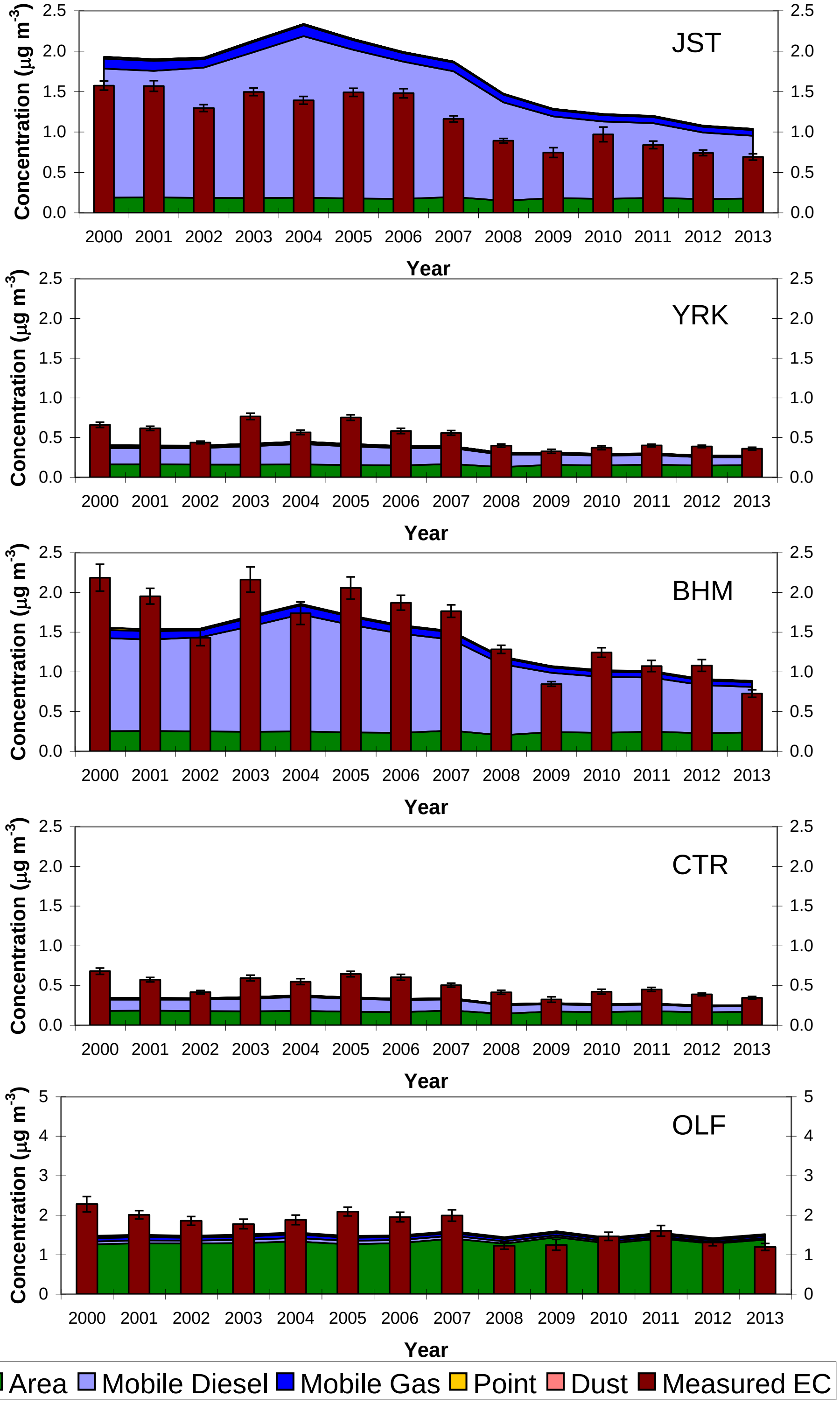

Figure S2. Apportionment of EC trends from chemical mass balance (CMB) receptor model predictions compared with observed mean annual EC concentrations at SEARCH sites. Model predictions were extended to 2012 and 2013 by using model parameters previously fit to data from 2000 – 2011 (Blanchard et al., 2013) along with regional emissions from 2012 and 2013 (Hidy et al., 2014).

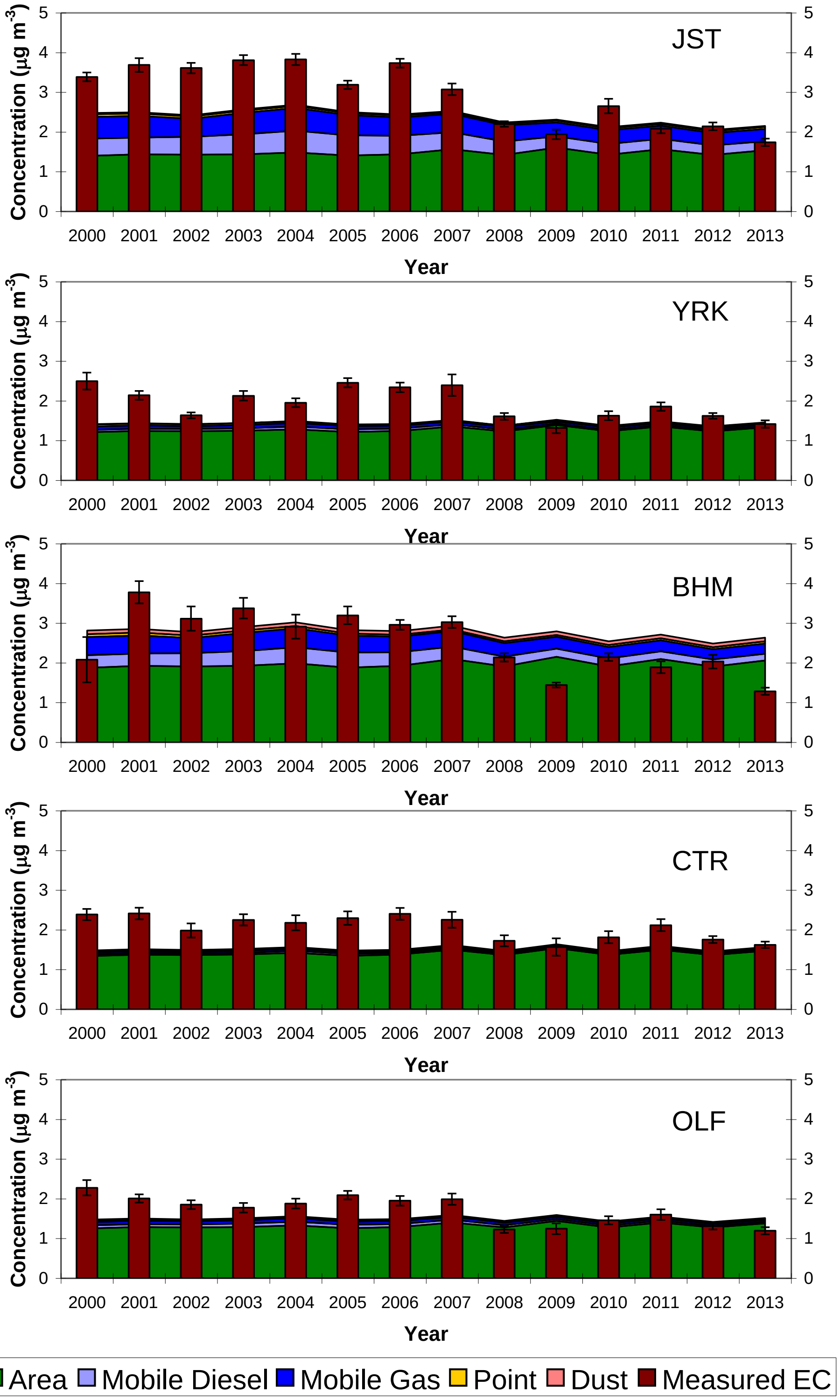

Figure S3. Apportionment of OC trends from chemical mass balance (CMB) receptor model predictions compared with observed mean annual OC concentrations at SEARCH sites. Model predictions were extended to 2012 and 2013 by using model parameters previously fit to data from 2000 – 2011 (Blanchard et al., 2013) along with regional emissions from 2012 and 2013 (Hidy et al., 2014).

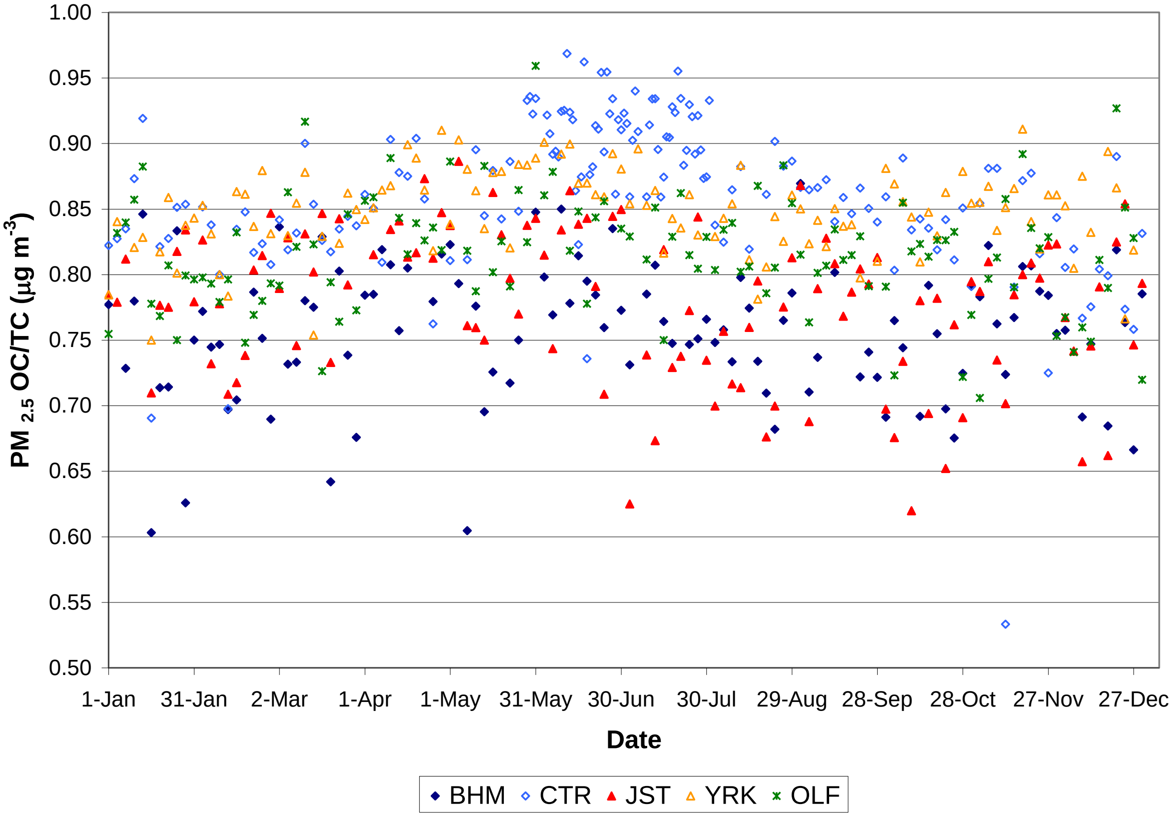

Figure S4. Ratio of OC/TC in daily-average $PM_{2.5}$ filter samples collected during 2013 vs. date. The highest OC/TC ratios occur at CTR during the SOAS campaign.

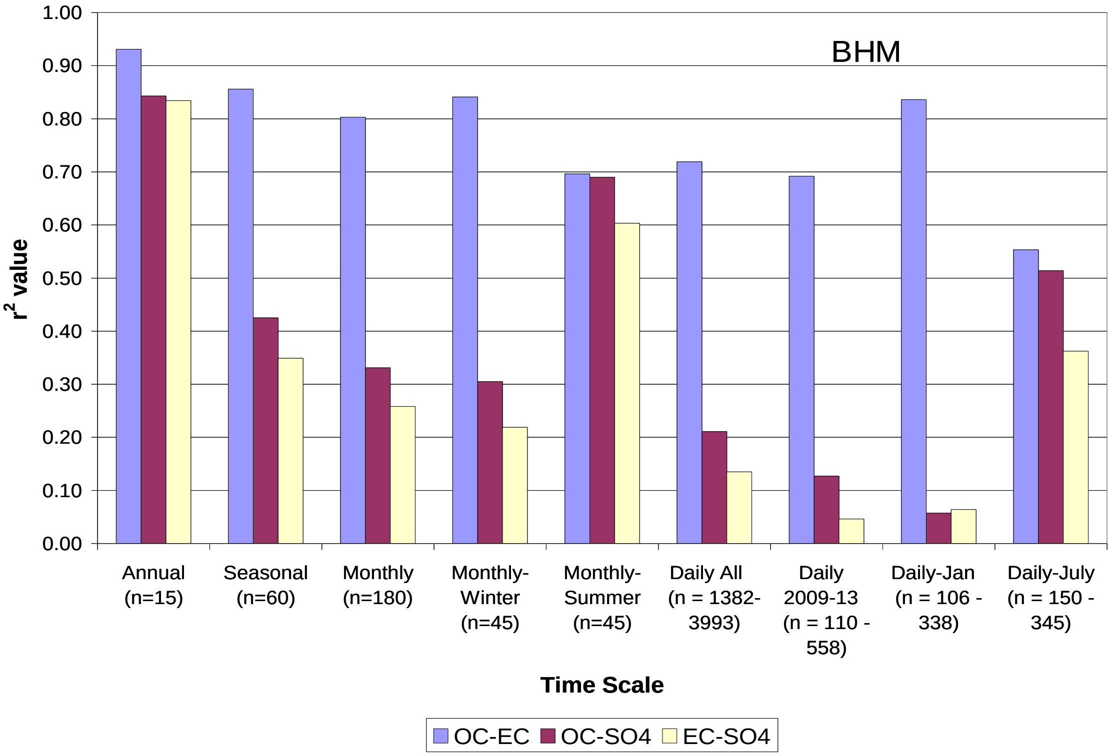

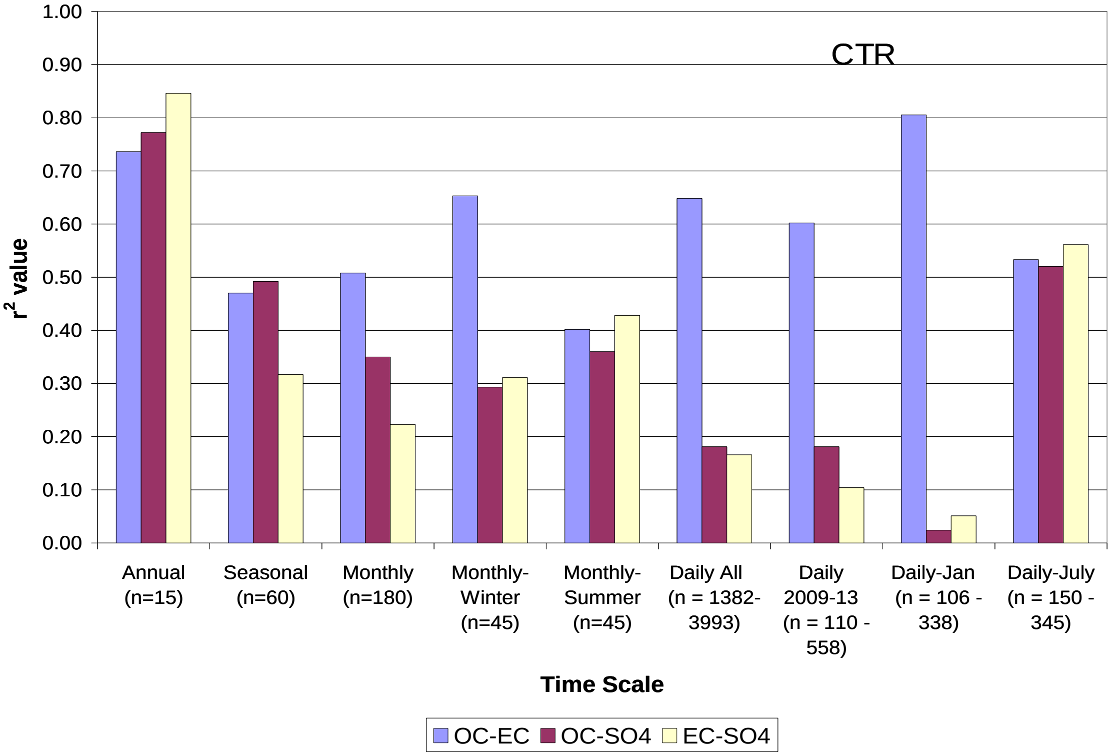

Figure S5. Correlations (r^2) among mean OC, EC, and SO_4 based on annual, seasonal, and monthly averaging periods and on daily measurements. Summer is defined as June through August, winter is December through February, autumn is September through November, and spring is March through May.

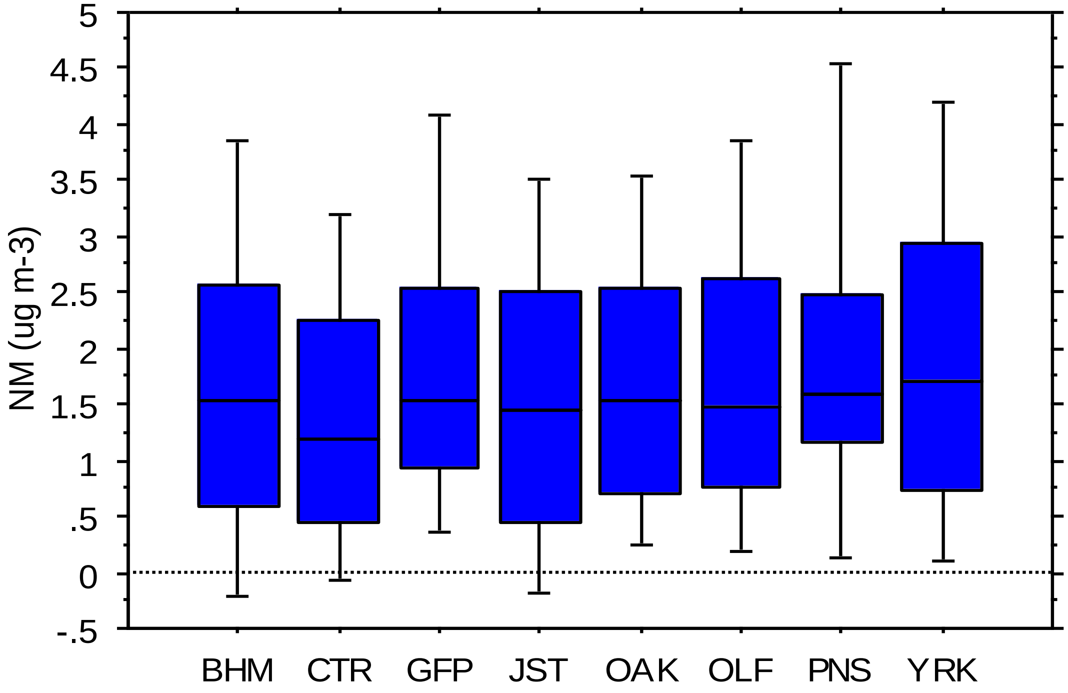

Figure S6. Distributions of non-measured (NM) $PM_{2.5}$ computed from 2009 – 2013 daily data as described in the text. Distributions indicate the 10th, 25th, 50th, 75th, and 90th percentiles. No measurements were made at PNS after 2009, at OAK after 2010, and at GFP after 2012 (GFP EC and OC data were not available after 2010).

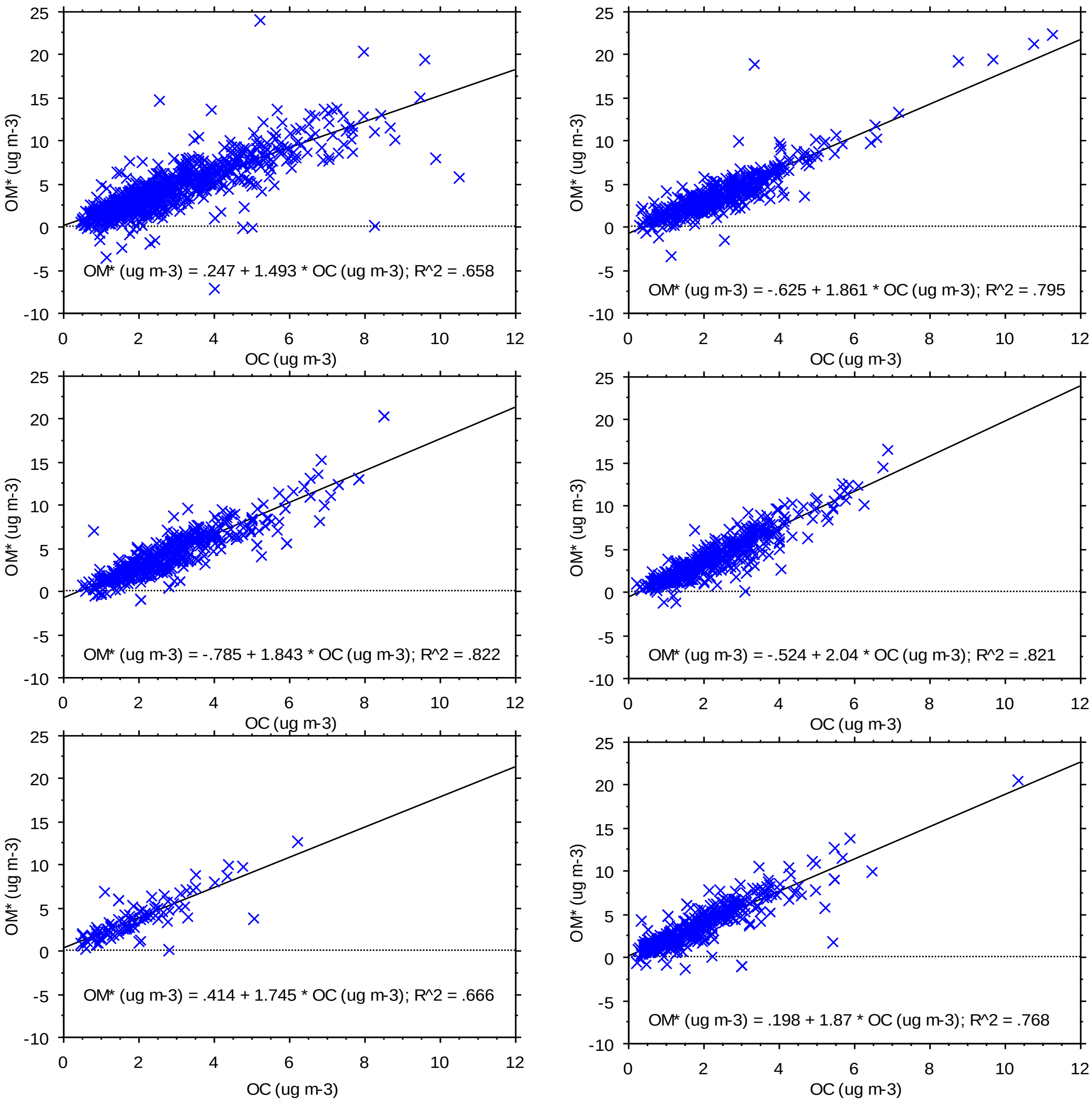

Figure S7. OM* vs. OC at SEARCH sites, 2009 – 2013. OM* is the sum of measured OC and the computed difference of $PM_{2.5}$ mass minus the sum of measured species concentrations. OM* is an upper bound for OM (see text).

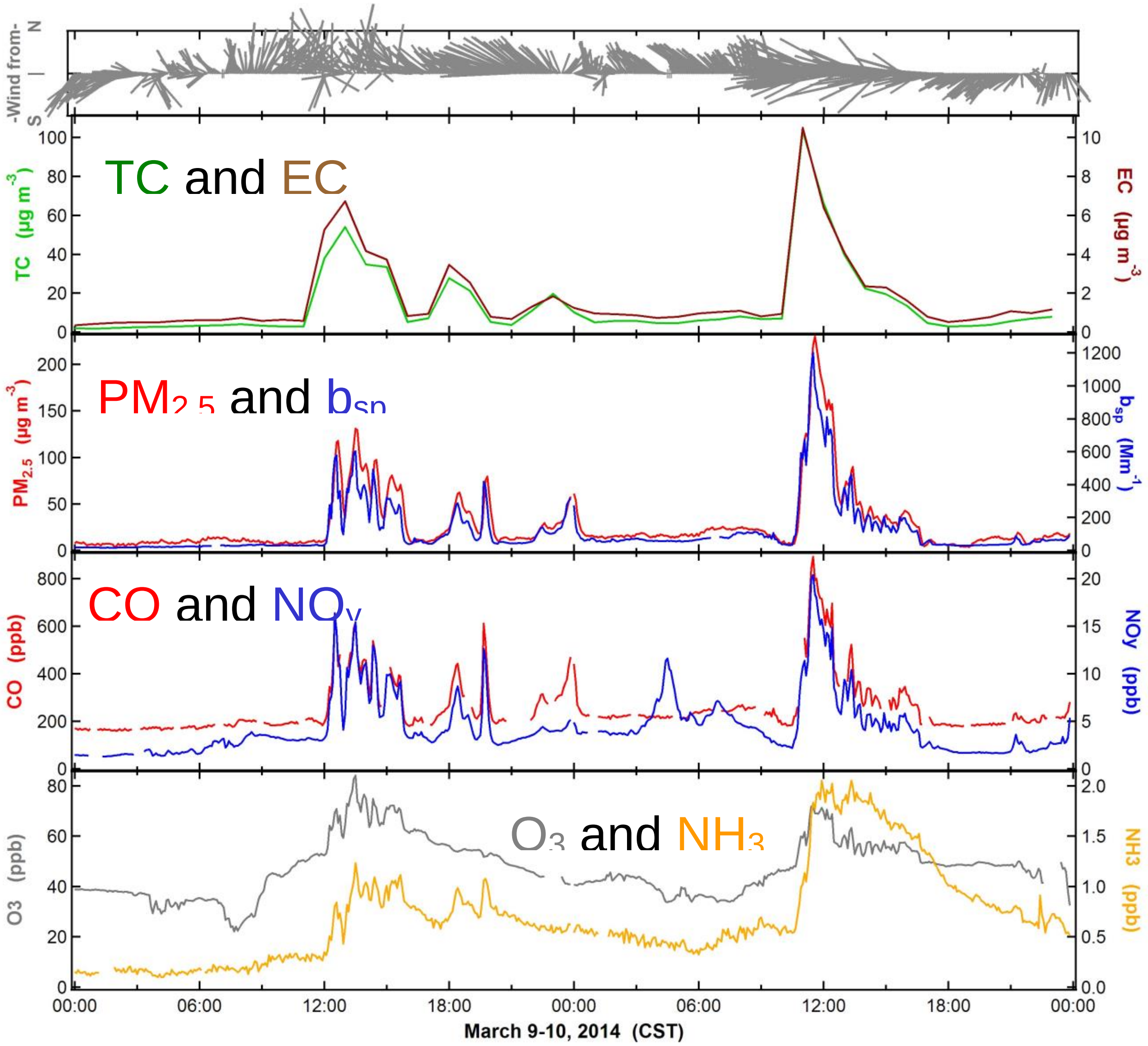

Figure S8. Observed biomass burning impacts at CTR on March 9 – 10, 2014. The burn was located ~10 km northwest of CTR on a ~1000 acre parcel. EC and TC data are hourly; all other measurements are 5-minute resolution. The surface wind directions potentially trace the plume but other factors (e.g., nocturnal inversion, fire intensity) also affect observed concentrations. NW winds occurred briefly on March 9 with weaker NW winds later in the day. The winds on March 10 show a persistent NW-SW direction followed by a shift to SW. The TC levels in the plume are very high relative to baseline: ~60 – 100 µg m^{-3} vs < ~ 5 µg m^{-3}. OC/EC ratios for the peak periods are about 9:1 to 11:1 (similar to the fire emission ratio in Table S2). The midday O_3 concentration peaks on the two days parallel the NO_y concentrations, but it is unclear if this pattern is directly related to the smoke plume or to more general effects from multiple mission sources in the region. The association of the NH_3 peak with the smoke plume is not explained, but could relate to fire chemistry.

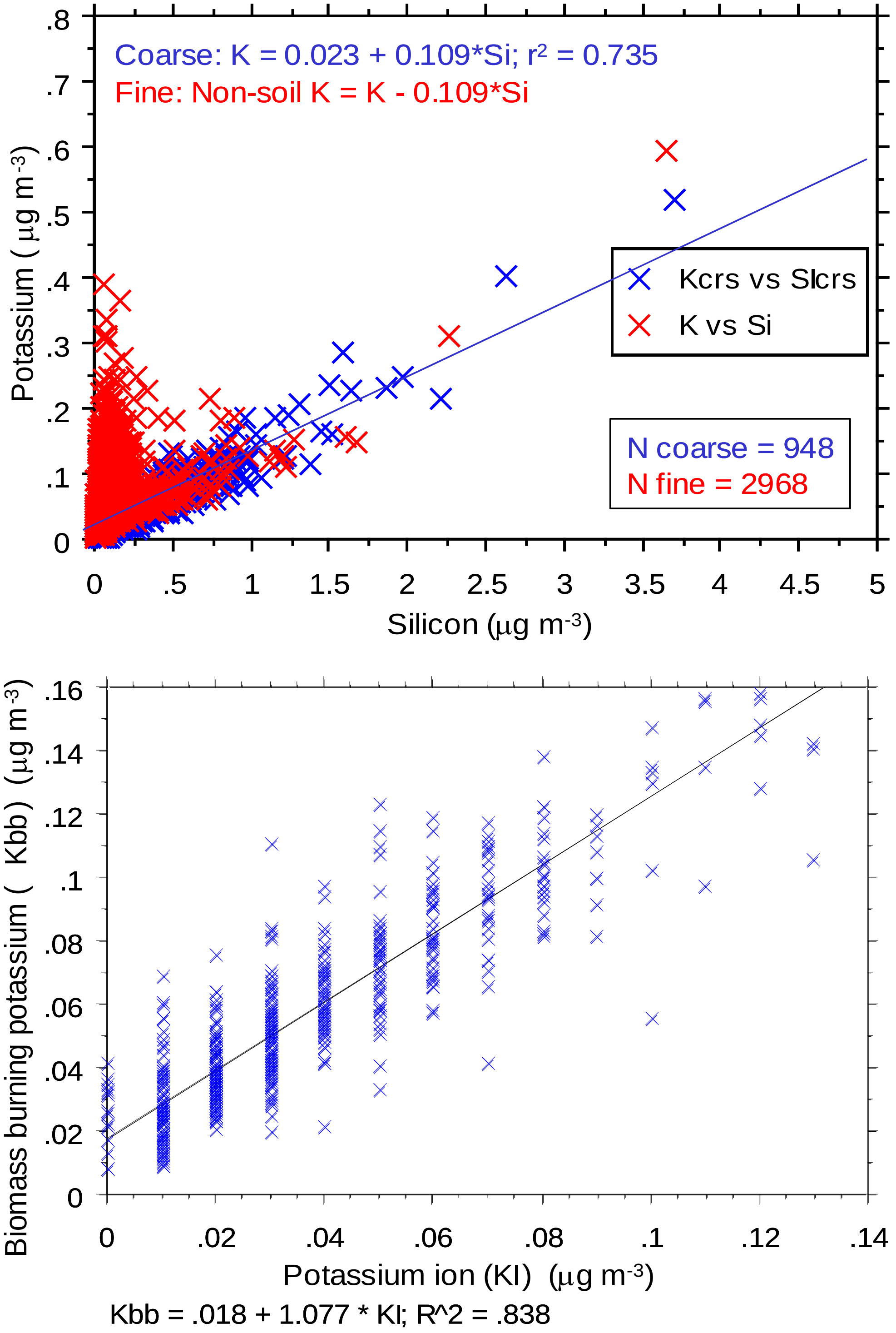

Figure S9. PM_{coarse} and $PM_{2.5}$ K vs. Si at CTR (top) and computed non-soil K (inferred as biomass burning K) vs. water soluble K (K ion) (bottom).

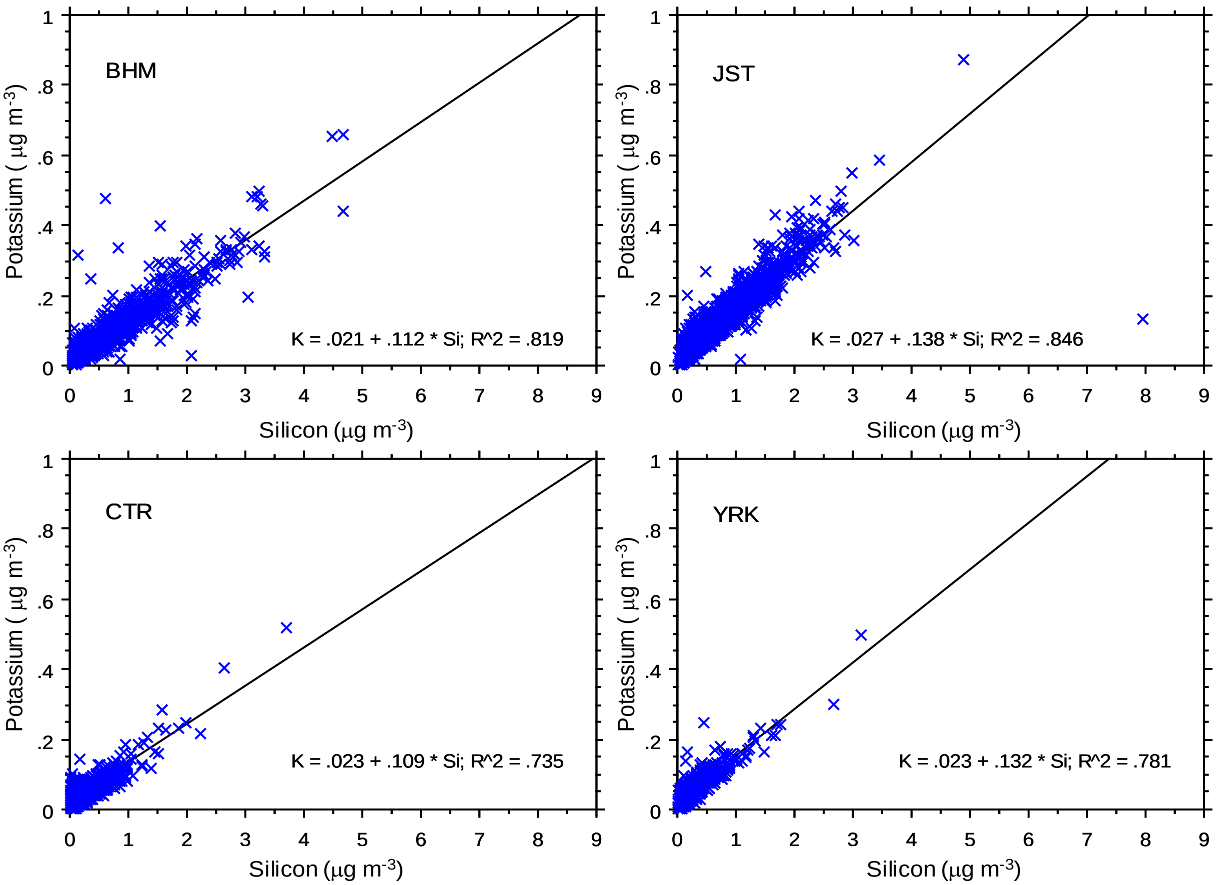

Figure S10. $PM_{10\text{-}2.5}$ K vs. Si.

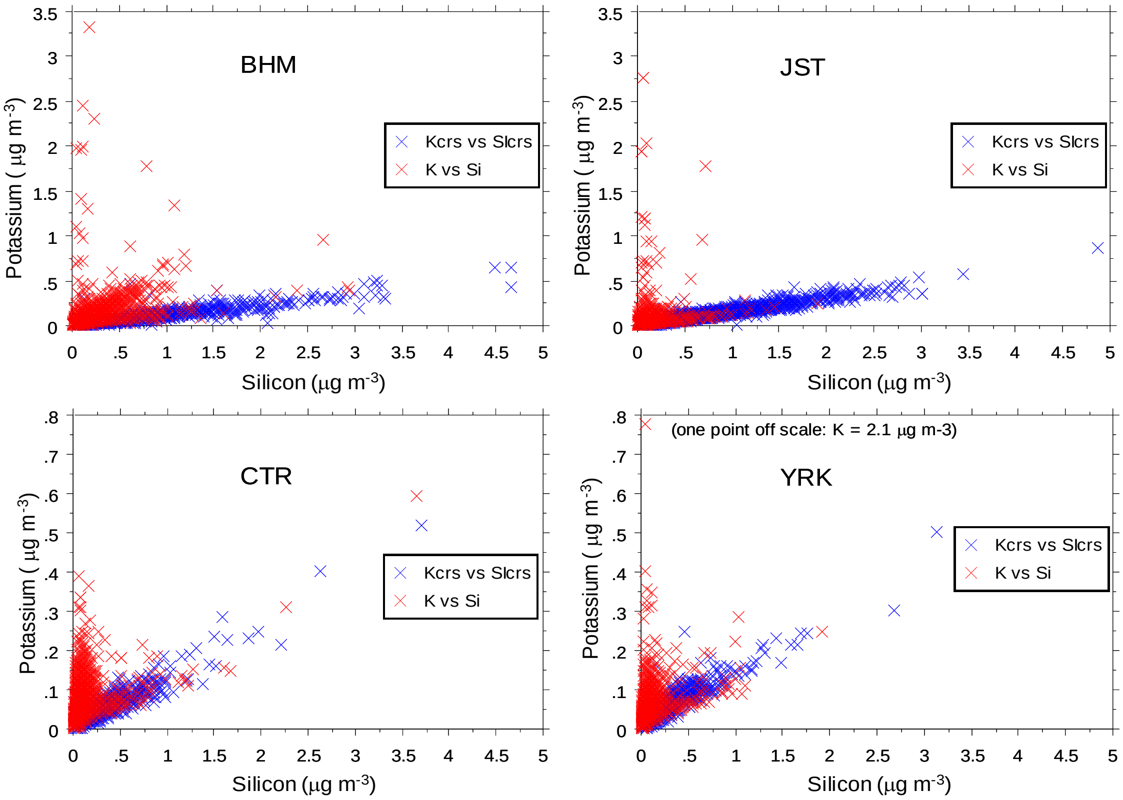

Figure S11. PM$_{crs}$ (PM$_{10-2.5}$) K vs. Si and PM$_{2.5}$ K vs. Si. Units are µg m^{-3}.

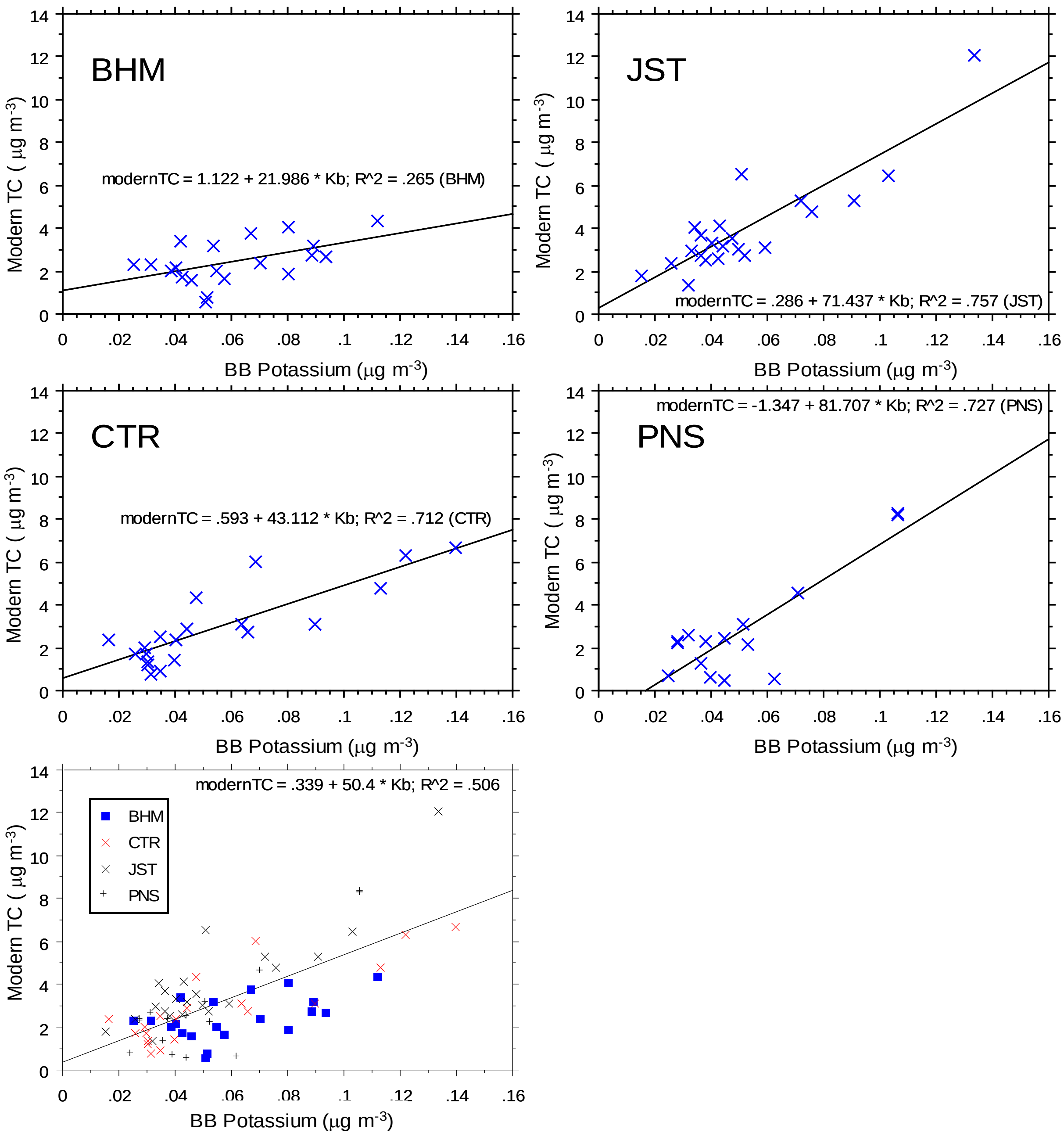

Figure S12. Modern total carbon (TC) (Blanchard et al., 2011) vs. biomass burning (BB) potassium (Kbb) for daily-average samples collected from the months of October through May (2004 and 2005).

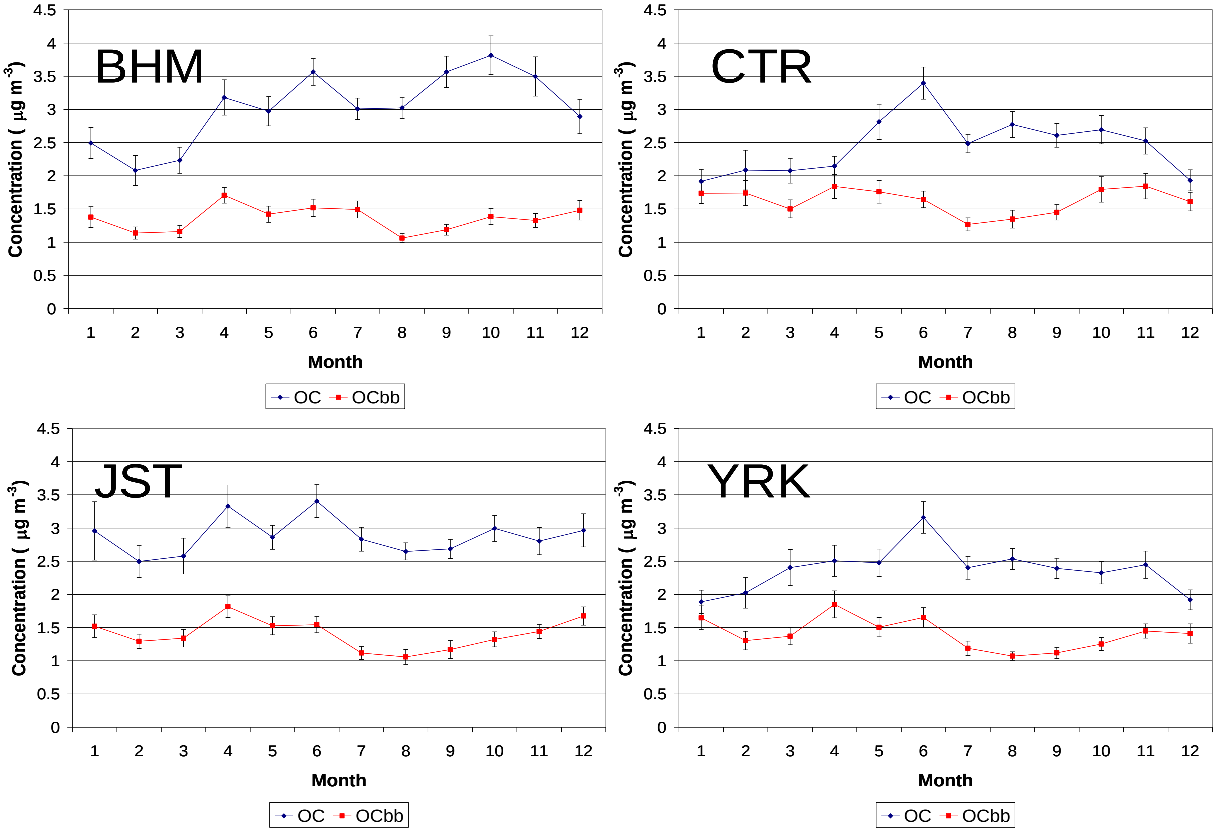

Figure S13. Monthly-average OC and OCbb at inland SEARCH sites, 1999-2013. Uncertainties are one standard error of the means.

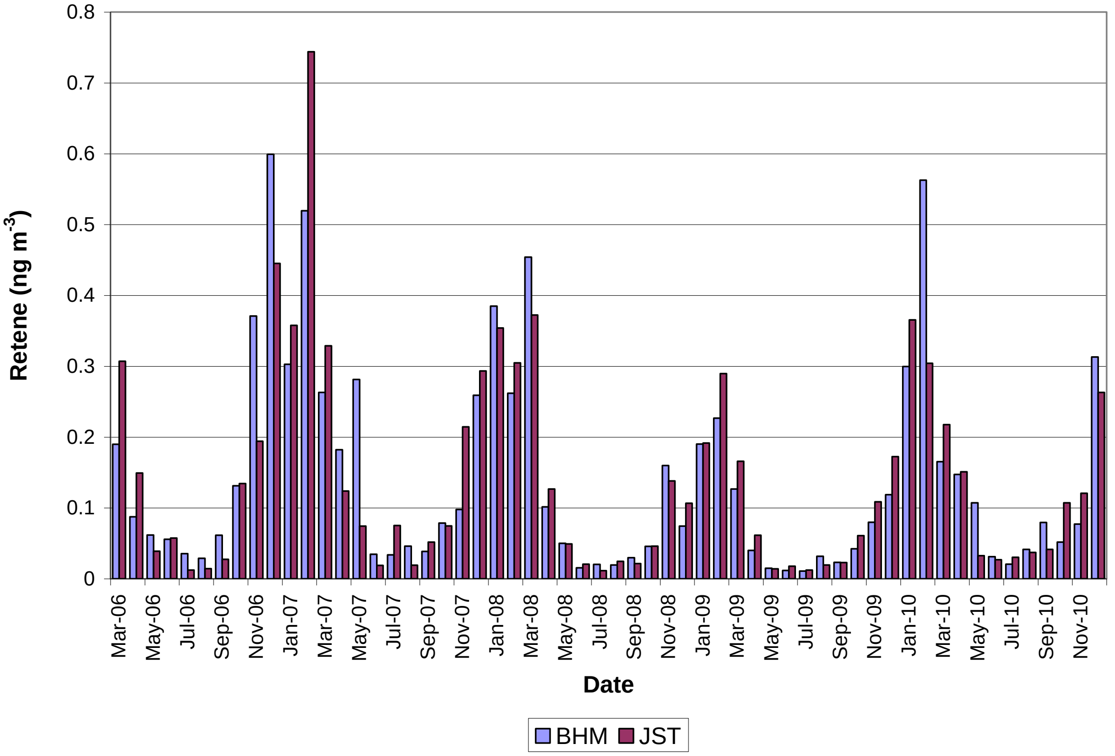

Figure S14. Monthly-average PM$_{2.5}$ retene concentrations at urban sites BHM and JST (Blanchard et al., 2014).

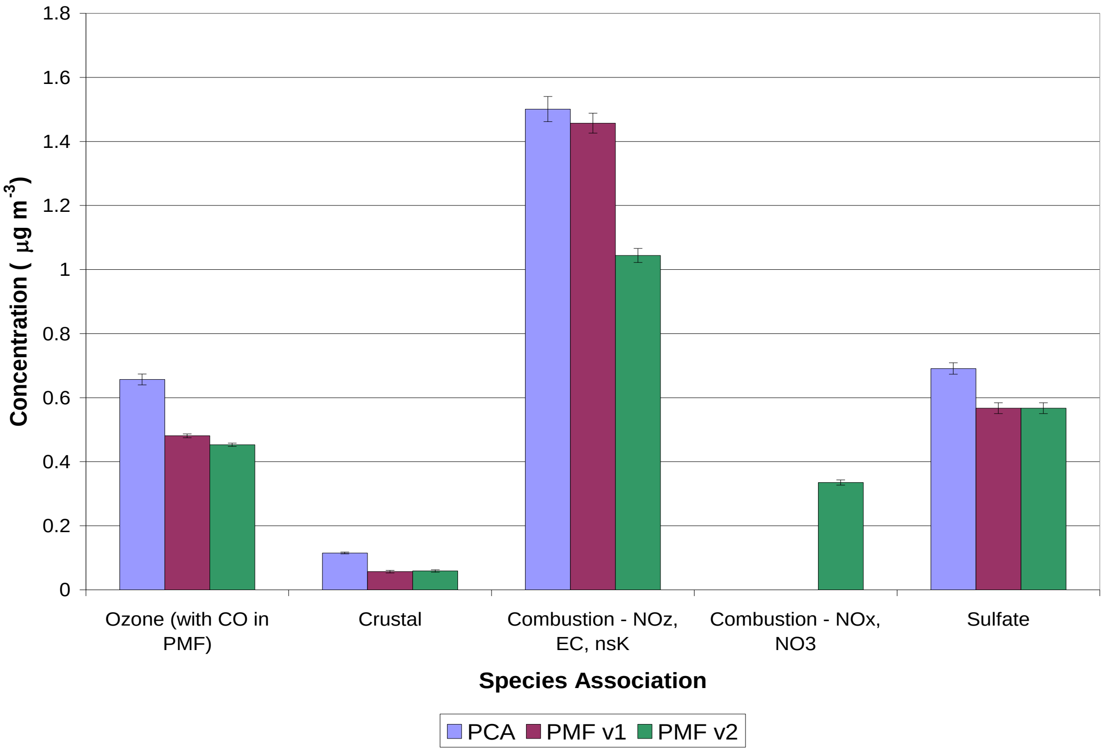

Figure S15. Comparison of CTR mean OC concentrations apportioned to PCA and PMF components. Uncertainties are one standard error of the means.

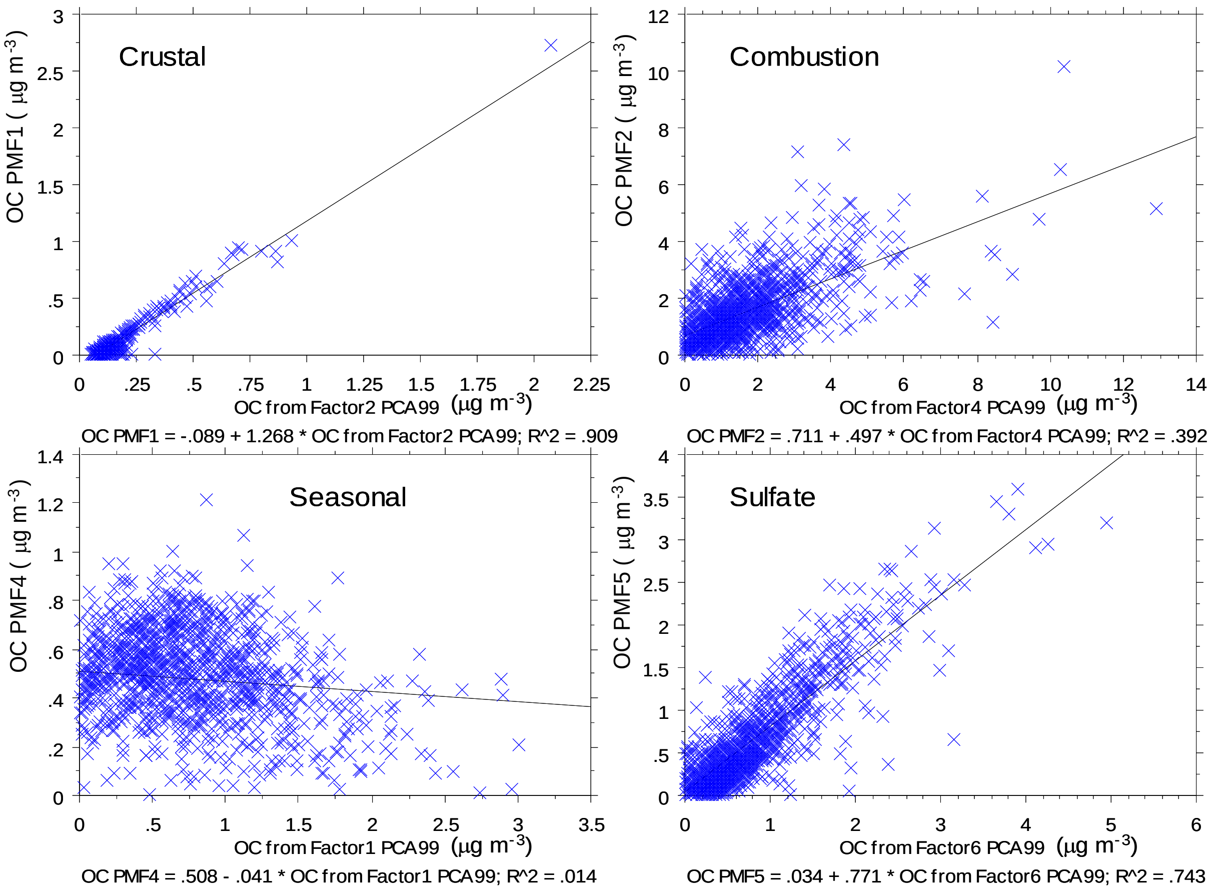

Figure S16. Comparison of CTR OC apportioned to PMF and PCA factors. PMF and PCA factor numbers are arbitrary and are matched by species associations. PCA99 refers to PCA2 beginning in 1999.

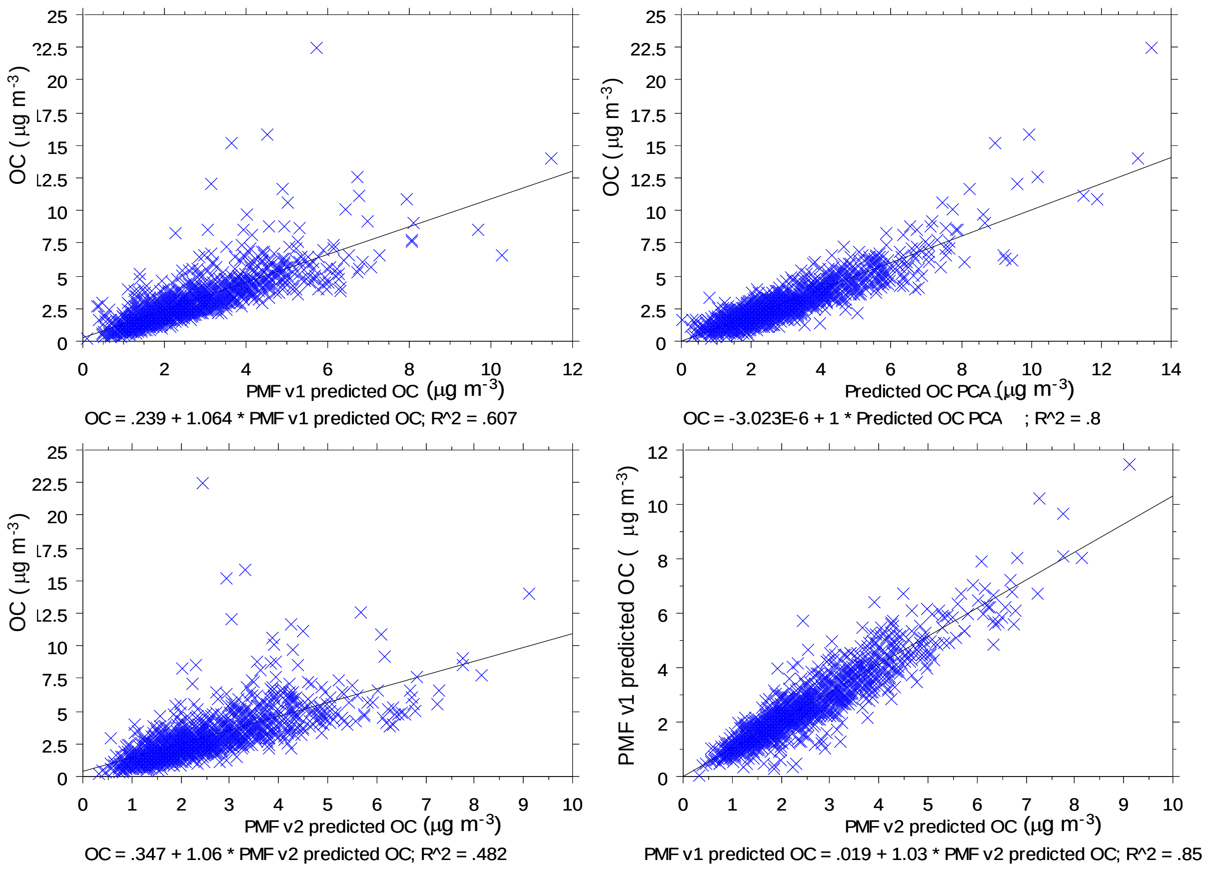

OC = .239 + 1.064 * PMF v1 predicted OC; R^2 = .607

OC = -3.023E-6 + 1 * Predicted OC PCA ; R^2 = .8

OC = .347 + 1.06 * PMF v2 predicted OC; R^2 = .482

PMF v1 predicted OC = .019 + 1.03 * PMF v2 predicted OC; R^2 = .85

Figures S17. Prediction of measured CTR OC by PMF and PCA. Both PMF applications underpredict the highest OC concentrations (upper left; lower left). The two PMF applications provide comparable predictions (lower right).

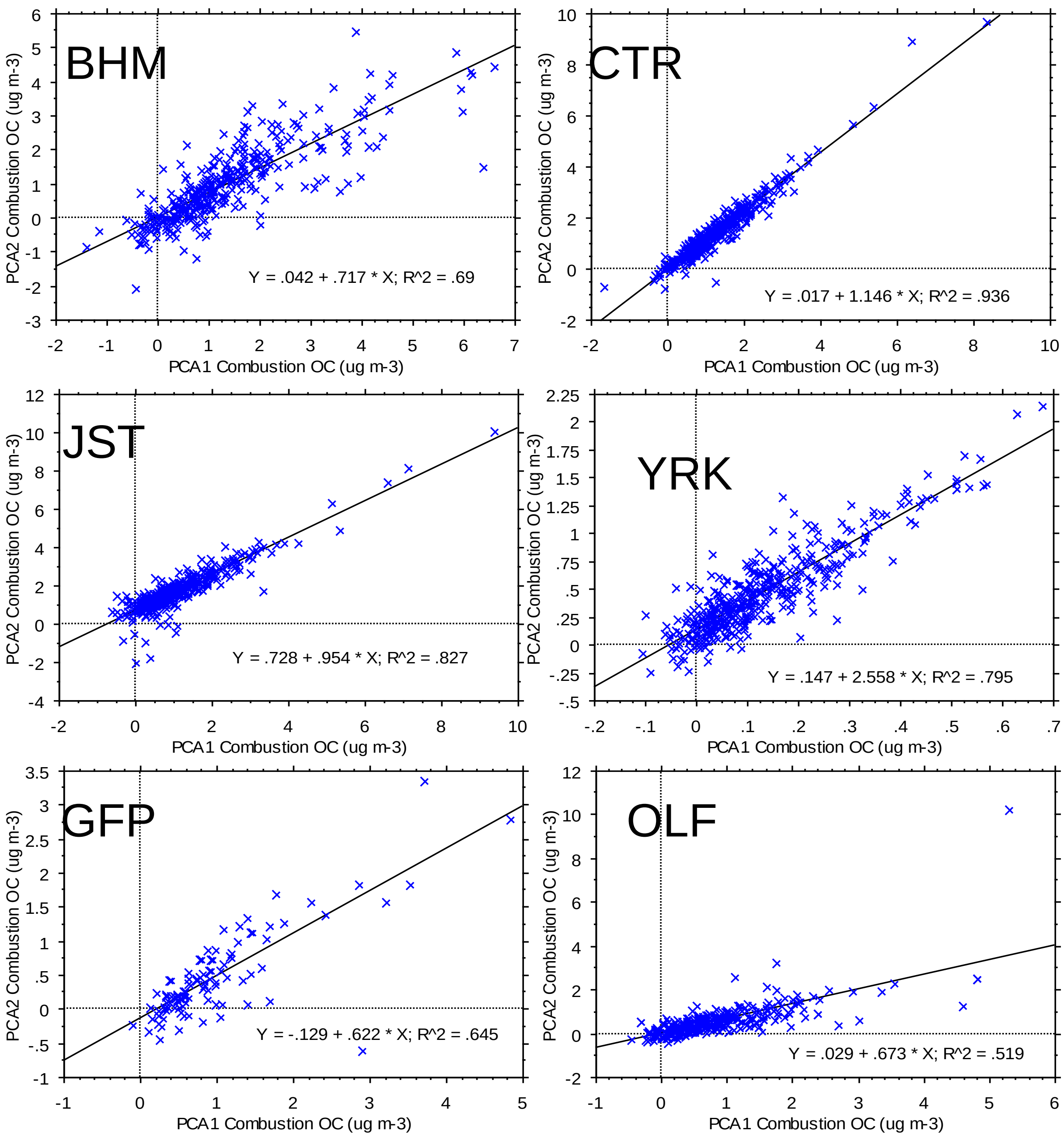

Figure S18. Comparison of PCA1 and PCA2 combustion-derived OC.

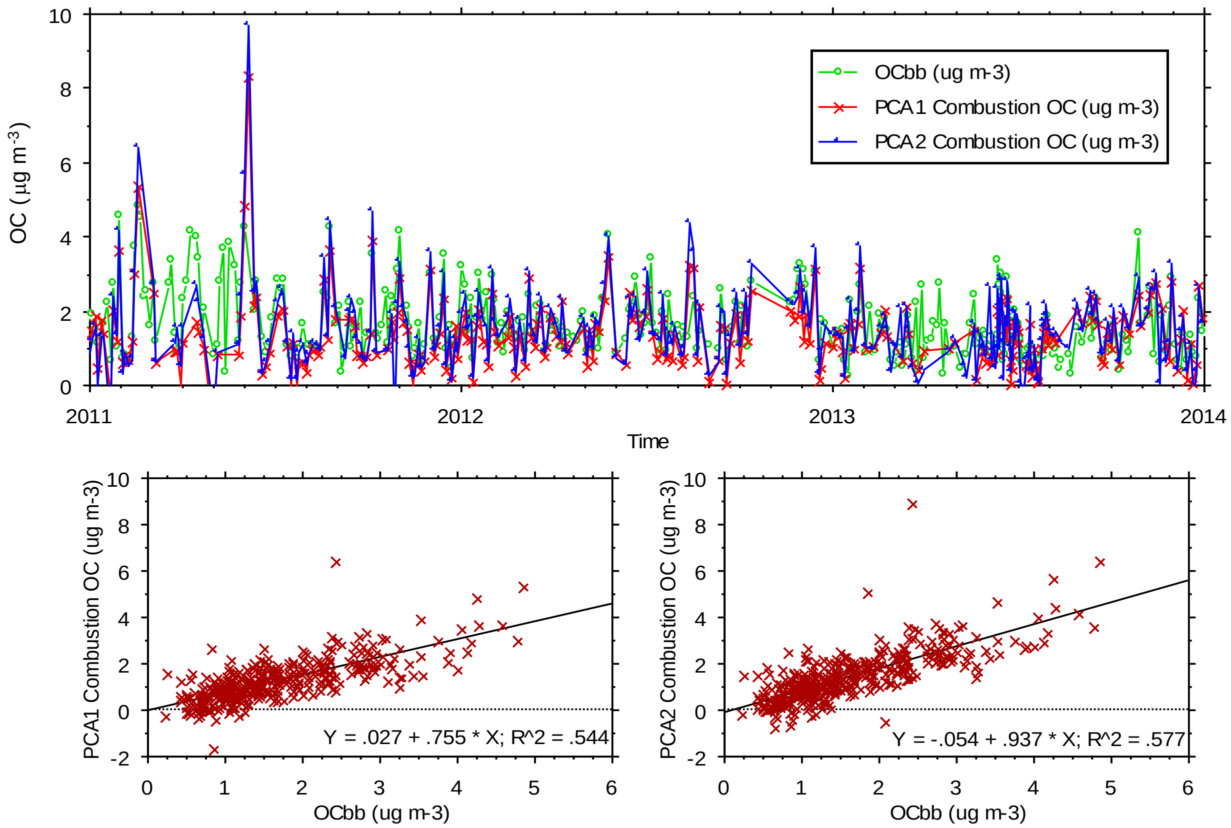

Figure S19a. Comparison of OCbb, PCA1 combustion OC, and PCA2 combustion OC at CTR. The scatter plots show all data points in 2008 – 2013. OCbb correlates significantly ($p < 0.0001$) with both PCA1 and PCA2 combustion OC. Whereas OCbb is computed from Kbb, PCA1 and PCA2 combustion OC concentrations are determined by concentrations of CO and EC in addition to K ion (PCA1) or Kbb (PCA2). On average, OCbb is ~10 – 20% higher than PCA1 or PCA2 combustion OC.

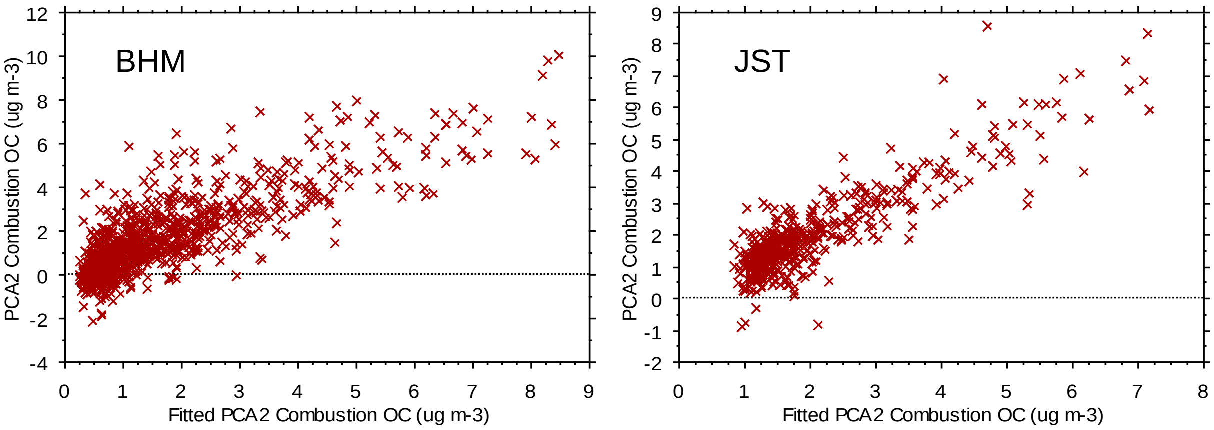

Figure S19b. PCA2 combustion OC vs predicted combustion OC as predicted by multiple regression on species not included in the PCA. (Left) BHM, predictor species 1-hour daily maximum NO and condensed-phase sums of n-alkanes, iso- and anteiso-alkanes, hopanes, and polycyclic aromatic hydrocarbons (PAHs) ($R^2 = 0.67$, $p < 0.0001$ for all species). (Right) JST, predictor species 1-hour daily maximum NO, condensed-phase sum of n-alkanes, gas-phase sum of aromatics ($R^2 = 0.78$, $p < 0.0001$ for all species). Gas-phase species data were not available for BHM. The correlations indicate that PCA2 combustion OC is associated with fresh emissions (NO) and with non-oxidized organic compounds.

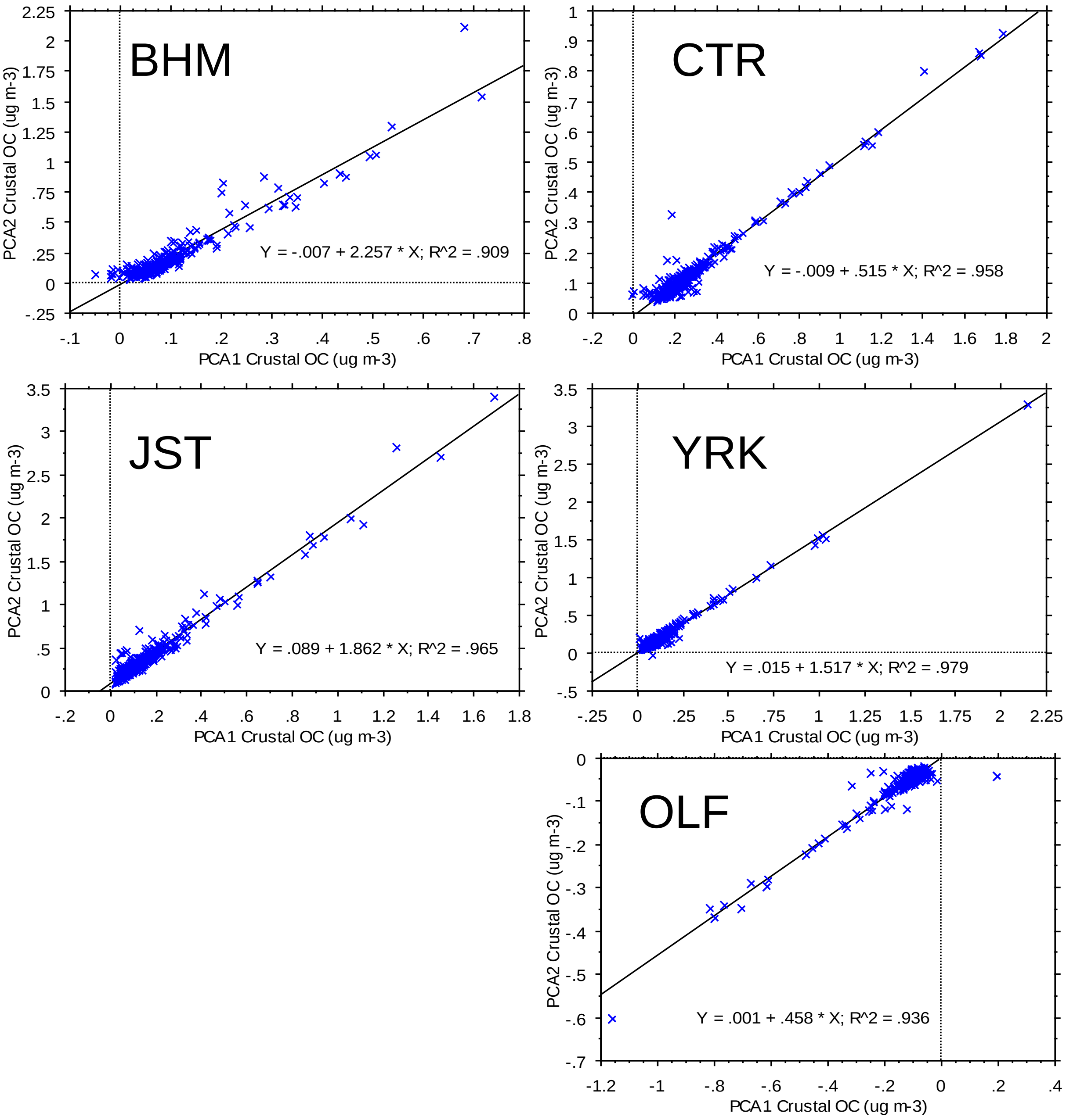

Figure S20. Comparison of PCA1 and PCA2 crustal OC.

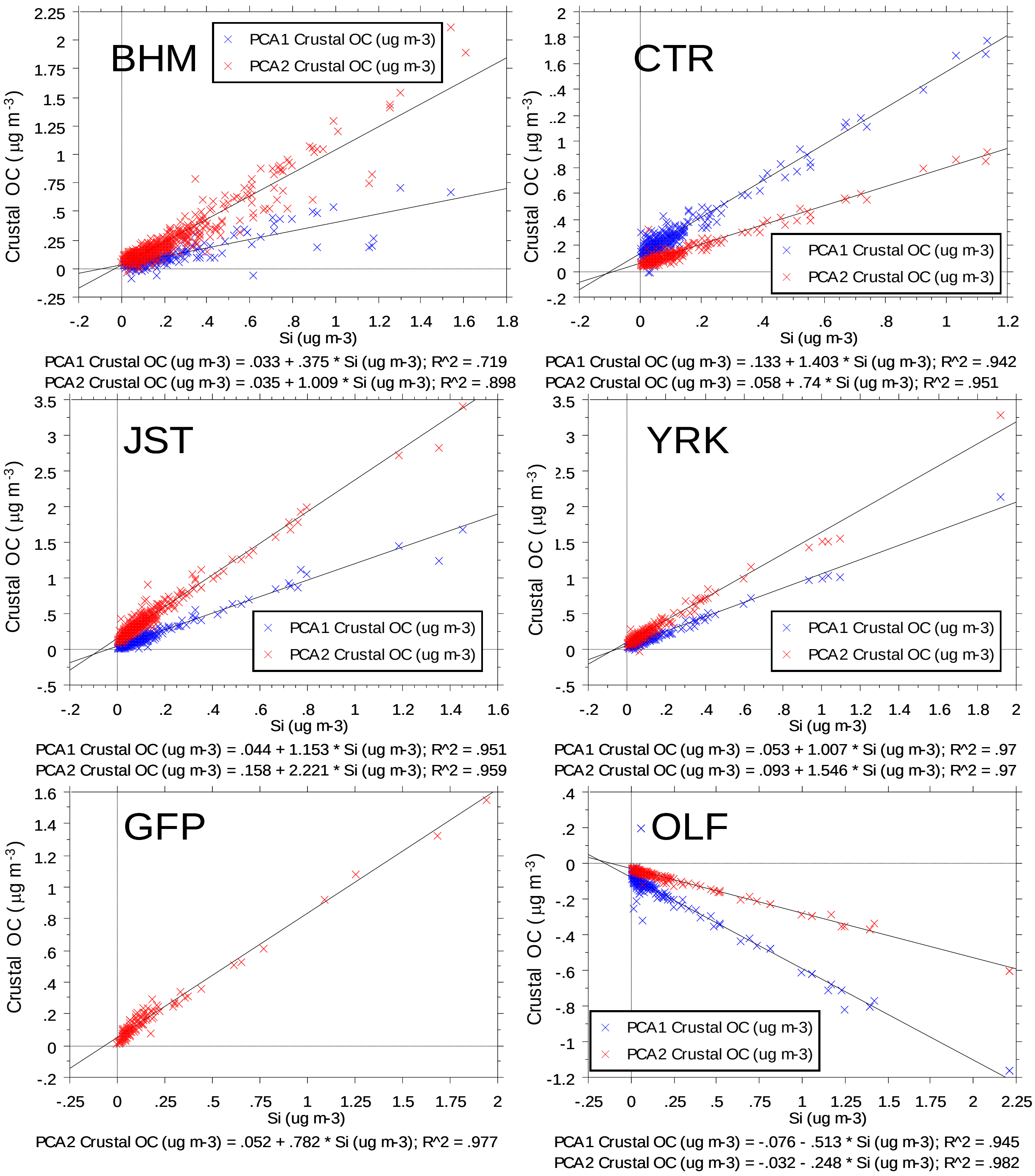

Figure S21. PCA1 and PCA2 crustal OC vs. silicon.

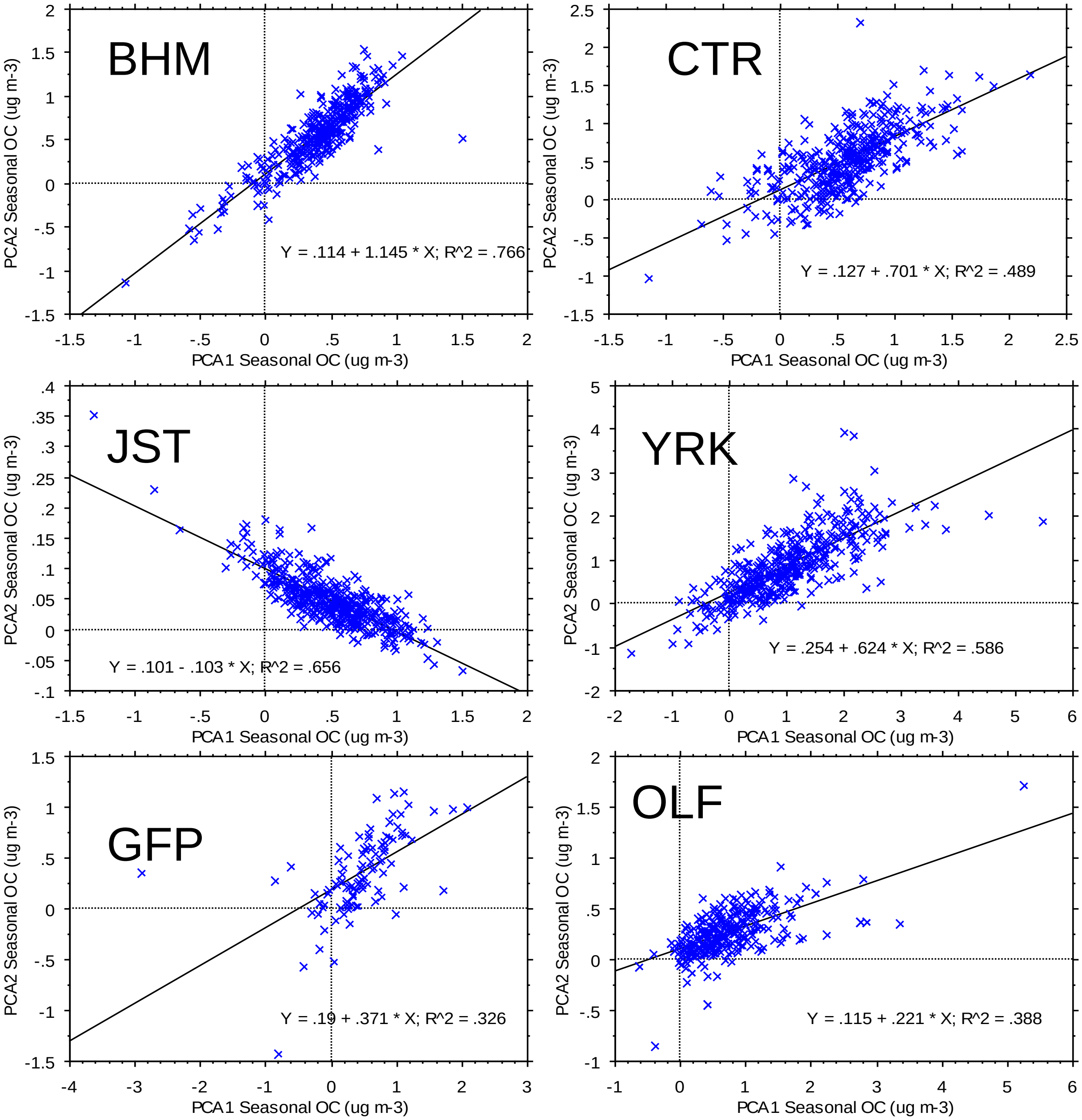

Figure S22. Comparison of PCA1 and PCA2 seasonal-component OC.

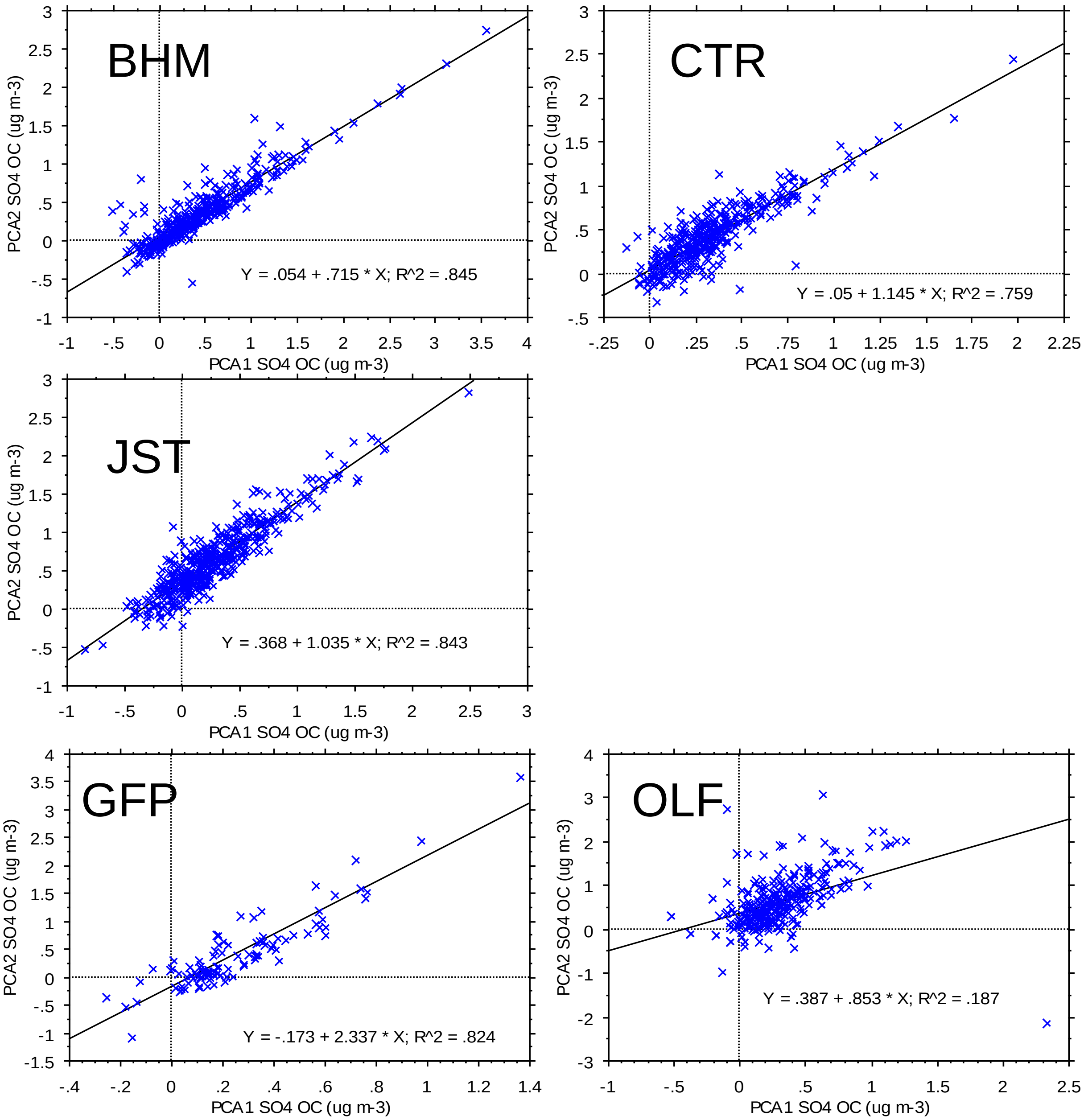

Figure S23. Comparison of PCA1 and PCA2 SO_4 OC.

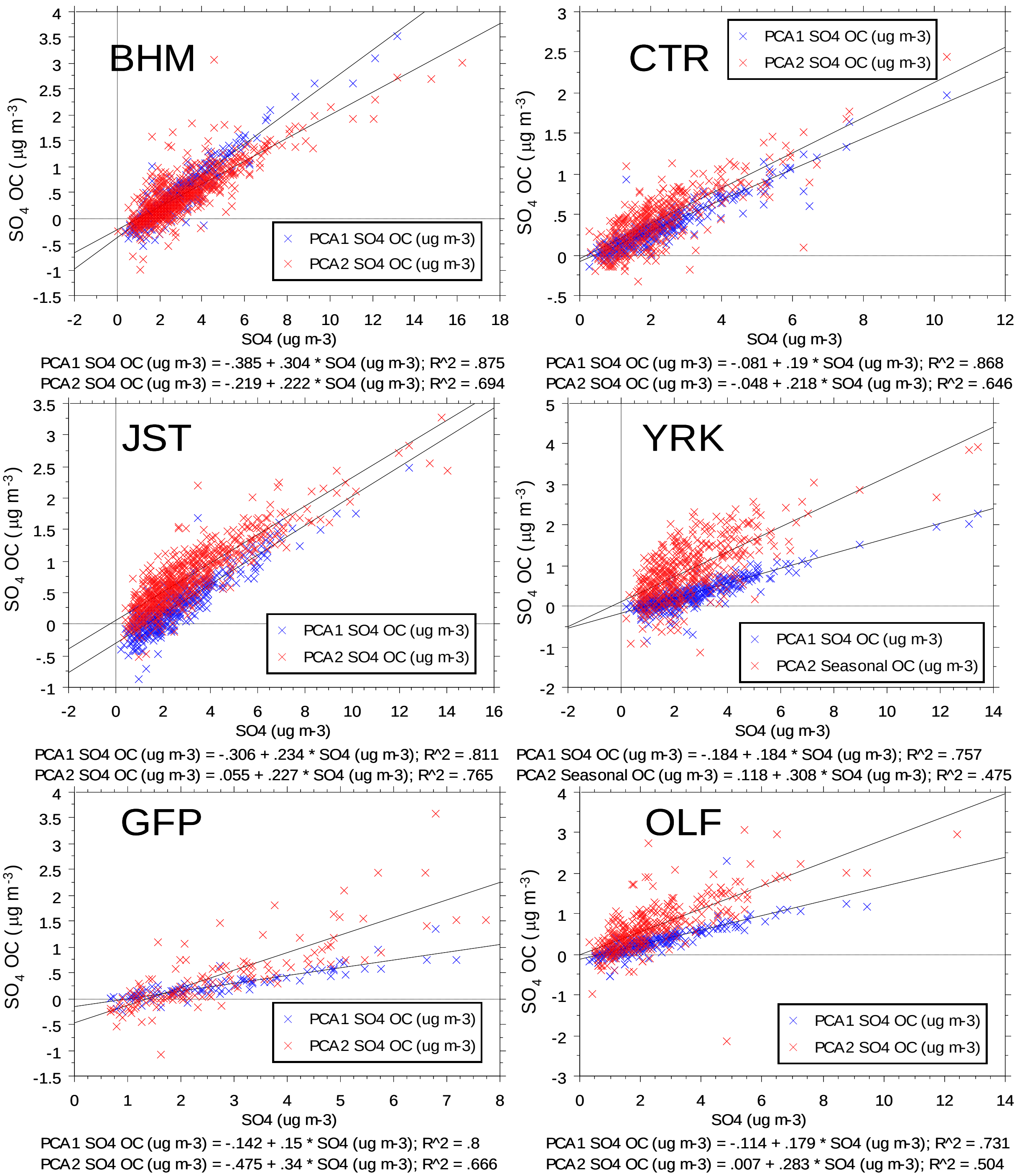

Figure S24. PCA1 and PCA2 SO_4 OC vs. SO_4. PCA2 did not separate seasonal and SO_4 components at YRK.

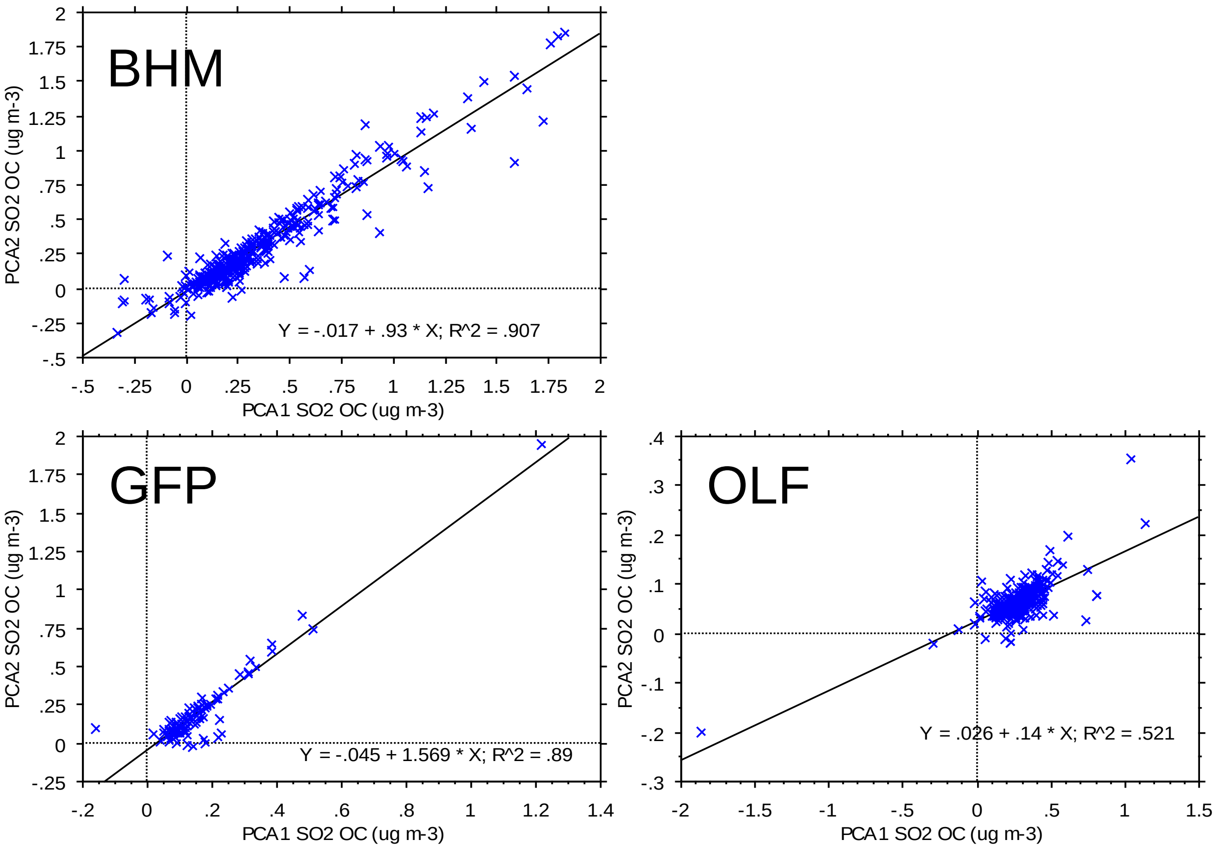

Figure S25. Comparison of PCA1 and PCA2 SO$_2$ OC.

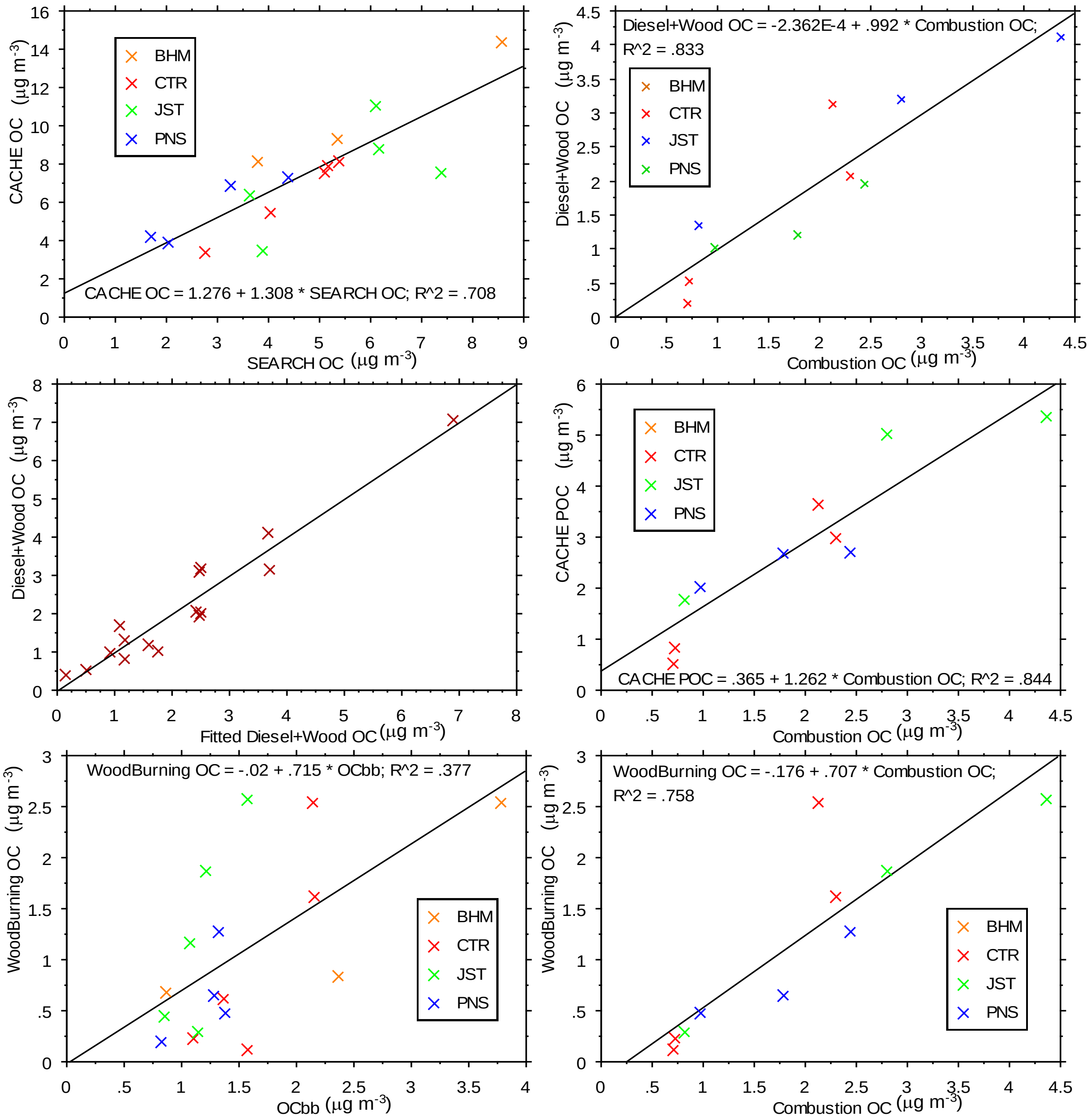

Figure S26. CACHE sampler OC source apportionments (Kleindienst et al., 2010) vs. SEARCH PCM sampler OC measurements and computed source contributions. SEARCH combustion OC was determined using PCA2 and is OC that is associated with CO, EC, Kbb, and NO$_x$ (Section 3.5). SEARCH OCbb was determined from Kbb (Section 3.4). CACHE POC is the sum of seven source categories described by Kleindienst et al. (2010).

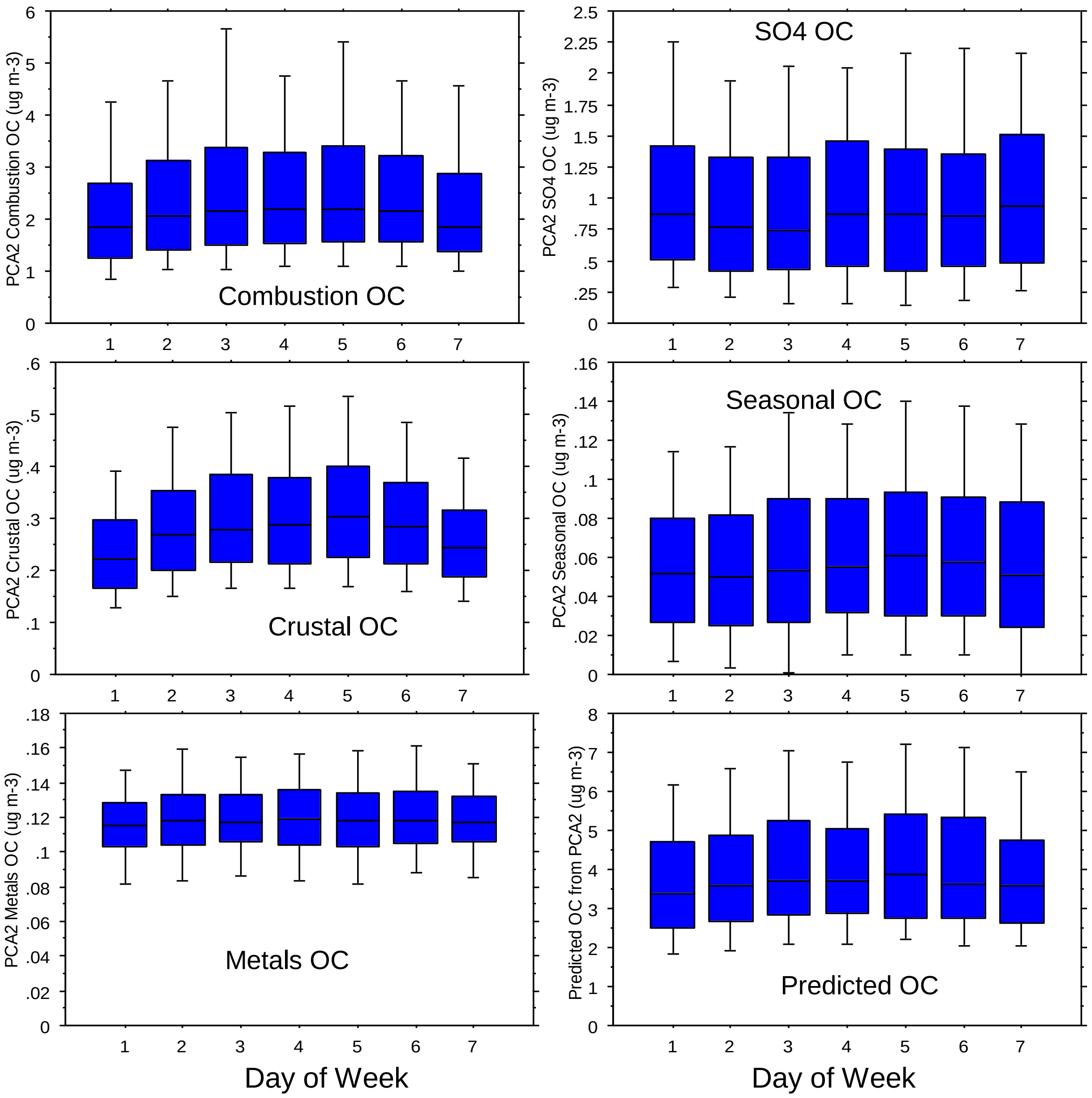

Figure S27. OC associated with PCA2 factors at JST vs. day of week, 1999 – 2013. Day of week begins with Sunday (1). Distributions indicate the 10th, 25th, 50th, 75th, and 90th percentiles. Units are μg m^{-3}.

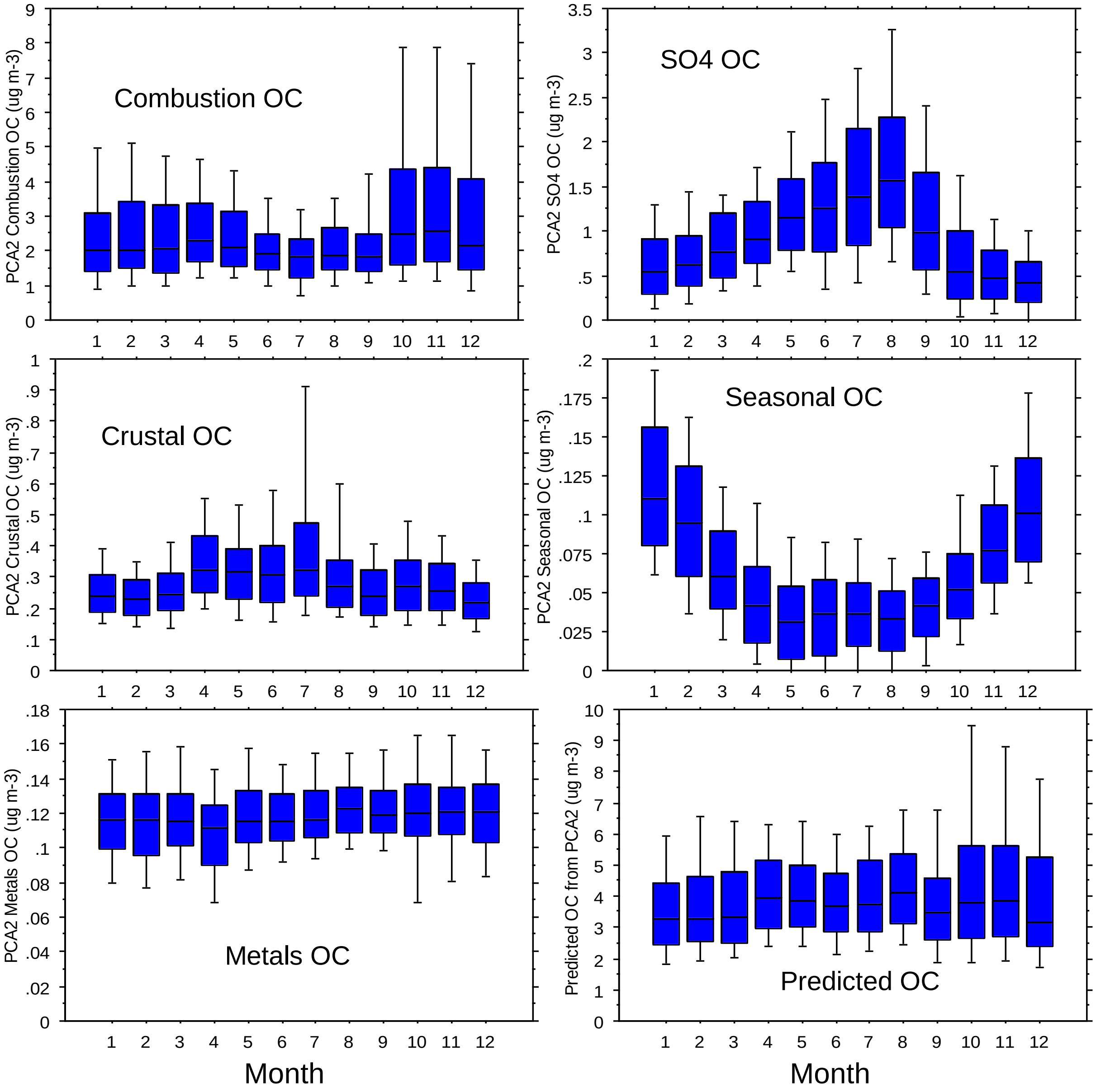

Figure S28. OC associated with PCA2 factors at JST vs. month, 1999 – 2013. Distributions indicate the 10th, 25th, 50th, 75th, and 90th percentiles.

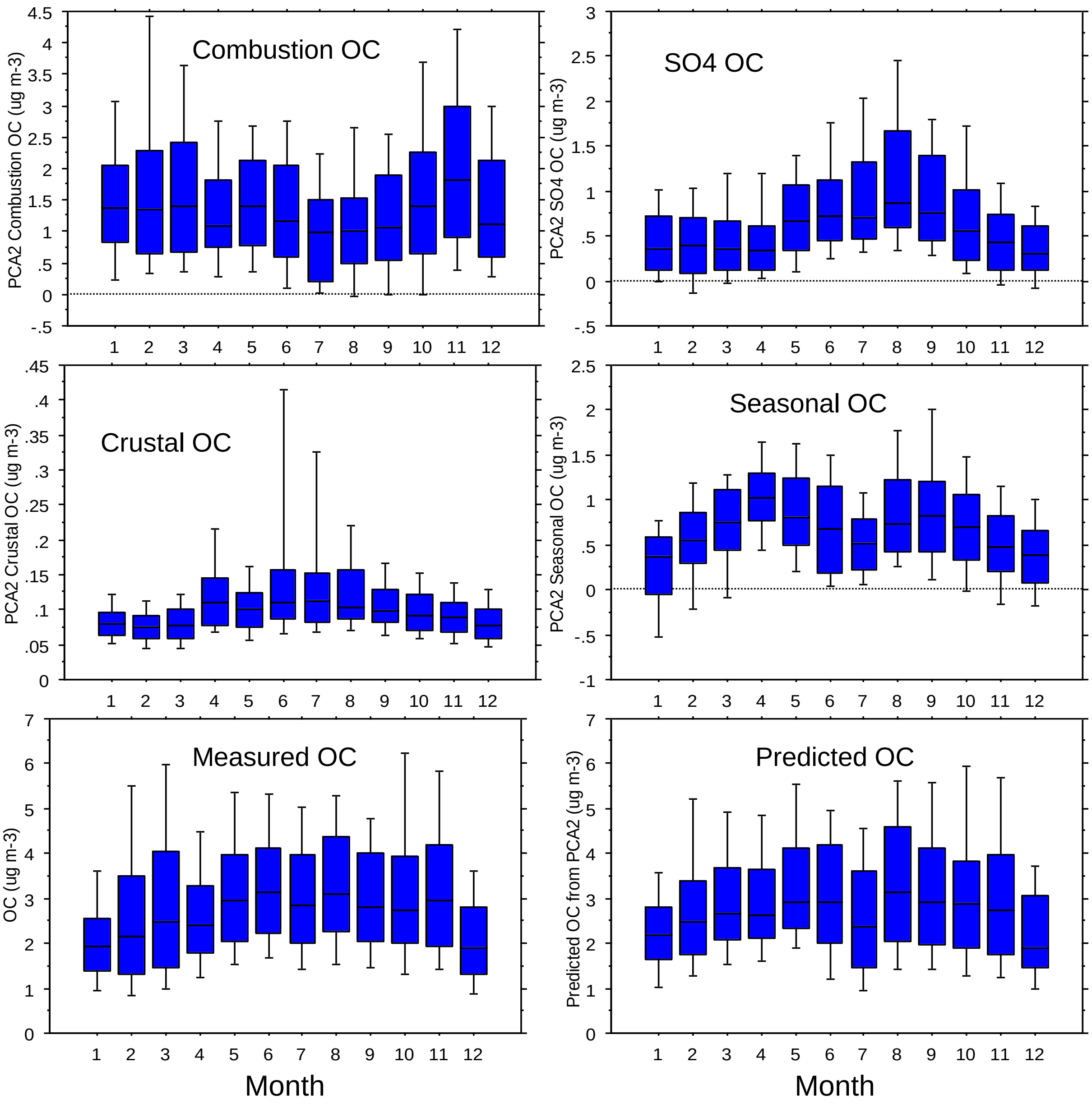

Figure S29. OC associated with PCA2 factors at CTR vs. month, 1999 – 2013. Distributions indicate the 10th, 25th, 50th, 75th, and 90th percentiles.

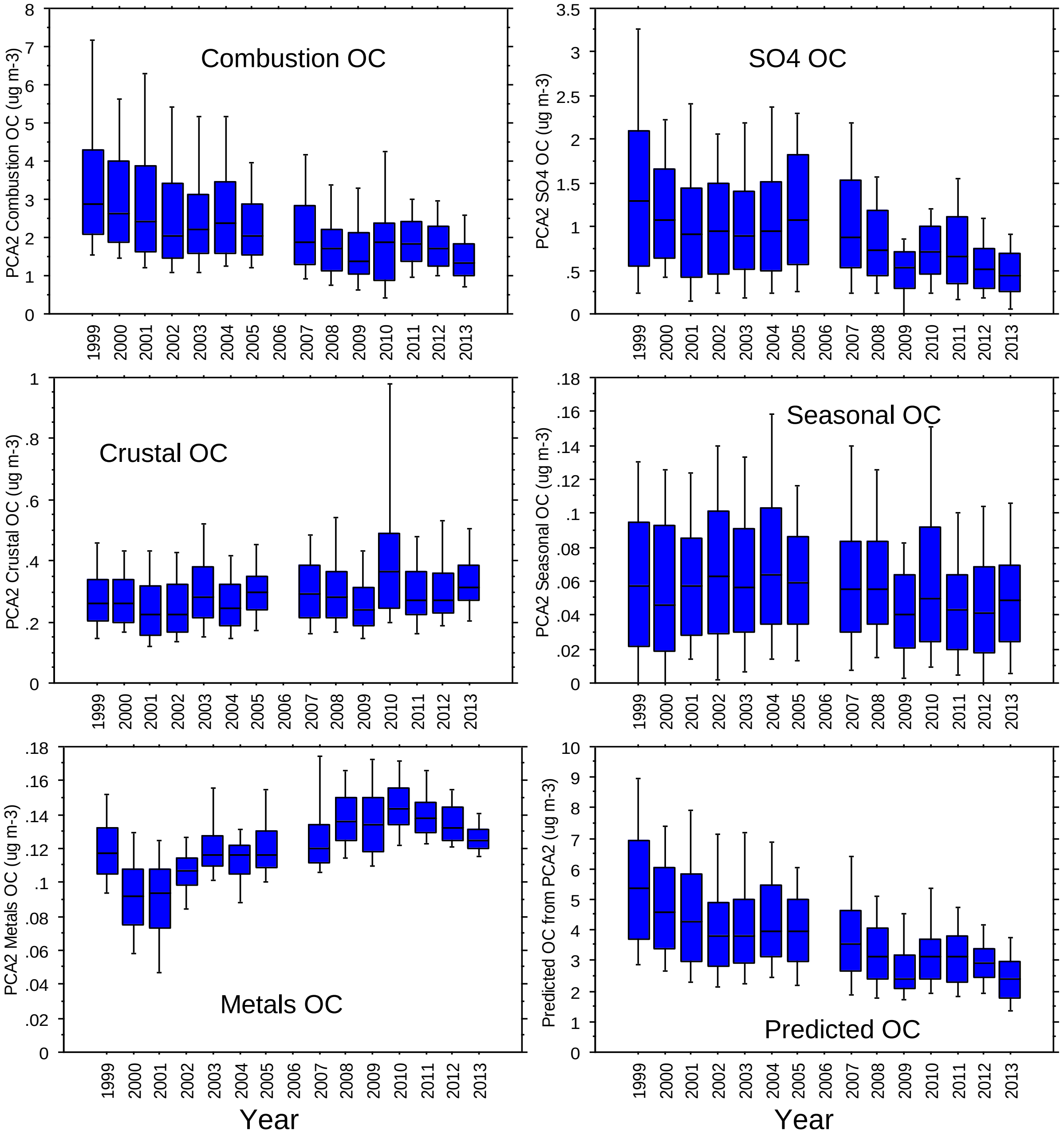

Figure S30. OC associated with PCA2 factors at JST vs. year, 1999 – 2013. Distributions indicate the 10th, 25th, 50th, 75th, and 90th percentiles. No predictions were made for 2006 due to missing CO and NO measurements.

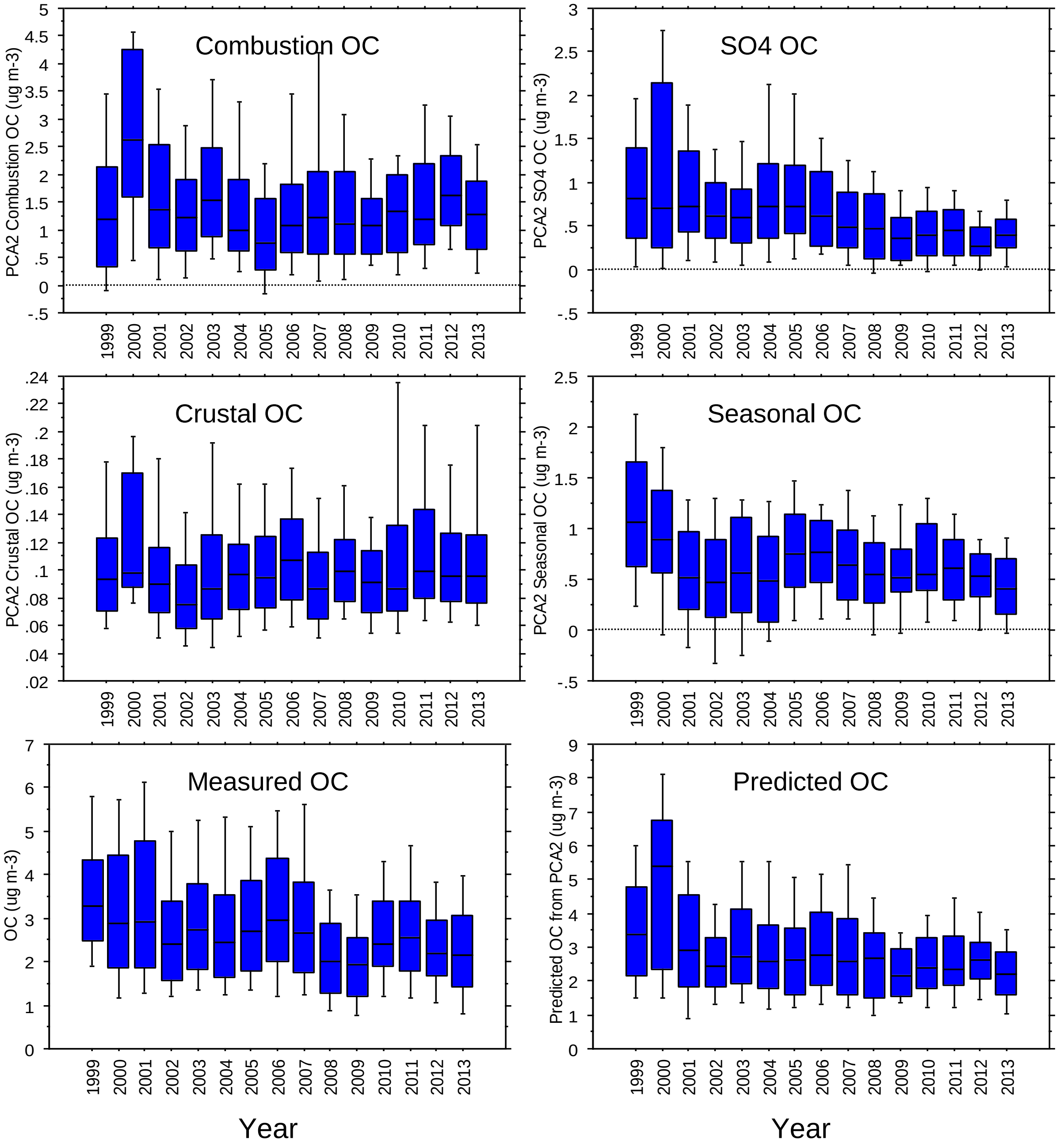

Figure S31. OC associated with PCA2 factors at CTR vs. year, 1999 – 2013. Distributions indicate the 10th, 25th, 50th, 75th, and 90th percentiles. Years with fewer sampling days are 2000 (n=11), 2009 (n=31), and 2010 (n=38).

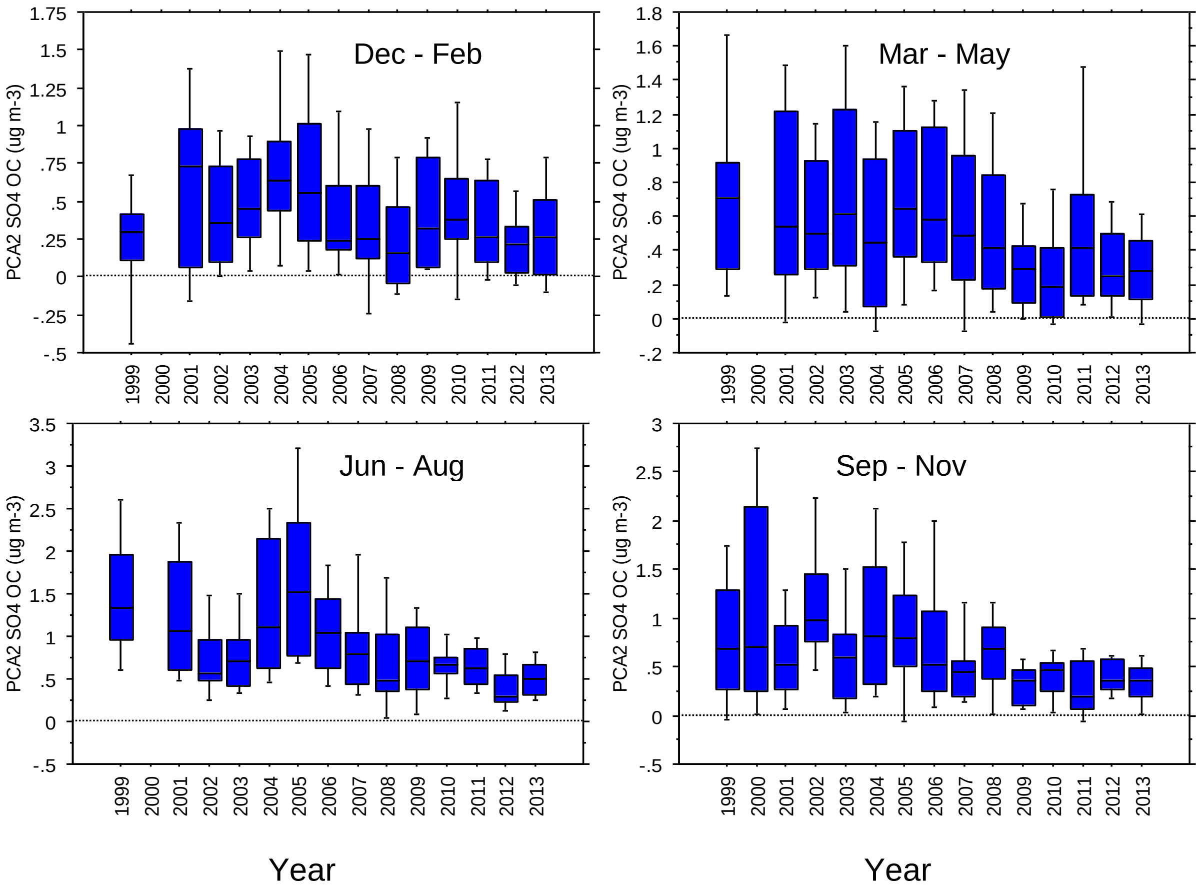

Figure S32. OC associated with PCA2 SO_4 factor at CTR vs. year, 1999 – 2013, shown by season. Distributions indicate the 10th, 25th, 50th, 75th, and 90th percentiles. Years with fewer sampling days are 2000 (n=11), 2009 (n=31), and 2010 (n=38).

Supplement References

Blanchard, C. L., Hidy, G. M., Tanenbaum, S., Edgerton, E., Hartsell, B., and Jansen, J.: Carbon in southeastern aerosol particles: empirical estimates of secondary organic aerosol formation, Atmos. Environ., 42, 6710-6720, 2008.

Blanchard, C. L., Tanenbaum, S., and Hidy, G. M.: Source attribution of air pollutant concentrations and trends in the Southeastern Aerosol Research and Characterization (SEARCH) network, Environ. Sci. Technol., dx.doi.org/10.1021/es402876s, 2013.

Budisulistiorini, S., Canagaratna, R., Croteau, P., Marth, W., Baumann, K., Edgerton, E., Show, S., Knipping E., Worsnop, D., Jayne, J., Gold, A., and Surratt, J.: Real-time continuous characterization of secondary organic aerosol derived from isoprene epoxydiols in downtown Atlanta, Georgia, using the Aerodyne Chemical Speciation Monitor, Environ. Sci. Technol., 47, 5686-5694, 2013.

Chan, M. N., Surratt, J. D., Claeys, M., Edgerton, E. S., Tanner, R. L., Shaw, S. L., Zheng, M., Knipping, E. M., Eddingsaas, N. C., Wennberg, P. O., and Seinfeld, J. H.: Characterization and quantification of isoprene-derived epoxydiols in ambient aerosol in the southeastern United States, Environ. Sci. Technol., 44, 4590–4596, 2010.

Ding, X., Zheng, M., Edgerton, E., Jansen, J., and Wang, X.: Contemporary or fossil origin: Split of estimated secondary organic carbon in the southeastern United States, Environ. Sci. Technol., 42, 9122-9128, 2008.

Gao, S., Surratt, J., Knipping, E., Edgerton, E., Shahgholi, M., and Seinfeld, J.: Characterization of polar organic compounds in fine aerosols in the southeastern United States: identity, origin and evolution, J. Geophys. Res., 111, doi 10.1029/2005JD006601, 2006.

Hu, W., Campuzano-Jost, P., Palm, B., DSay, D., Ortega, A., Hayes, P., Krechner, J., Chen, Q,Kuwata, M., Liu, Y., De Sa, S., Martin, S., Hum, M., Budisulistiorini, S., Riva, M., Surratt, J., St. Clair, J., Isaacman-VanWertz, G., Yee, L., Goldstein, A., Carbone, S., Artaxo, P., DeGouw, J., Koss, A., Wisthaler, A., Mikoviny, T., Karl, T., Kaser, L., Jud, W.,Hansel, A., Docherty, K., Robinson, N., Coe, H., Allan, J., Canagaratna, M., Paulot, F., and Jimenez, J.: Characterization of a real-time tracer for isoprene epoxidiols-derived secondary organic (IEPOX-SOA) from aerosol mass spectrometer measurements, Atmos. Chem. Phys. Discuss., 15, 11223-11276, 2015.

Kim, P., Jacob, D., Fisher, J., Travis, K., Yu, K., Zhu, L., Yantosca, R., Sulprizio, Jiminez, J., Campusano-Jost, P., Froyd, K., Liao, J., Hair, J., Fenn, M., Butle, C., Wagner, N., Gordon, T., Welti, A., Wennberg, P., Crounsem J., St. Clair, j., Teng, A., Millet, D., Schwarz, J., Markovic, M., and Perring, A.: Sources, seasonality and trends of Southest US aerosol: an integrated analysis of surface, aircraft, and satellite observations with the GEOS-CHEM chemical transport model, Atmos. Chem. Phys. Discuss., 15, 17651-17709, 2015.

Kleindienst, T., Lewandowski, M., Offenburg, J., and Edney, E.: Contribution of primary and secondary sources of organic aerosol and PM2.5 at SEARCH network sites, J. Air Waste Manage., 60, 1388-1399, 2010.

Lee, D., Balachandran, S. Pachon, J., Shankaran, R., Lee, S., Mulholland, J. A., and Russell, A. G. Ensemble-trained $PM_{2.5}$ source apportionment approach for health studies, Environ. Sci. Technol., 43, 7023–7031, 2009.

Lewandowski, M., Piletic, I., Kleindienst, T., Offenburg, J., Beaver, M., Jaoui, M., Docherty, K., and Edney, E.: Secondary organic aerosol characterization at field sites across the United States during the spring-summer period, Intern. J. Environ. Anal. Chem. 93, 1084-1103, 2013.

Liao, J., Froyd, K., Murphy, D., Keutsch, F., Yu, G., Wennberg, P., St. Clair, J., Crounse, J., Wisthaler, A., Mikoviny, T., Jiminez, J., Campuzano-Jost, P., Day, D., Hu, W., Ryerson, T., Pollack I., Peischl, J., Anderson, B., Ziemba, L., Blacke, D., Meinhardi, S., and Diskin, G.: Airborne measurements of organosulfates over the continental U.S., J. Geophys. Res. Atmos., 120, doi:10.1002/so14JD022378, 2015.

Lim, H. and Turpin, B.: Origins of primary and secondary organic aerosol in Atlanta: results of time-resolved measurements during the Atlanta Supersite experiment, Environ. Sci. Technol., 36, 4489-4496, 2002.

Lin, Y., Knipping, E., Edgerton, E., Shaw, S., and Surratt, J.: Investigating the influences of SO_2 and NH_3 levels on isoprene-derived secondary organic aerosol formation using conditional sampling approaches, Atmos. Chem. Phys., 13, 8457-8470, 2013.

Weber, R.J., Sullivan, A.P., Peltier, R.E., Russell, A., Yan, B., Zheng, M., de Gouw, J., Warneke, C., Brock, C., Holloway, J.S., Atlas, E.L., and Edgerton, E.: A study of secondary organic aerosol formation in the anthropogenic-influenced southeastern United States, J. Geophys. Res., 112, D13302, 2007.

Xu, L., Guo, H., Boyd, C. M., Klein, M., Bougiatioti, A., Cerully, K. M., Hite, J. R., Isaacman-VanWertz, G., Kreisberg, N. M., Knote, C., Olson, K., Koss, A., Goldstein, A. H., Hering, S., de Gouw, J., Baumann, K., Lee, S-H., Nenes, A., Weber, R., and Ng, N. L.: Effects of anthropogenic emissions on aerosol formation from isoprene and monoterpenes in the southeastern United States, P. Natl. Acad. Sci. USA, 112, (1) 37-42, doi:10.1073/pnas.1417609112, 2015a.

Xu, L. Suresh, S., Guo, H., Weber, R., and Ng, N.: Aerosol characterization over the southeastern United States using high-resolution aerosol mass spectrometry: spatial and seasonal variation of aerosol composition and sources with a focus on organic nitrates, Atmos. Chem. Phys., 15, 7307-7336, 2015b.

Yu, S., Bhave, P., Dennis, R., Mathur, R.: Seasonal and regional variations of primary and secondary organic aerosols over the continental United States: semi-empirical estimates and model evaluation, Environ. Sci. Technol., 41, 4690-4697, 2007.

Zhang, X., Hecobian, A., Zheng, M., Frank, N., and Weber, R.: Biomass burning impact on PM2.5 over the southeastern US during 2007: integrating chemically speciated FRM filter measurements, MODIS fire counts and PMF analysis, Atmos. Chem. Phys., 10, 5839-6853, 2010.

Zheng, M., Ke, L., Edgerton E. S., Schauer, J. J., Dong, M., and Russell, A. G.: Spatial distribution of carbonaceous aerosol in the southeastern United States using molecular markers and carbon isotope data, J Geophys Res, 111, D10S06, doi:10.1029/2005JD006777, 2006.